JIMMA UNIVERSITY
JIMMA INSTITUTE OF TECHNOLOGY
SCHOOL OF GRADUATE STUDIES
FACULTY OF CIVIL AND ENVIRONMENTAL ENGINEERING
GEOTECHNICAL ENGINEERING STREAM

NUMERICAL ANALYSIS OF UNSUITABLE TROPICAL RED SUBGRADE SOILS FOR ASSESSING UNDERCUT DEPTH: A CASE STUDY OF MEREWA-SEKA ROAD PROJECT

A Thesis Submitted to School of Graduate Studies, Jimma University, Jimma Institute of Technology, Faculty of Civil and Environmental Engineering in Partial Fulfillment of the Requirements for the Degree of Master of Science in Geotechnical Engineering

by

Binyam Gezahegn Kassa

June 2024

Jimma, Ethiopia

JIMMA UNIVERSITY
JIMMA INSTITUTE OF TECHNOLOGY
SCHOOL OF GRADUATE STUDIES
FACULTY OF CIVIL AND ENVIRONMENTAL ENGINEERING
GEOTECHNICAL ENGINEERING STREAM

NUMERICAL ANALYSIS OF UNSUITABLE TROPICAL RED SUBGRADE SOILS FOR ASSESSING UNDERCUT DEPTH: A CASE STUDY OF MEREWA-SEKA ROAD PROJECT

A Thesis Submitted to School of Graduate Studies, Jimma University, Jimma Institute of Technology, Faculty of Civil and Environmental Engineering in Partial Fulfillment of the Requirements for the Degree of Master of Science in Geotechnical Engineering

Main advisor: Alemineh Sorsa (PhD)

Co-advisor: Shelema Amena (MSc)

June 2024

Jimma, Ethiopia

DECLARATION

I, the undersigned, hereby declare that the work presented in this thesis, entitled "**Numerical Analysis of Unsuitable Tropical Red Subgrade Soils for Assessing Undercut Depth: A Case Study of Merewa-Seka Road Project,**" is my own original work and has not been submitted for any other degree or qualification at Jimma University or elsewhere. I also declare that I have acknowledged all sources of information used in the preparation of this thesis.

Candidate:

Mr. Binyam Gezahegn

_____________________ _________________

Signature Date

As Master's research advisers, we hereby certify that we have read and evaluated the MSc thesis prepared under our guidance by **Binyam Gezahegn** entitled "Numerical Analysis of Unsuitable Tropical Red Subgrade Soils For Assessing Undercut Depth: A Case Study of Merewa-Seka Road Project." We believe that the thesis report is of a high standard and that it meets the requirements for the degree of Master of Science in Geotechnical Engineering.

Alemineh Sorsa (PhD)	_____________________	_________________
Main advisor		
Shelema Amena (MSc)	_____________________	_________________
Co-advisor	Signature	Date

APPROVAL PAGE

As members of the examining board of the final M.Sc. open defense, we verify that we have read and evaluated the thesis prepared by Binyam Gezahegn, entitled "**Numerical Analysis of Unsuitable Tropical Red Subgrade Soils for Assessing Undercut Depth: A Case Study of Merewa-Seka Road Project,**" and recommended for acceptance as a fulfillment of the requirement for the Degree of Master of Science in Civil Engineering (Geotechnical Engineering).

Main Advisor
Alemineh Sorsa (PhD)

	Signature	Date

Co-Advisor
Shelema Amena (MSc)

	Signature	Date

Members of Examining Board:

1. **Tadesse Abebe (PhD)**		02/07/2024
External Examiner	Signature	Date
2. **Chemeda Alemu (MSc)**		
Internal Examiner	Signature	Date
3. **Hashim Ware (MSc)**		
Chairperson of Examiner	Signature	Date

ABSTRACT

Unsuitable tropical red subgrade soils form in situ by the intense weathering of parent material in tropical and sub-tropical climatic environments. They cover a wider area of the Western part of Ethiopia, including the project under study. Due to the absence of an adequate classification system, they are well known to be misunderstood and are deemed unsuitable, considering only index properties without assessing the engineering properties of the soils. This leads to a conservative treatment approach with an undercut depth suggested for expansive soils in their application for flexible pavements. The aim of this study is to investigate the geotechnical properties and deformation characteristics of unsuitable tropical red subgrade soils under vehicular loading. After modeling the subgrade soils, the researcher examined the degree of weakness present in these soils and determined the appropriate undercut depth using numerical solutions in the PLAXIS 2D software. In this study, three different categories (1, 2, and 3) of subgrade were selected, and disturbed and undisturbed samples collected and investigated using field and laboratory test programs. The test programs included determination of moisture content, Atterberg limits, specific gravity, grain size distribution, moisture-density relation, California bearing ratio, dynamic cone penetration, triaxial shear strength, consolidation parameters, free swell index, swelling pressure, geochemical properties, and X-ray diffraction analysis. The numerical analysis program used cyclic (dynamic) pulse loading on top of flexible pavement and the Hardening-Soil Model with Small-Stiffness Material Model for simulating the behavior of unsuitable subgrade soils. The subgrade soils were classified as fine grained that are inactive and have a non-expansive nature. The mineral analysis indicated the presence of dominant minerals like quartz, chloritoid, heulandite, and kaolin, and chemical analysis revealed that the soils are true laterites. In addition, category-1 subgrade soil was found to have adequate bearing capacity and strength that could be used for subgrade without treatment (having a soaked CBR value of 10.2%, a cohesion value of 78.3 kPa, and a friction angle value of 17.11^o), while categories 2 and 3 were found to be inadequate, requiring treatment (having a soaked CBR value of 7.2% and 2.5%; a cohesion value of 40.71 kPa and 32.64 kPa; and a friction angle value of 12.11^o and 10.56^o, respectively). Moreover, from in-situ testing, DCP values were determined to be 23 mm/blow, 25 mm/blow, and 49 mm/blow for categories 1, 2, and 3, respectively. The numerical deformation analysis revealed that 60 cm and 100 cm undercut depth treatments are adequate for categories 2 and 3, respectively. The effectiveness of undercut treatment in relation to deformation resulting from numerical simulation and the comparison of this study's findings with the current practice in Ethiopia are also presented in this paper. Furthermore, conducting additional geotechnical investigations and numerical analysis on a large number of unsuitable tropical red subgrade soils is recommended in order to obtain reliable and comprehensive information on how they behave.

***Keywords**: Tropical red soil, Unsuitable subgrade soils, Numerical analysis, Flexible pavement, minimum undercut.*

ACKNOWLEDGMENTS

I want to start by saying how grateful and thankful I am to the Almighty God, whose constant presence, support and direction have been essential to every stage of my life.

My most profound appreciation goes to my main research advisor, Dr. Alemineh Sorsa, PhD, and co-advisor, Eng. Shelema Amena, MSc, for their time, effort, unwavering encouragement, helpful advice, and understanding in helping me succeed during the preparation of this thesis.

I also want to express my gratitude to the academic staff at Jimma University, Jimma Institute of Technology's faculty of civil and environmental engineering (geotechnical engineering chair).

I would like to thank the following people and firms for helping with this research project: China Tiseju Civil Engineering Group Co. Ltd., Ethiopia branch, Guo Jian, Su Meixu, Li Xing, Sun Guo Qeng, Song Chen, Chala Woji, Hundera Tolina, Hana Alemayehu, Liranso Wabato, Dereje Moges, Gashaw Jibril, Samson Gebreab, Firew Bekele, and his wife Bethel Kassahun, Haile Tsegay G/Samuel, Selamawit Tadesse, Afework Debaleke, Binyam Getachew and Samson Abate.

I am grateful to my colleagues, partners, and friends who shared their experiences with me and voluntarily took part in this study.

Lastly, I want to thank my family, especially Aynalem Tefera (my mother), Bethelehem Gezahegn (my sister), Yakob Gezahegn (my brother), Genet Gossaye (my wife), and our children, Be’emnet and Eliab, for their constant inspiration, support, motivation, and prayer.

TABLE OF CONTENTS

LIST OF TABLES

LIST OF FIGURES

ACRONYMS

A	Activity of clay
AAS	Atomic absorption spectroscopy
AASHTO	American Association of State Highway Transpiration Officials
a.m.s.l	Above Mean Sea Level
ASTM	American Society for Test and Materials
BS	British Standard
CBR	California Bearing Ratio
DC	Design Class
DCPI	Dynamic Cone Penetration Index
DOT	Department of Transportation
E	Easting
ECDSWC	Ethiopian Construction Design and Supervision Works Corporation
ERA	Ethiopian Road Administration (Former Ethiopian Roads Authority)
ESA	Equivalent Single Axle
ETB	Ethiopian Birr
FEM	Finite Element Modeling
IS	Indian Standard
JiT	Jimma Institute of Technology
LL	Liquid Limit
MDD	Maximum Dry Density
N	Northing
OMC	Optimum Moisture Content
PDM	Pavement Design Manual
PI	Plasticity Index
PL	Plastic Limit
PVC	Potential volume change
SL	Shrinkage Limit
SPT	Standard Penetration Test
S-S ratio	Silica-Sesquioxide ratio
STS	Standard Technical Specifications and Method of Measurement for Roads
USCS	Unified Soil Classification System
URRAP	Universal Rural Road Access Program

UU	Unconsolidated Undrained Triaxial test
Wt.	Weight
XRD	X-ray Diffraction

CHAPTER 1

INTRODUCTION

1.1 Background of the Study

Red soils cover 13% of the land area and are mostly found in tropical and subtropical areas, making them the third most important soil in the world [1]. To think of them as a single, well-defined soil type, however, would be to overlook the vast range of soils that they comprise, each with significantly different material and engineering characteristics [2]. This difference may be seen in the literature on tropical soils, where red and reddish-brown soils are referred to as latosols, tropical red clays, laterites, lateritic soils, and non-lateritic tropically weathered soils [2–5].

Tropical red subgrade soils, or tropical red soils in this study, refer to residual soils having a red or reddish-brown color formed in situ by the intense weathering of parent material in tropical and sub-tropical climatic environments [2]. These soils are commonly recognized as having iron or aluminum oxides, also known as sesquioxides (Fe_2O_3 or Al_2O_3), which are responsible for the soils' reddish coloration [6].

For the engineering application of tropical red soils, employing global classification systems is called into doubt, as such methods are dependent on the grain size distribution and Atterberg limits of soils [4]. The difficulties of using conventional identification and classification approaches meant for temperate soils for engineering behavior prediction are related to the weathering of the soils, the presence of unusual clay minerals, or the effects of sesquioxides [5–7]. However, standard classification systems are commonly used for these soils, making them well known worldwide to be identified as problematic or unsuitable [2,6], regardless of their satisfactory field performance for subgrade applications [8].

According to ERA standard [9], tropical red soils could be easily identified as unsuitable materials if their liquid limit (LL) value is greater than 60%, their plasticity index value is greater than 30%, or their CBR-swell value is greater than 3%, despite having a higher (> 5%) CBR value. With this in mind, the project under study (Merewa-Seka road project) is characterized by a significant portion of unsuitable tropical red subgrade soils [10]. During the project's construction phase, 39.4% of the subgrade soil was classified as unsuitable, despite 77.9% of it having a CBR value greater than 5%, as shown in Table 1-1.

Table 1-1 Subgrade soil category for the study based on construction phase data [10]

Description	Category-1	Category-2	Category-3	Category-4	Total
	Unsuitable Subgrade soils (CBR ≥ 5 & CBR-Swell ≤ 3)	Unsuitable Subgrade soils (CBR ≥ 5 & CBR-Swell > 3)	Unsuitable Subgrade soils (CBR < 5)	Suitable Subgrade soils	
Length of tested road section [m]	12,640.0	13,884.0	7,500.0	52,440.0	86,464.0
Percentage	14.6%	16.1%	8.7%	60.6%	100.0%
Average LL	67	68	70	55	62
Average PI	26	25	28	18	22
Average CBR	8.6	6.9	3.4	9.7	7.9
Average CBR-Swell	2.0	4.2	6.2	1.7	3.0
Minimum undercut depth required [cm]	60*	100**	100**	Nil*	-

* Based on ERA standard specification [9] and judgement of the engineer or consultant.
** Based on ERA standard specification [9,11,12] and project specification.

As a consequence, after considering these soils as expansive or problematic, the researcher has practically observed that removal and replacement (undercutting) equivalent to black cotton or highly expansive soils is recommended as a treatment [9,13]. There are also no studies in the project area that deal with the unsuitable tropical red subgrade soils and their undercut treatment depth. If such soils are left unstudied in depth, not only misinterpretation will follow, but also the commonly practiced conservative method may lead to an uneconomical, time-consuming, and environmentally unfriendly subgrade construction approach.

Without a doubt, misunderstanding unsuitable tropical soils is a recurring problem for many areas of the country, especially the south-western part of Ethiopia [14,15], and it will have a negative impact on the progress of current and future road construction projects. It is in this context that the researcher hopes to learn more about the district geotechnical properties of unsuitable tropical red subgrade soils and deformation characteristics.

This thesis aims to investigate the geotechnical characteristics of the unsuitable tropical red subgrade soils of the Merewa-Seka road project and determine an appropriate undercut depth based on the deformation characteristics of the same under vehicular load using numerical analysis.

1.2 Statement of the Problem

Tropical red soils, characterized by unique properties resulting from weathering and pedogenesis [4,7], present a challenge in predicting their engineering behavior using standard geotechnical classification methods developed for temperate soils [5,16,17]. This has led to their popularity as problematic [6], and despite several attempts to identify and classify these soils, a comprehensive method has not yet been established to address all of the soil varieties [18,19].

In Ethiopia, according to ERA standard [9], conventional geotechnical classification methods are used for tropical red soils in their identification as unsuitable, despite the recognition of their special feature of satisfactory performance while having higher plasticity characteristics [20]. In this context, as presented in Table 1-1, 39.4% of the tropical red subgrade soils of the project under study are classified as unsuitable material and deemed to be treated to a minimum removal and replacement (undercut) depth of either 60 or 100 cm.

The essential issue is that a substantial portion of the subgrade soils of the project are considered unsuitable solely based on their Atterberg limit value, CBR-swell value, or both, in spite of having an acceptable CBR value for the corresponding design subgrade class. Additionally, in Ethiopia, there is no appropriate removal and replacement (undercut) treatment depth guideline for such soils based on the level of detrimental effect they pose, regardless of the fact that they are commonly undercut to a predetermined depth.

Given their index properties, the unsuitable tropical red subgrade soils of the project are easily considered expansive soils, and the subsequent required treatment is expensive and will negatively affect the progress of the project. In addition to this, a predetermined undercutting depth requires additional land for a suitable replacement material source and disposal of undercut material, despite its grave scarcity. Furthermore, the acquisition of lands for such purposes will result in considerable environmental degradation as the road traverses through populated areas and agricultural lands.

In light of these challenges, assessing unsuitable tropical red soils will provide greater understanding to determine their engineering properties and distinct strength for their economical, durable, and environmentally friendly subgrade application.

This research aims to evaluate the problematic nature of tropical red subgrade soils of the project that have been deemed unsuitable through an in-depth geotechnical investigation, as the researcher noted a lack of existing studies focusing on unsuitable tropical red subgrades that were explicitly conducted on soils in the Jimma zone, Oromia region, Ethiopia. Aside from that, the research used the finite element method to conduct deformation analysis of these soils under vehicular loading in order to establish the optimum undercut depth for the appropriate treatment that follows.

1.3 Research Questions

This study attempted to answer the following research questions:

1. What distinguishing geotechnical properties do the unsuitable tropical red subgrade soils have?
2. How can the permanent deformation of unsuitable subgrade soils under vehicular load be addressed using finite element modeling?
3. To what extent does the removal and replacement treatment method reduce deformation in unsuitable tropical red subgrade soils when applied up to a depth of 100 cm?

1.4 Objectives

1.4.1 General Objective

The general objective of this study is to analyze the effects of the undercut depth of unsuitable tropical red subgrade soils under flexible pavement.

1.4.2 Specific Objectives

1. To investigate the geotechnical properties of unsuitable tropical red subgrade soils.
2. To develop a finite element model for simulating the behavior of unsuitable tropical red subgrade soils under vehicular load.
3. To evaluate the undercut depth of unsuitable tropical red subgrade soils using the finite element model.

1.5 Scope and Delimitation of the Study

This study is to focus on analyzing the effects of the undercut depth of unsuitable tropical red subgrade soils under flexible pavement using numerical analysis. The researcher used the geotechnical properties of unsuitable tropical red subgrade soils, vehicular loading, and undercut depth to measure the deformation and stress distribution of unsuitable tropical red subgrade soils.

Three test pit samples and respective in-situ testing that correspond to separate subgrade categories as well one replacement material sample served as the study's input for investigation, modeling using finite elements, and analysis of undercut depth up to 100 cm. This study was conducted from February to May 2024 within the right-of-way boundaries of the Merewa-Seka road project, Jimma zone, Oromia region, Ethiopia.

The samples and in-situ testing locations were selected by performing purposive non-probability sampling to ensure that there would be at least one representative in each subgrade category of the predetermined index property.

The researcher collected test data after conducting geotechnical tests on both disturbed and undisturbed samples to assess the properties of unsuitable tropical red subgrade soils and replacement material. The collected data was used as an input for finite element modeling of flexible pavement using PLAXIS 2D software to assess the optimum undercut depth.

This study didn't take into account every aspect that influences the undercut depth determination of unsuitable tropical red subgrade soils but rather considers deformation as a primary criterion. Further, the study didn't consider long-term deformation analysis, as dynamic analysis of the model will require extensive computation times and sophisticated computer technology.

1.6 Significance of the Study

The project understudy, the broader road construction sector, researchers, and academic scholars will benefit from this study in the following aspects:

- The study will increase understanding of the engineering properties and deformation characteristics of tropical red soils that are classified as unsuitable materials based on their index properties.

Further, it will fill the knowledge gaps about unsuitable tropical red soils, their numerical analysis, and their adequate undercut treatment under flexible pavements.

- The outcome of this study will help identify the most problematic type of unsuitable tropical red soil and its subsequent treatment with the most economical undercut depth.
- It will serve as an additional resource that helps identify unsuitable tropical red soils for their economical, effective, and environmentally friendly application.
- The findings of this research will provide information that will enable stakeholders in road construction projects with the same type of subgrade soil to look for an economical and technically acceptable construction approach.
- The analysis presented in this study will convey valuable information for future research exploring the properties of unsuitable tropical red soils and their successful utilization.

CHAPTER 2
LITERATURE REVIEW

2.1 Overview

This chapter's primary goal is to provide evidence from the literature in favor of studying and modeling unsuitable tropical red subgrade soils in order to evaluate undercut depth options. The researcher will also discuss the importance of the issue being studied. The chapter is structured into three main parts based on the significant topics that emerged throughout the problem's examination. The definition, formation, geotechnical characteristics, and identification of unsuitable tropical red subgrade soils are covered in the first part. The modeling of tropical red subgrade soils using the finite element method is the main topic of the second section. And lastly, the third section covers undercut (removal and replacement) treatment methods using both regional and international practices.

2.2 Unsuitable Tropical Red Subgrade Soils

2.2.1 Definition

The subgrade, or earth roadbed portion that receives the base or surface material, is built in a way that closely adheres to the lines, grades, and cross-sections depicted on the plans. The depth below the completed level of the road at which soil properties have a major impact on pavement behavior (i.e., 800mm to 1,200mm depending on the traffic class) is where subgrade may extend, provided that the nominal subgrade strength chosen for the design is not exceeded [9,11]. But while constructing a subgrade, a variety of soils could be encountered, tropical red soils being one of them.

Tropical red soils are a type of residual soil that is usually found in tropical and subtropical regions. They are characterized by their high iron content, which gives them their characteristic red color [21,22].

Unsuitable material consists of a broad range of subgrade and/or roadbed materials. Table 2-1 below lists the primary categories of subgrade materials that are not suitable for use in road construction, as per Ethiopian standards.

Table 2-1 Unsuitable material type [9]

Type	Unsuitable material description
1	Peat and other organic materials from swamps, marshes, and bogs that contain compressible soils and excessive amounts of degradable organic matter, such as decomposing wood and other vegetation.
2	Clay material having a liquid limit (LL) exceeding 60; or a plasticity Index (PI) exceeding 30; or a CBR value less than 3% at 95% of modified AASHTO compaction (AASHTO method T-180) after 4 days of soaking; or a swell value of more than 3% (with two surcharge rings) when determined in accordance with AASHTO T-193 at 95% of modified AASHTO compaction.
3	Other problem soils such as expansive clays; collapsible sands; dispersive soils; saline soils; micaceous soils; and low strength soils.
4	Any material that is sufficiently wet and soft to prevent it from being trafficked or excavated by normal bulk earth-moving equipment

2.2.2 Formation

Residual soils form through decaying vegetation, weathering, leaching, and disturbance, forming parallel horizons. The soil profile can change as depth increases, affecting engineering properties and mineralogy [7]. Thus, even though there are some circumstances in which it might be the case, it can be said that it is highly unlikely that the residual soil profile is homogeneous. With a gradual change in properties with depth and the potential to contain joint or fault planes, it is far more likely to be heterogeneous.

2.2.3 Geotechnical characteristics

The unsuitable subgrade soils of the project studied falls into one or more classes of unsuitable material defined in Table 2-1. Yet, it should be noted that the broad tropical red subgrade soils include laterite soils, depending on climate conditions and the surrounding environment [23].

Accordingly, understanding the overall nature and formation of tropical red soils requires an understanding of their geotechnical properties. Several studies have been published concerning the characteristics of tropical red clay soils. [24] surveyed tropical red clay soils across different parts of the world, including Ethiopia.

It is reported that average index values range in a suitable category for subgrade except for some marginal soils. Liquid limit values range from 32% to 52%; plasticity index values range from 14% to 31%; CBR values range from 18% to 67%; and activity values range from 0.77 to 1.0.

Likewise, Akalu [25] has also investigated red clay soils found in western Addis Ababa and assessed their suitability as per the existing codes and standards. The findings of the study were clay content ranging from 55% to 65%, liquid limit value from 39% to 106%, plasticity index values from 9% to 40%, and free swell value ranging from 5% to 80%.

Teferi [15] investigated the suitability of tropical red soils (lateritic soils) for road construction material along the project route. For towns located along the project under study, he has found that there are both suitable and unsuitable subgrade materials when examined as per ERA standards. He concluded that lateritic soils from Seka Kebele are poor subgrade, while samples from Babu and Limu towns are good subgrade.

Most of the literature reviewed in the study area focuses on the identification of suitable subgrade soils or construction materials. They did not adequately address the extent to which these subgrade soils are unsuitable, the detrimental impacts they would have if used for pavement applications, or the necessary treatments if they were troublesome. In addition, in order to properly and effectively utilize such subgrade soils, performance characterization under pavements and vehicular load must be included. Hence, it is important to further study unsuitable tropical red subgrade soils for appropriate treatment measures.

2.2.4 Identification

Before beginning any construction activity, such as constructing pavement infrastructure, a geotechnical engineer must identify any unsuitable soils, especially expansive soils. The main issue with unsuitable tropical subgrade soils is their propensity for expansive soil properties, which could negatively impact the pavement structure that will be built on them. Numerous studies have provided guidance on how to recognize these qualities.

Chen [26] has offered a thorough method for carrying out these kinds of tasks. He proposed three different approaches to classifying expansive soils: mineralogical identification, direct measurement, and indirect methods.

2.2.4.1 Mineralogical Identification

A crucial step in assessing the properties of clay materials with regard to swelling is the identification of the clay minerals they contain using the mineralogical identification method. X-ray diffraction, a widely used technique in Ethiopia, could be used to implement this method.

Teferi [15] determined the mineralogical composition of Jimma City, Limu Woreda, and Seka Kebele, which are situated along the project under study, using X-ray diffraction analysis. He discovered that the soils in Jimma City contain 32.6% quartz, 32.6% albite, and 34.9% ferrosililite. The soils in Limu Woreda, on the other hand, contain 40.4% keolinite and 50.6% ferrinatrite. Finally, the soils in Seka Kebele contain 66.3% Quartz, 15.1% Goethite, and 18.6% Lindgrenite.

2.2.4.2 Direct Measurement

The direct measurement method offers an excellent way of determining the swelling potential and swelling pressure of an expansive clay. This method can be achieved by using the conventional one-dimensional consolidometer. It accurately simulates the site conditions.

Muhammed et al. [27] have studied Jimma City's soils, particularly the tropical red clay soils. His research, however, did not address the swelling pressure in these soils. His consideration of these tests was limited to other categories of expansive soils; nevertheless, since the research project starts in Jimma city, the results are presented here. According to their investigation, expansive soils in Jimma have swelling pressures between 135 and 210 kPa.

Consequently, the researcher noted a gap in the literature when he was unable to locate any local studies on the subject of tropical red soils' swelling pressure.

2.2.4.3 Indirect Methods

Indirect methods that are useful for assessing the swelling property of soil include the activity method, the potential volume change (PVC) method, and the index property. Index properties and activity methods are more prevalent in Ethiopia [20].

Gidigasu [18] in his comprehensive review of laterite soils, however, stated that these identification techniques might be deceptive.

This is because index properties like Atterberg limits, which are greatly influenced by pretest preparations and testing procedures, may not produce repeatable results. Additionally, because clay-size content and plasticity index vary depending on sample preparation and testing methods, the activity method may be misleading for some laterite soils.

In conclusion, this study will employ direct measurement and mineralogical identification techniques since they are more dependable and accurate for identification.

2.3 Modeling of Tropical Red Subgrade Soils

2.3.1 PLAXIS 2D software

Geotechnical engineering and rock mechanics use PLAXIS 2D, a robust and intuitive commercial finite-element software, for 2D deformation and stability analysis. Initiated by the Dutch Department of Public Works and Water Management, PLAXIS development started in 1987 at the Technical University of Delft. The original objective was to create a user-friendly 2D finite element code for river embankment analysis on the soft soils of the Holland lowlands. Even now, the primary aim of PLAXIS is to offer geotechnical engineers, who may not be numerical experts, a practical analysis tool. Leading institutions and engineering firms in the geotechnical and civil engineering sectors use PLAXIS globally. Applications such as tunneling, mining, oil and gas, reservoir geomechanics, embankments, and foundations are all well suited for PLAXIS 2D. With the exception of creep, steady state groundwater or thermal flow, consolidation analysis, or any time-dependent effects, PLAXIS 2D has all the necessary components to conduct deformation and safety analyses for soil and rock [28].

The use of PLAXIS in the road and highway industries is likewise well established. PLAXIS 2D was used by several researchers to examine subgrade and pavement deformation. Using PLAXIS 2D, [29,30] carried out finite element analysis on flexible pavements. Also, [31–36] used the same application to study the deformation of the subgrade and pavement structures. Relatedly, [37] examined the damaging impact of expansive soil on pavement overlaying. Therefore, with an accurate and reasonable estimate, PLAXIS 2D could be used to assess the deformation of unsuitable subgrades of the project under study.

2.3.2 Finite Element Modeling Approach

Finite Element Analysis (FEA), sometimes referred to as Finite Element Modeling (FEM), is a numerical technique used to forecast the behavior of physical systems, including thermal, fluid, electromagnetic, and structural ones. The technique necessitates breaking down the component under study into discrete elements, which produce a finite element mesh.

The behavior of the individual elements is then modeled by assembling the simple equations that describe them into a larger system of equations that models the entire problem. A direct or iterative solver is used to solve the resulting system of equations, depending on whether nonlinear effects are present [38].

Because they are made of so many different layers, materials, and boundary conditions, flexible pavements are complex engineering structures [39]. Hence, finite element modeling of flexible pavements should follow proper methodology for accurate analysis.

2.3.2.1 Geometry and General Inputs

Two types of models can be used to simulate real-world scenarios: axisymmetric models and plane strain models. With the help of a practical graphical user interface, users of PLAXIS 2D can quickly create a geometry model and finite element mesh using a representative vertical cross section of the given scenario. Plane strain analysis is based on the assumption that the problem is infinitely long and normal to the plane section of the analysis. In a plane strain analysis, the out-of-plane displacement (strain) is, by definition, zero. The axisymmetric analysis allows for the analysis of a 3D problem which is rotationally symmetric about an axis. Although the input is two-dimensional, one is actually analyzing a symmetric three-dimensional problem due to the rotational symmetry [28]. The axisymmetric analysis consisting of 15-node triangular elements is commonly applied to flexible pavement modeling. Researchers, [29,32,34], could be taken as examples.

A large variety of inputs are available in PLAXIS 2D, making modeling simple for users. In general, there are two input modes available for modeling: geometry modes and calculation modes. The geometric configuration of the model is defined in geometry modes, which enable all geometry modifications (e.g., creation, relocation, modification, or removal of entities).

The two modes that make up the geometry mode are the soil and structure modes. The definition of soil stratigraphy, the overall water levels, and the initial conditions of the soil layers are all made possible by the soil mode. On the other hand, the structural components, forces, and geometric entities in the model are defined in the structure mode. Within the calculation modes, the calculation process is defined. Flow conditions, staged construction, and mesh make up the calculation mode. Additionally, phase definition modes are the flow conditions and staged construction modes [28].

2.3.2.2 Materials

In PLAXIS 2D, there are seven different types of material sets grouped as data sets for: soil and interfaces, discontinuities, plates, geogrids, embedded beams, cables and anchors [28]. Considering the scope of the study, only soils and interfaces are discussed to model flexible pavements on unsuitable subgrade.

Depending on the constitutive models chosen, PLAXIS 2D can be used to model both the subgrade and multi-layer pavement materials. Whenever subgrade modeling and analysis is made, for simplicity and to save calculation time, researchers like, [29,32,33,37], preferred the use of either the linear elastic or Mohr-Coulomb models for pavement layers. Nonetheless, more practical and precise models, such as the hardening soil model, are employed whenever modeling unsuitable soils or generally subgrade soils [31,34].

2.3.2.3 Load and Tire-Pavement Contact Area

Vehicular loading is transferred to the pavement through the vehicle's axle and tires. The contact area between the tires and the pavement must somehow be precisely determined in order to calculate the stress and strain that are generated. Better accuracy in contact area determination is necessary for proper vehicular load modeling. Vuuren [40] developed a curve that shows the general relationship between tire contact pressure and tire inflation pressure for tires used on road vehicles, as presented in Figure 2-1. Also, Yap [41] showed that the contact area of 11R24.5 dual tires is 114 inch^2 for a 4,250 lbs load. However, the contact area recommended by Huang [42] is commonly used for modeling. He assumed that the contact area is composed of a rectangle and two semicircles for each tire, as shown in Figure 2-2. Considering length L and width $0.6L$, the area of the contact, $A_c = 0.5227 L^2$. Using one equivalently larger circle rather than two separate circles, as shown in Figure 2-2, is recommended for simplicity and to obtain more approximate results in calculations [36,42].

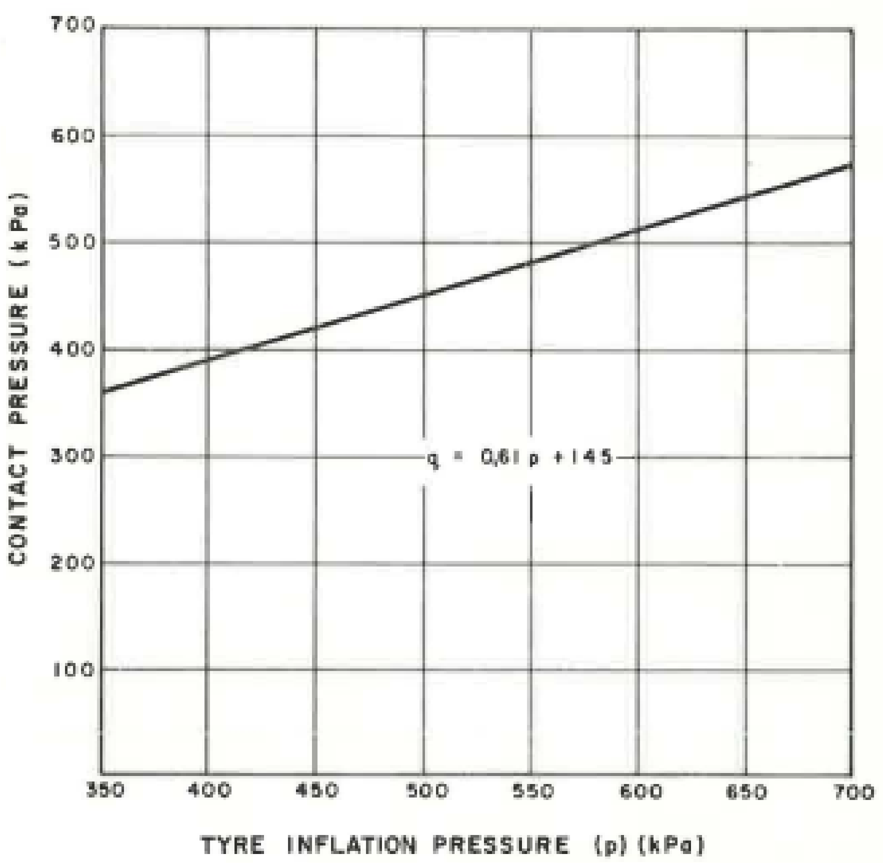

Figure 2-1 Average straight-line relationship between contact pressure and inflation pressure (for recommended combinations of wheel load and inflation pressure) [40]

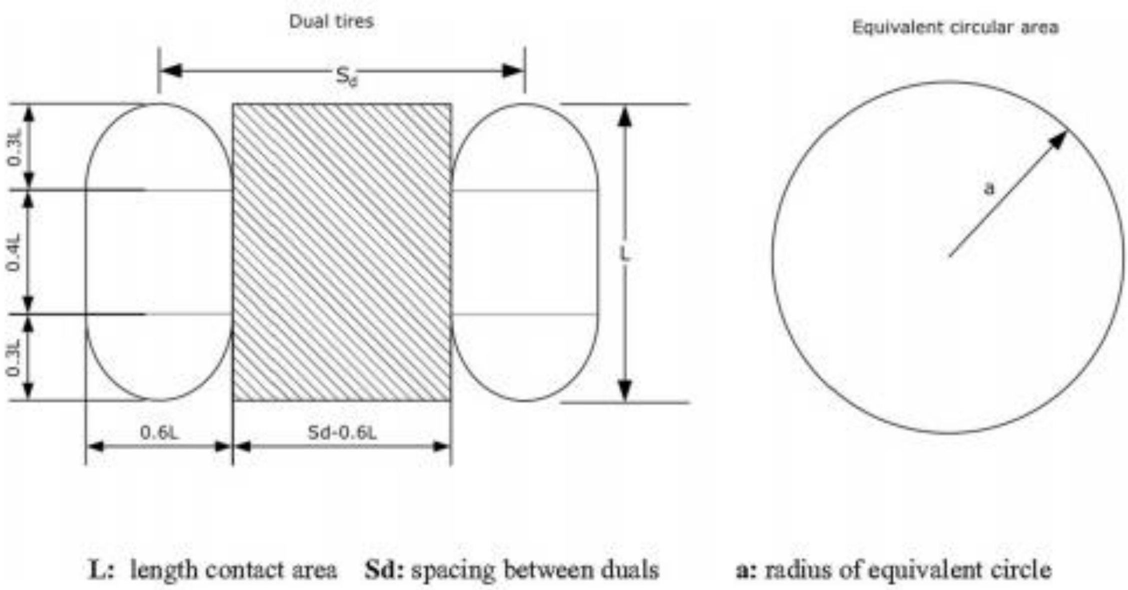

Figure 2-2 Dual tires' contact area transformed to a circle with radius 'a' [42] cited in [36]

2.3.3 Constitutive Models

Different models are supported by PLAXIS 2D to simulate the behavior of soil and other materials under vehicular or cyclic loading. The linear Elastic, Mohr-Coulomb, and hardening soil models are the most widely used. Additionally, the hardening-soil model with small-stiffness is used in the literature to estimate deformations under cyclic loading more accurately [34,43].

2.3.3.1 Linear Elastic Model

Hooke's law is the foundation for PLAXIS's linear elastic model, which is used to simulate isotropic linear elastic behavior. It has two parameters: the effective Poisson's ratio (ν') and the effective Young's modulus (E'). Although simulating non-linear soil behavior is generally inappropriate, it is useful for simulating structural behavior like thick concrete walls or plates, whose strength properties are typically much higher than those of soil [28].

When compared to soils, asphalt concrete layers show stronger properties, and researchers commonly use the linear elastic model for numerical analysis [29,31,32,36].

2.3.3.2 Mohr-Coulomb Model (MC Model)

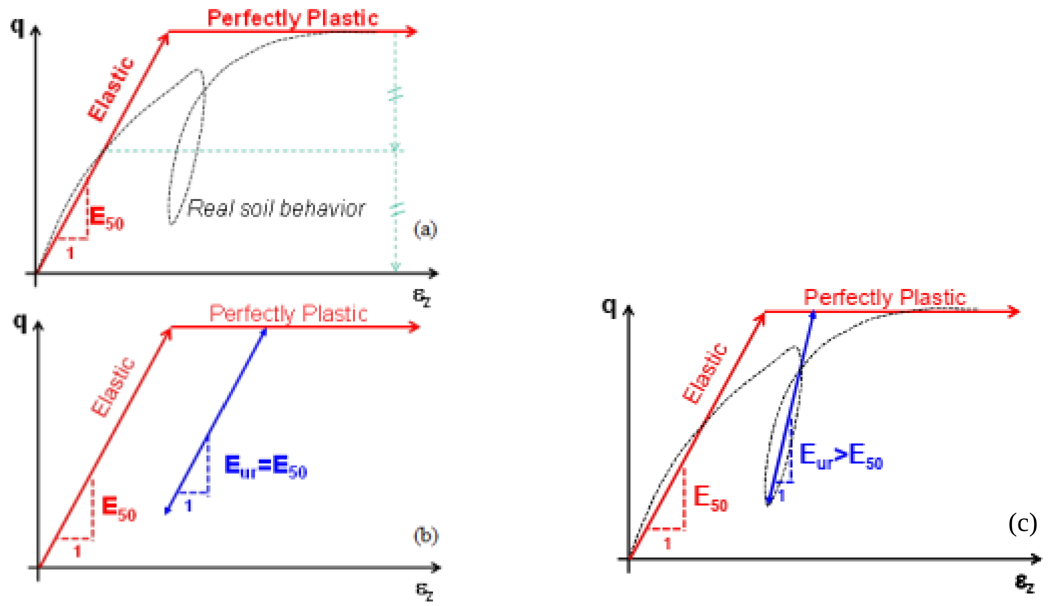

Figure 2-3 Mohr Coulomb Model [44]

The Mohr-Coulomb model, also known as the elastic perfectly-plastic constitutive model, uses Hooke's law and the Mohr-Coulomb failure envelope to model linear elastic deformation behavior in soils below the failure envelope [45].

As shown in Figure 2-3 (a), the Mohr-Coulomb bilinear elastoplastic approach divides soil's nonlinear behavior into two bilinear lines, with soil stiffness constant, defined as E_{50}, until stress reaches the plastic zone. However, soil exhibits nonlinear behavior, varying according to stress levels within the soil mass. The model can over-predict ground movement at stress levels less than 50% of the ultimate strength and under-predict it at stress levels higher than 50%. Additionally, as shown in Figure 2-3 (b), the Mohr-Coulomb model assumes that the stiffness modulus of soil unloading and reloading, E_{ur}, equals the stiffness of soil loading, E_{50}.

This results in inaccurate predictions of soil movement when compared to the actual conditions shown in Figure 2-3 (c), and it has limitations when analyzing undrained problems because it overpredicts the shear strength of the undrained soil [44].

The model requires two stiffness properties: elastic modulus, E, and Poisson's ratio, ν; and three shear strength properties in a drained condition: cohesion, c, friction angle, φ, and dilatancy angle, ψ. Because of its simplicity to get rapid rough estimates, several scholars and researchers, like [29,32,36] used the Mohr-coulomb model for analyzing pavement layers below the asphalt concrete layer.

2.3.3.3 Hardening-Soil Model (HS Model)

Schanz et al. [46] have developed a constitutive formulation using a double-stiffness model for elasticity and isotropic strain hardening, replacing Hooke's single-stiffness model with ideal plasticity. This model, called the Hardening-Soil Model, greatly outperforms the earlier models because it incorporates soil dilatancy, applies the yield cap, and applies the theory of plasticity rather than the theory of elasticity. In contrast to an elastic perfectly-plastic model, the hardening plasticity model distinguishes between shear and compression hardening types by allowing plastic straining to expand its yield surface. The model contains both kinds. It is also frequently used to assess hard ground conditions or soft soils that make it suitable for flexible pavement modeling [28].

The hardening soils model was developed to simulate the fundamental macroscopic behaviors of soils, including plastic yielding, dilation, stress-dependent stiffness, densification, and soil stress history [47].

The hardening soil model has limitations, despite possessing all the best attributes for accurately analyzing geotechnical problems. Under cyclic loading, it is unable to capture the material model's incremental cumulative deformation. Furthermore, higher values of soil stiffness associated with very small strain levels are not taken into account [45]. The hardening soil model is widely used to analyze unsuitable or even soft soils, despite its limitations.

2.3.3.4 Hardening-Soil Model with Small-Stiffness (HSS Model)

The Hardening Soil model with small-strain stiffness used in PLAXIS is based on the Hardening Soil model and has essentially identical properties.

To characterize stiffness changes with strain, just two factors are required: the initial or very small-strain shear modulus and the shear strain level at which the secant shear modulus is lowered to around 70% of the initial shear modulus [28].

2.3.4 Model Parameters for Hardening Soil Model

The basic parameters for the hardening-soil model are - failure parameters: cohesion, c, friction angle, φ, and dilatancy angle, ψ; Basic parameters for stiffness: E_{50}^{ref}, E_{oed}^{ref}, E_{ur}^{ref} and m; and advanced parameters: ν_{ur}, P^{ref}, K_0^{nc} and R_f [46]. This subsection will address the parameters of the hardening soil model as well as the laboratory tests required to determine those parameters.

2.3.4.1 Reference Secant Stiffness (E_{50}^{ref})

Its purpose is to explain plastic straining at a chosen reference pressure resulting from primary deviatoric loading. The test required to ascertain the parameter is: test of drained triaxial compression. Considering Figure 2-4, stiffness parameter E_{50}^{ref}, a selected confining pressure can be determined from triaxial compression test results using equation (2-1). E_{50} is equal to 50% of the peak deviatoric stress divided by the corresponding axial strain [48].

$$E_{50} = E_{50}^{ref}\left(\frac{c\cos\varphi - \sigma_3'\sin\varphi}{c\cos\varphi + p^{ref}\sin\varphi}\right)^m \tag{2-1}$$

p^{ref} is the referenced confining pressure, and in PLAXIS, a default setting p^{ref}= 100 stress units is used. σ_3' is effective confining pressure.

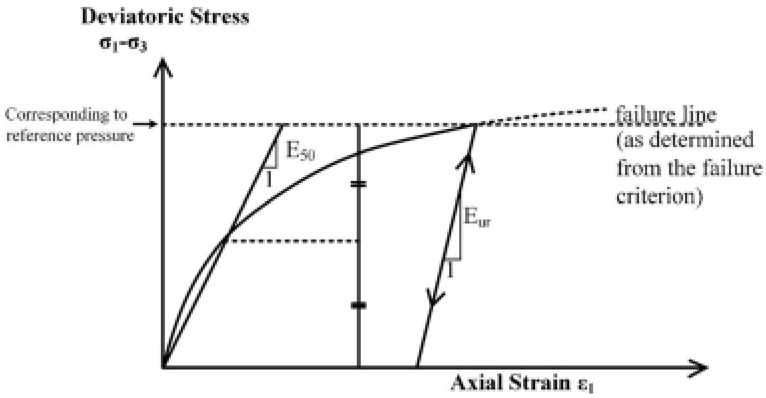

Figure 2-4 Determination of soil model parameters $\boldsymbol{E_{50}}$ and $\boldsymbol{E_{ur}}$ from triaxial compression test results [39]

2.3.4.2 Reference Tangent Stiffness ($\boldsymbol{E_{oed}^{ref}}$)

Its purpose is to explain plastic straining at a chosen reference pressure resulting from primary compression. The test required to ascertain the parameter is: Principal loading in oedometer tests. Then, equation (2-2) is used for the computation. Figure 2-5 shows how to determine E_{oed}^{ref}; however, $E_{oed}^{ref} \approx E_{50}^{ref}$, the default value recommended by PLAXIS, could be used if an oedometer test of the soil is not performed [48].

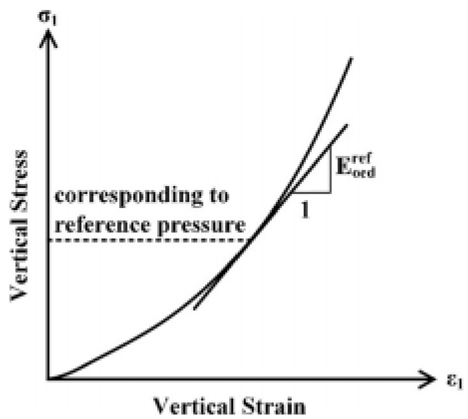

Figure 2-5 Determination of soil model parameter E_{oed}^{ref} at a selected reference pressure from oedometer test results [48]

$$E_{oed} = E_{oed}^{ref} \left(\frac{c \cos\varphi - \sigma_1' \sin\varphi}{c \cos\varphi + p^{ref} \sin\varphi} \right)^m \tag{2-2}$$

σ_1' is vertical stiffness or primary loading.

2.3.4.3 Reference Unloading/reloading Stiffness (E_{ur}^{ref})

It is used to characterize elastic unloading/reloading behavior at a selected reference pressure. Unloading/reloading in triaxial compression tests is required to determine the parameter (default value suggested by PLAXIS: $E_{ur}^{ref} \approx 3E_{50}^{ref}$). Considering Figure 2-4, stiffness parameter E_{ur}^{ref}, a selected confining pressure can be determined from triaxial compression test results using equation (2-3) [46,48].

$$E_{ur} = E_{ur}^{ref}\left(\frac{c\cos\varphi - \sigma_3'\sin\varphi}{c\cos\varphi + p^{ref}\sin\varphi}\right)^m \tag{2-3}$$

2.3.4.4 Failure Parameters c, φ and ψ

The cohesion c, friction angle, φ, and dilatancy angle, ψ requires drained triaxial compression test loaded to failure and a drained triaxial test with measurement of volume change, respectively. c and φ, could be determined from the Mohr-coulomb failure envelope. On the other hand, ψ can be determined from the volume change curve obtained from drained triaxial tests, as shown in Figure 2-6 [48].

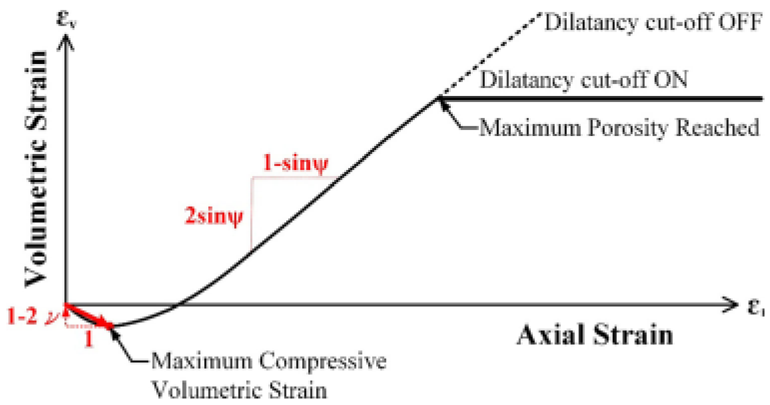

Figure 2-6 Determination of dilation angle ψ and unloading-reloading (elastic) Poisson's ratio $\boldsymbol{\nu_{ur}}$ by the initial part of volume change curve obtained from drained triaxial tests [48]

2.3.4.5 Elastic Poisson's Ratio (ν_{ur})

Test required to determine the parameter: Unloading/reloading in triaxial compression tests. Figure 2-6 illustrates how the volume change curve's initial portion can be used to estimate it. However, the default value suggested by PLAXIS ν_{ur}= 0.2 could be used [48].

2.3.4.6 Power (m)

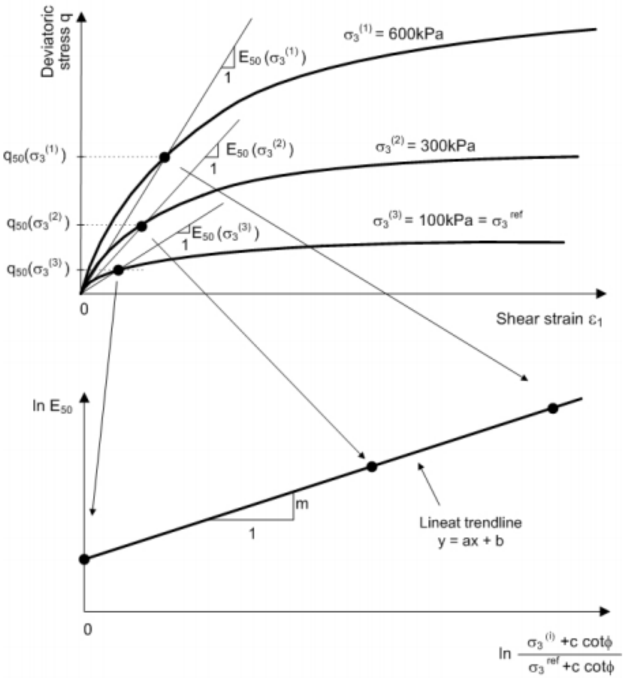

Figure 2-7 Determination of the stiffness stress dependency parameter *m* from three curves derived from the triaxial drained compression tests [47].

Power of a power law used to describe the level of stress dependency of soil stiffness. Test needed to determine the parameter: drained triaxial compression test. Typical range of value: 0.5 ≤ m ≤ 1; default value suggested by PLAXIS: m = 0.5 (m = 1 for logarithmic stress dependency (as in soft clay); m = 0.5 in Norwegian sands and silts) [48]. The parameter determination is as shown in Figure 2-7.

2.3.4.7 Reference Pressure (P^{ref})

Introduced to make parameter m independent of units used for stresses: $E_{oed} = E_{oed}(\sigma/P^{ref})^{m}$. No test is needed to determine the parameter. Default value suggested by PLAXIS is P^{ref} = 100 kPa [48].

2.3.4.8 Failure Ratio (R_f)

$R_f = (\sigma_1 - \sigma_3)_{failure}/(\sigma_1 - \sigma_3)_{ultimate}$ Test needed to determine the parameter: drained triaxial compression test. Default value suggested by PLAXIS is R_f = 0.9 [48].

2.3.4.9 Value For Normal Consolidation (K_0^{nc})

No test is needed to determine the parameter. Default value suggested by PLAXIS is $K_0^{nc} = 1 - \sin\phi$ (coefficient of earth pressure at rest) [44,48].

2.3.5 Additional Model Parameters for HSS Model

2.3.5.1 Reference Shear Modulus at Very Small Strains (G_0^{ref})

This parameter could be measured in laboratories (triaxial tests) and/or field tests (geophysical). Using data from the triaxial test, it is determined using equation (2-4). In the absence of test data, it could be estimated using correlation from geotechnical tests [28,49].

$$G_0 = G_0^{ref}\left(\frac{c\cos\varphi - \sigma_3'\sin\varphi}{c\cos\varphi + p^{ref}\sin\varphi}\right)^m \tag{2-4}$$

2.3.5.2 Shear Strain ($\gamma_{0.7}$)

Identification of the parameter $\gamma_{0.7}$ at which the secant shear modulus, G_s^{ref}, is reduced to $0.722G_0^{ref}$, requires the use of advanced laboratory devices in order to determine the S-shape curve at very small strain levels. In practice, it may prove to be time-consuming and expensive, and therefore, it is suggested to estimate $\gamma_{0.7}$ by means of typically observed experimental curves. In cohesive materials, $\gamma_{0.7}$ may mostly depend on the plasticity index (PI). To identify the parameter $\gamma_{0.7}$ that reduces the secant shear modulus, G_s^{ref}, to $0.722G_0^{ref}$, modern laboratory instruments are required to detect the S-shape curve at extremely tiny strain levels. To save effort and cost, it is recommended to estimate $\gamma_{0.7}$ using commonly observed experimental curves. In cohesive materials, $\gamma_{0.7}$ may primarily depend on the plasticity index (PI) [47].

2.4 Treatment with Undercut or Removal and Replacement

In Ethiopia, a range of techniques are suggested and used for treating unsuitable or problematic subgrade soil under specific project requirements. Undercutting (removal and replacement), soil stabilization with chemical and mechanical modifiers, and soil stabilization with geotextiles and geogrids are some of the techniques used [50]. Nonetheless, removal and replacement treatments are most frequently employed, particularly in situations where undercut material spoilage areas and suitable replacement materials are abundant [13].

The main objective of the undercut or removal and replacement method of subgrade treatment is to completely eradicate any issues related to problematic soil up to a point where it significantly affects the structure of the pavement [51].

As discussed in the subsections below, various authorities and scholars have different undercut criteria for various kinds of conditions.

However, given their geotechnical characteristics, the researcher was unable to track down undercut criteria developed specifically for unsuitable tropical red soils in the literature; therefore, the assessment uses the currently established criteria.

2.4.1 Undercut Criteria and Depth

2.4.1.1 International Agencys' or Autorities' Practices

The undercut and backfill criteria of the Illinois Department of Transportation's guidelines have been succinctly presented by Chou et al. [51]. The thickness requirements they presented for the backfill (replacement) material are based on a modified design approach developed by the Corps of Engineers. Generally speaking, they recommended the thickness of the granular layer needed for subgrade soils depending on their CBR value.

Remedial action is optional for CBRs between 6 and 8 and required for CBRs below 6, but it is not required for CBRs above 8. For CBR values of 1 through 8, the recommended thicknesses are roughly 58.42, 40.64, 33.02, 30.48, 25.4, 22.86, 22.86, and 22.86 cm.

As thoroughly discussed by Mousavi et al. [45], in order to replace the poor subgrade soils with selected fill, North Carolina developed undercutting criteria. The DCP test must be performed, and a value greater than 38 mm/blow is deemed weak and requires undercutting.

Additionally, as illustrated in Table 2-2, they have provided a thorough synopsis of the guidelines and practices followed by a number of agencies for unsuitable subgrade treatment. On the other hand, Borden et al. [52] proposed undercut criteria based on numerical analyses and prototype scale testing in the laboratory. They assessed the impact of shallow layer shear strength on surface rutting and deep layer stiffness on pumping using axisymmetric and plain strain models. An acceptable rut of less than 1-inch and a performance capacity ratio of 1.5 served as the foundation for the undercut criterion.

Table 2-2 Summary of agencies' practice on treating unsuitable subgrade soils [51]

Agency	**Subgrade treatment**	**Remark**
Pennsylvania DOT	Soils with a CBR below 5 are enhanced either with a cut and backfill or stabilization	CBR is governing parameter
Michigan DOT	45 cm removal and replacement with granular layer	
Indiana DOT	Three options; 60 cm compaction undercut; 40 cm chemical treatment; 30 cm undercut with aggregate replacement.	Based on soil boring data and test on undisturbed samples
Minnesota DOT	Cut and backfill	Based on soil boring data

For both the plain strain condition and the axisymmetric load condition, they offered sets of design charts and graphs. Elastic modulus (E), cohesion (c), angle of internal friction (φ), and performance capacity ratio (ζ) were the required input parameters for the charts. They have also shown that field tests/data like the Dynamic Cone Penetratio Index (DCPI) could be effectively used to assess subgrade soils with the proposed undercut citeria.

Furthermore, Mousavi et al. [45] evaluated the undercut criteria proposed by Borden et al. [52]. They came to the conclusion that, when subjected to fewer than 1000 truck passes, the design charts were consistent with field observations and that they could reliably assess the effectiveness of stabilization measures.

2.4.1.2 Minimum undercut Depth Based on Ethiopian Roads Authority

It is necessary to treat any subgrade or roadbed soils that meet the criteria listed in Table 2-1 as being deemed unsuitable. Unlike international practices, with the exception of expansive or black cotton soils, however, the undercut depth and degree of treatment with alternative techniques have not been specified; instead, they are left up to specific contract requirements and the engineer's guidance [9,11].

On the other hand, expansive or black cotton soils are required to be treated as follows [9]:

- If the finished road level is designed to be less than two meters above natural ground level, the problematic soil must be removed to a minimum depth of 60 centimeters throughout the entire road's width.

- Remove the problematic soil to a depth of 60 cm below ground level beneath the unsurfaced area or shoulder of the road structure if the finished road level is designed to be higher than two meters above natural ground level; or
- Remove the expansive soil to its full depth if it is less than or equal to one meter in depth.

2.4.1.3 Minimum undercut Depth Based on Merewa-Seka road project specification

With only minimal modifications, the treatment criteria and level of treatment provided in subsection 2.4.1.2 remain in effect. That is, the problematic soil must be excavated to a minimum of 100 centimeters throughout the whole width of the road if the final road level is designed to be lower than two meters above the naturally existing ground level.

In addition, it is required to include the following requirements: when the subgrade CBR is less than 5% and the section is classified as S1 or S2, it must be excavated to a minimum depth of 60 cm. Then, S3 or better borrow material - which has a minimum CBR of 5% and a swell index of less than 2% - must be replaced, making sure that the earthwork cover is at least 1 meter high, or at least 60 cm deep (replacement plus an additional 40 cm fill).

As a result, only expansive soils and weak subgrade soils (CBR<5%) are designated for undercut treatment options with appropriate depth, leaving the other unsuitable soils without a specified treatment option. This will typically lead to a conservative and ambiguous approach; that is, all unsuitable soils may be labeled as expansive, and instructions to treat them as such may appear.

Table 1-1 presents the actual test results of the project under study (secondary data), and it could be noted that around 8.7%, or 7.5Km of the subgrade soils are required to be treated using the requirements stated above. However, around 30.7% of the subgrade soils are unsuitable as per requirement despite having a CBR value greater than 5% by considering Atterberg limit values and CBR-Swell values. Such soils are required to be treated by the same standard specification; however, it doesn’t specify the extent or type of treatment to be applied; rather it leaves it open for the engineer to decide.

The actual test results for the project under study are shown in Table 1-1, where it can be seen that 8.7%, or about 7.5 km, of the subgrade soils must be treated in accordance with the aforementioned requirement.

Even though the subgrade soils have a CBR value of more than 5%, about 30.7% of them are not suitable according to [9] requirements when Atterberg limit values and CBR-Swell values are taken into account. These soils need to be treated according to the same standard specification, but it leaves it up to the engineer to determine how much and what kind of treatment should be applied.

Ultimately, determining the proper treatment for each category of unsuitability is crucial. In order to address this gap, this study assesses the proper undercut depth for unsuitable tropical red subgrade soils.

CHAPTER 3
RESEARCH METHODOLOGY

3.1 Introduction

The goal of the study is to determine the undercut depth required to lessen the influence of unsuitable tropical red subgrade soils that take deformation as a primary criterion. Specifically, the distinctive geotechnical properties of these soils were investigated and modeled using a finite element method. This section presents methods for soil sampling, laboratory testing, modeling, and analysis.

An experimental program was used to determine the geotechnical properties of the subgrade soils that were collected (for each of the three categories and replacement material), and PLAXIS 2D was employed to numerically model the subgrade soils underneath flexible pavement. The laboratory tests were carried out in the project laboratory, Jimma University's geotechnical engineering, materials science, and agricultural laboratories, the Ethiopian Construction Design and Supervision Works Corporation's (ECDSWC) geotechnical laboratory, and the Geological Institute of Ethiopia's geochemical laboratory. A personal computer was used for PLAXIS 2D finite element modeling with experimental data input. Subgrade soils were then evaluated for the appropriate undercut depth using the model analysis and experimental data. A few additional relevant data points were obtained for the modeling from the literature.

This study provides valuable insights into the deformation characteristics of tropical red subgrade soils. The findings will contribute to the understanding of essential soil properties and interventions aimed at economical and environmentally friendly utilization of these soils.

3.2 Study area

The study has explored the Merewa-Somodo-Seka and Somodo-Limu Junction spur Design and Build Road Project in Ethiopia, a key link road connecting Addis-Jimma-Metu and Addis-Ambo-Nekempt-Gimbi. The project road, starting in Jimma City and ending at Seka Kebele, will have a total length of 93.95 km, including a 5.06 km spur, meeting the DC5 design standard as per [53].

The project starts at Addis-Ababa-Jimma-Agaro road and ends at Seka Kebele, accessible via standard gravel road from Limu Junction and partially via URRAP road from Merewa to Somodo. The location map of the project area is shown in Figure 3-1.

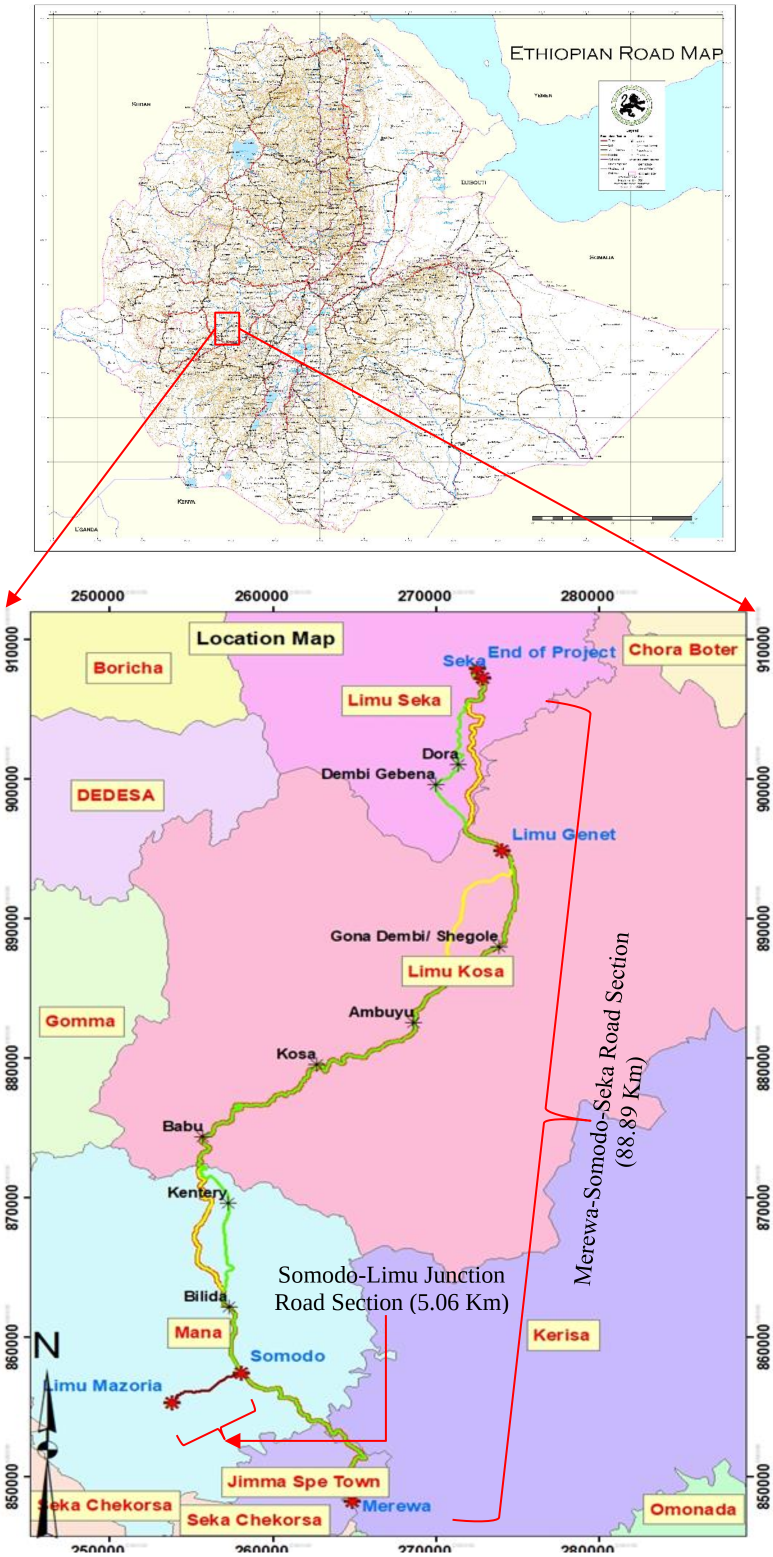

Figure 3-1 The location map of the project [10]

3.2.1 Climate

The climatic condition analysis uses meteorological data from Jimma City Meteorological Station, the closest station to the project region, encompassing 31 years (from 1986 to 2017). As a result, the temperature distribution shown in Figure 3-2 is used to classify the climate of the project area according to the ERA manual [20] recommendation. Therefore, the climate zone of the road project is warm-cool, or Weina Dega. In addition, the maximum and minimum average annual temperature recorded are 27.7°C and 12.2 °C, respectively.

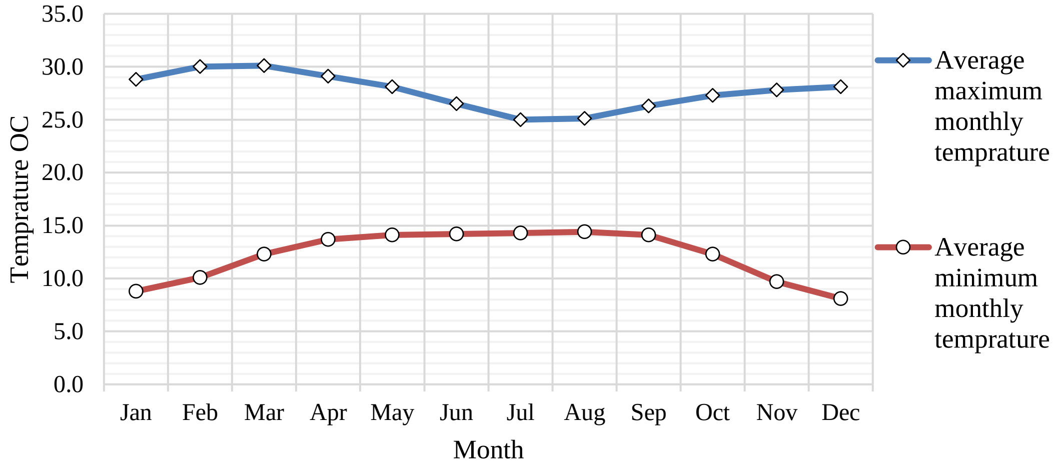

Figure 3-2 Average monthly temperature distribution of the road project [10]

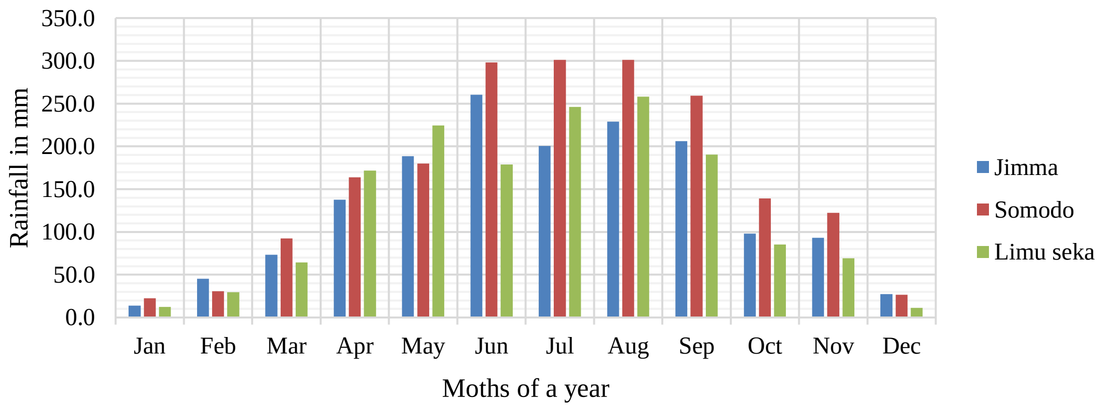

Figure 3-3 Average monthly rainfall distribution of the road project [10]

Figure 3-3 presents rainfall data that was collected for three stations (Jimma, Somodo, and Limu Seka) during a ten-year period from 2010 to 2019. According to these meteorological data, Jimma, Somodo, and Limu Seka have annual average rainfalls of 1573.3 mm, 1936.3 mm, and 1541.7 mm, respectively.

The project area receives rainfall in all months of the year, even during relatively dry seasons, with monthly rainfall below 60 mm extending from December to February. Accordingly, the area could be considered as seasonally wet region.

3.2.2 Geological Condition

The geology of the road project could be obtained from two studies by Haro et al. [55] and Alemu et al. [54] for the Jimma map and the Arjo map, respectively, as shown in Figure 3-4.

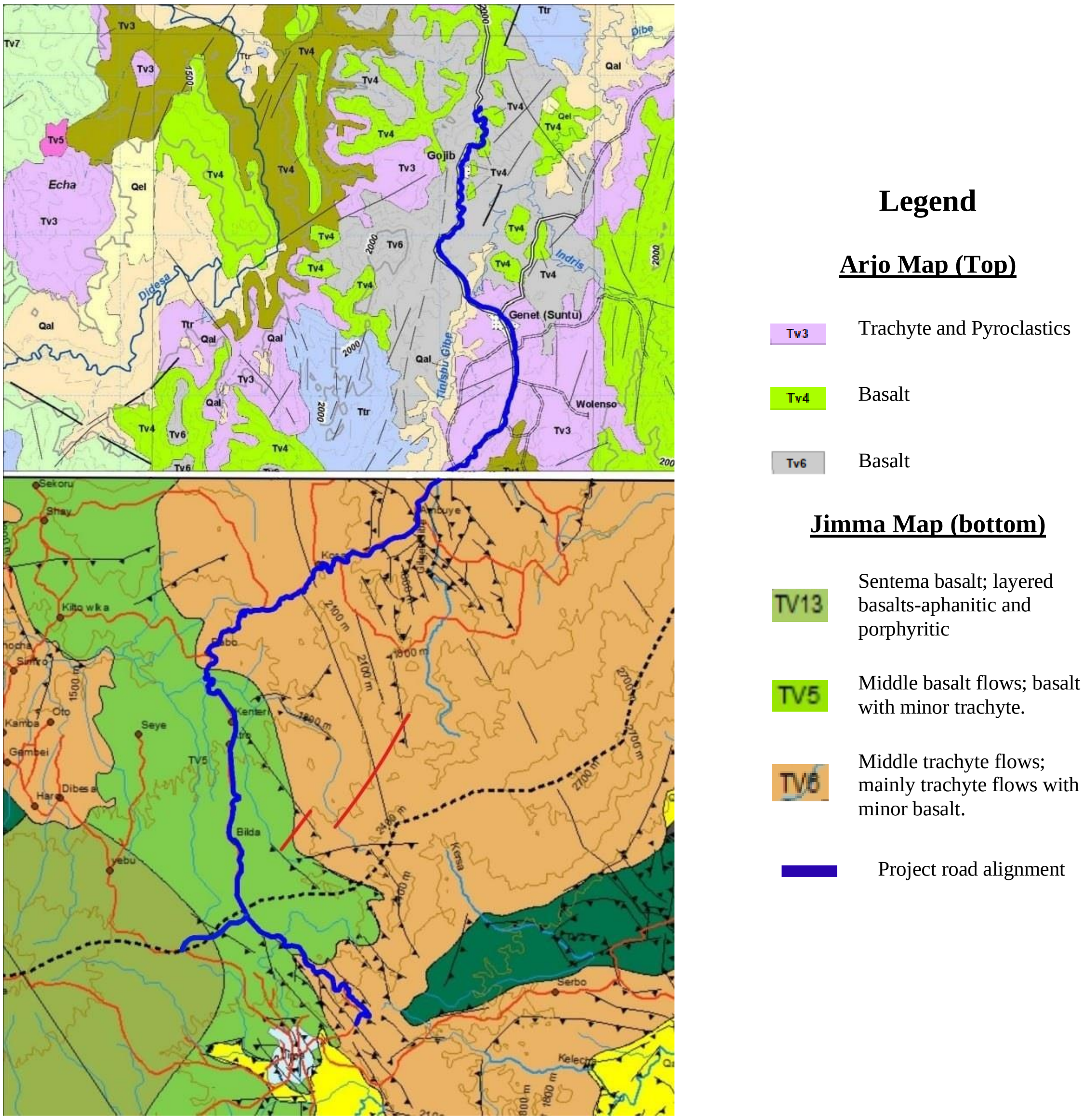

Figure 3-4 Regional geological setting of the project area; at the top Arjo map [54] and at the bottom Jimma map [55]

Further, joining the geological map of the two studies will give better understanding of the general geology of the project area. The project route up to Ambuye Kebele consists of Sentema basalt, Middle trachyte flows (TV6), and Middle basalt flows (TV5). Sentema is composed of porphyritic to aphanitic basalt, while TV6 is light gray, fine to medium grained trachyte [44]. From Amubye Kebele to the end of project, the Arjo geological map reveals Trachyte and pyroclastics (TV3), Basalt (TV4), and Basalt (TV6) lithology. TV3 rock has light gray to grayish black coloration, texture ranging from aphanitic to phyric, and porphyritic characteristics [45]. Generally, the project area is predominated by the weathering products of these rock formations having reddish or reddish-brown soils at the top shallow depth, which are apparently used as subgrades or bedding for the flexible pavement [10,56].

3.3 Research Design

This research study employed a quantitative research design that included field and laboratory testing to investigate the geotechnical properties of unsuitable tropical red subgrade soils for measuring undercut depth in the Merewa-Seka Road Project after modeling it with the finite element method.

PLAXIS 2D software was used to create finite element models, assess soil undercut depth, and evaluate the effectiveness of undercut treatment for unsuitable tropical red subgrade soils.

The research design was implemented in four stages before recommendations and conclusions were given. The first part involved doing a literature research, consultation, and site observation to develop a comprehensive framework for the thesis. The following step was the investigation phase, which included field and laboratory investigations to select the appropriate subgrade categories and acquire information on the geotechnical properties of the subgrade soils for the road project. Furthermore, the geotechnical property data obtained during the research phase was employed in the modeling phase to simulate vehicle loading by modeling subgrade soils on PLAXIS 2D software. Finally, the analysis step used the simulation data and the finite element model to establish the undercut depth. A flow chart to show the research design is presented in Figure 3-5.

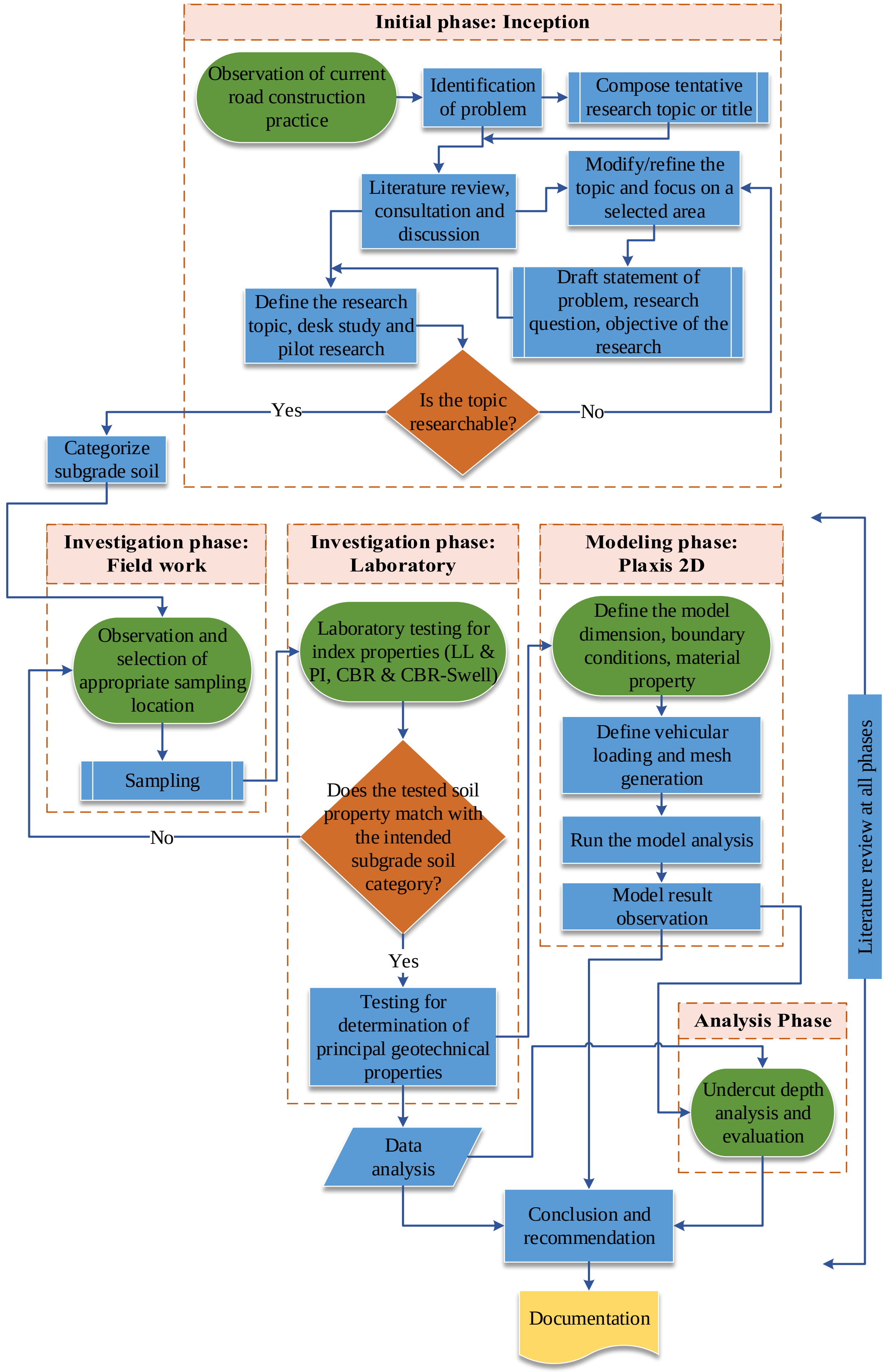

Figure 3-5 Research design

3.4 Sample Collection Methods

3.4.1 Sampling Size and Selection

As assessing the entire population (Unsuitable subgrade soils of the project under study) is beyond the scope of the study, a smaller sample of groups has to be identified, from which the researcher actually collects data. As described in sub-section 3.4.2, three test pits of 1 m depth were excavated for each unsuitable subgrade soil category, and sampling bags were used to collect a representative disturbed soil sample from each pit. Likewise, a representative disturbed sample was acquired from a suitable borrow source to determine replacement material properties. In addition, nine undisturbed samples (i.e., three for each category) using Shelby tubes for testing in a triaxial shear test apparatus and three more for tests in a consolidometer for each unsuitable subgrade soil category.

3.4.2 Sampling Techniques and Procedure

Using secondary data presented in APPENDIX A, the unsuitable subgrade soils cover approximately 40% of the project. Purposive non-probability sampling, therefore, was employed for this study in order to obtain a smaller group that reflects the entire population as well as to create an acceptable category representative to express the behavior of a certain category of population. Accordingly, Table 1-1 presents predetermined characteristics of each subgrade soil category based on existing construction data utilized in this study as criteria for collecting appropriate representative subgrade soil samples.

The sampling procedure was as follows:

1. The unsuitable subgrade soils of the project were categorized into three types, as shown in Table 3-1 (based on Table 1-1, secondary data).

Table 3-1 Unsuitable subgrade categories and replacement material information

Description	Category-1	Category-2	Category-3	Replacement
Required property for the specific group	LL>60 and/or PI>30, CBR ≥ 5 & CBR-Swell ≤ 3	LL>60 and/or PI>30, CBR ≥ 5 & CBR-Swell > 3	LL>60 and/or PI>30, CBR < 5 & CBR-Swell ≤ 3	LL≤60 and PI≤30, CBR ≥ 5 & CBR-Swell ≤ 2
Sampling location	E-261656.208 N-878103.635 2034.937 m a.m.s.l	E-261512.213 N-877686.747 2036.850 m a.m.s.l	E-260872.922 N-877431.074 1985.575 m a.m.s.l	E-257488.552 N-876176.578 1832.767 m a.m.s.l

2. For each unsuitable subgrade soil category, representative test pits with an approximate 1.5 x 1.5 x 1.0 m (length x width x depth) dimension were dug by excavator to obtain both disturbed and undisturbed samples. In addition, suitable material, as shown in Table 3-1 was obtained from the borrow pit to be used as a replacement to backfill the undercut.

Figure 3-6 Test pits; (a) category-1, (b) category-2 and (c) category-3

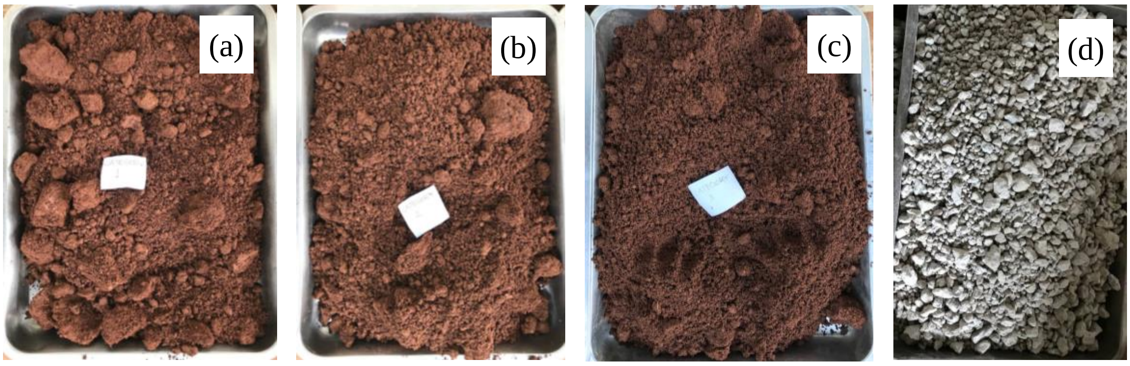

Figure 3-7 Disturbed samples; (a) category-1, (b) category-2, (c) category-3, and (d) replacement material

3. The materials excavated from the test pits (Figure 3-6 and Figure 3-7) were used as disturbed samples for determining geotechnical properties, XRD analysis, and chemical analysis. However, undisturbed soil samples (Figure 3-8) to determine shear strength, compressibility, and in situ density were collected using a Shelby tube sampler as per ASTM D 1587-08 protocol. Shelby tubes of a 42 mm diameter were used for triaxial compression testing, while 110 mm diameter were used for consolidometer testing. The Shelby tubes were driven firmly into the ground using a drop hammer. To prevent causing damage to the soil sample, the driving procedure was controlled and gradual. Lastly, the Shelby tubes with undisturbed soil samples were waxed and labeled before shipment to the testing laboratory, as shown in Figure 3-8.

Figure 3-8 Waxed, labeled, and sealed undisturbed samples; (a) for triaxial compression test, and (b) for consolidometer test

3.5 Study Variables

The research investigated the relationship between the independent variable that the researcher manipulates in order to affect the outcome of the experiment and the dependent variable that represents the outcome of the experiment. The goal is to develop a predictive model that can be used to estimate the undercut depth for each unsuitable subgrade soil category.

3.5.1 Dependent Variables

Deformation is the dependent variable that was observed and measured to determine the effect of the independent variables.

3.5.2 Independent Variables

Properties of subgrade soil category (i.e., Atterberg limits, CBR, swelling potential, and mineralogical composition), undercut and replacement depth, Vehicular load and subgrade soil strength (i.e., elastic modulus or stiffness modulus, cohesion, and friction angle) are the independent variables that were changed in order to see how they affect the observed phenomena.

3.6 Data Collection Methods

A comprehensive soil investigation of the study area, specifically unsuitable subgrade soils assigned to the designated category, has provided the input data for the study.

In this regard, the primary data was obtained from analysis and experimental laboratory and field testing. Additionally, a variety of published and unpublished sources, including books, journals, research reports, and project data (including test results, design data, and investigation reports), were the sources of secondary data collection.

3.6.1 Field Survey

Before starting any field operations, a thorough analysis of the study area's geological setting, the overall design of the roadway, previously completed subgrade soil investigations, and traffic count data were conducted. Once enough data has been gathered, a thorough observation of the roadway's key features, including the type of soil and formation, drainage system, vegetation cover, and state of the current road, is carried out both on foot and by vehicle. Additionally, subgrade soils that matched the required properties for the corresponding subgrade category, as shown in Table 3-1 were identified for sampling along the road project during site observation. Finally, the method described in subsection 3.4.2 was employed to sample the subgrade soils.

3.6.2 Laboratory Test Program

Following ASTM D 421-85 protocol, the disturbed soil samples collected were prepared for testing. After being taken from the field, the soil samples were allowed to air dry at room temperature, and some samples were kept sealed in plastic bags for tests at natural moisture content. The aggregations were pulverized completely in the mortar using a pestle wrapped with rubber. Using the quartering method (using a riffle box), a representative sample of the quantity needed was chosen to carry out the intended tests.

Table 3-2 Standard laboratory test protocols

Test method or determination of	**Standard designation**
Natural moisture content	ASTM D 2216-10
Specific gravity	ASTM D 854-14
Grain size distribution	ASTM D 422-63
Atterberg limits	ASTM D 4318-10
Volumetric shrinkage limit	ASTM D 427-04
Linear shrinkage	BS 1377 Part 2 1990
Maximum dry density and Optimum moisture content	AASHTO T 180-01
California bearing ratio (CBR) and CBR-Swell	AASHTO T 193-99
Triaxial compression test	ASTM D 2850-15
One-dimensional consolidation	ASTM D 2435-04

Test method or determination of	Standard designation
Free swell	IS 2720 Part XL 1977
X-ray diffraction	
Geochemical test	

When drying the subgrade soils, appropriate drying and pre-treatments were applied prior to testing. The test procedure and techniques outlined in Table 3-2 were utilized to determine the essential geotechnical characteristics of each category of unsuitable subgrade soil and replacement material.

3.6.2.1 Natural Moisture Content

To determine the amount of water contained in the natural state of the subgrade soils, two methods were adopted:

- Method 1 – Standard procedure of drying the soil in an oven at 110 ± 5^{o}C to a constant weight and determination of moisture content as per ASTM D 2216-10.
- Method 2 – is recommended for tropical soils that are sensitive to the standard oven drying, which shall be dried at 50 ^{o}C with a maximum relative humidity of 30% to avoid the loss of the molecular water [57].

Duplicate samples were prepared for each method and each subgrade category. Then, the values of the two methods were compared to assess the drying effect on the project's soils and select the appropriate moisture content determination method. According to Blight et al. [57], a significant difference is 4 – 6 % of the water content obtained by oven-drying at 105^{o}C.

3.6.2.2 Specific Gravity

The boiling method (using pycnometer) was used to determine the mass ratio of a unit volume of soil solids to the mass of the same volume of gas-free distilled water at 20°C for oven-dried duplicate specimens of each subgrade category in accordance with ASTM standards. The test data was utilized to calculate soil phase relationships such as void ratio and degree of saturation, as well as hydrometer analysis.

3.6.2.3 Grain Size Distribution

To determine the particle size distribution of the subgrade soils, two methods were used:

- Method 1 – standard wet sieve analysis for particle sizes larger than 75 µm (retained on the No. 200 sieve).
- Method 2 – hydrometer analysis for particle sizes smaller than 75 µm.

Duplicate samples were prepared for each method and each subgrade category (including replacement material). The data from the two methods were then merged to represent all particle sizes, including microparticles.

3.6.2.4 Atterberg Limits

To determine the liquid limit of the subgrade soils, two methods were used:

- Method 1 – is applying the conventional procedure of determining the liquid limit of subgrade soils using a hand-operated liquid limit device as per ASTM D 4318-10.
- Method 2 – is recommended for tropical soils that are sensitive to the duration of mixing, which shall be mixed for a maximum of 5 minutes to avoid the application of greater energy to the soil prior to testing [17,57]. The specimens were tested immediately upon receiving without any means of drying, and the mixing period was under five minutes. Additionally, for every test water content point, fresh soil specimens have been used.

Duplicate samples were prepared for each method and each subgrade category. Then, the values of the two methods were compared to assess the mixing time effect on the project's soils and select the appropriate Atterberg limit determination method. A considerable difference (>5% of the liquid limit determined from a test on a specimen mixed for 5 minutes) between the two methods suggests clay particle disaggregation in the soil [58]. Further, in order to assess the expansion potential, the linear shrinkage and shrinkage limit were determined as per BS and ASTM standards, respectively. AASHTO and USCS engineering classifications were used and the activity of clays in subgrades was assessed using Skempton's equation (3-1) [59].

$$A = \frac{PI}{Percent\ passing\ 0.002 - mm\ sieve} \tag{3-1}$$

where A = activity, which is the slope of the line correlating PI and % finer than 0.002 mm.

3.6.2.5 Moisture-Density Relationship

A modified compaction effort according to AASHTO T 180-01 (Method A & D) was utilized to establish the optimum moisture content (OMC) and maximum dry density (MDD) in order to study compaction characteristics and determine the laboratory CBR value.

3.6.2.6 California Bearing Ratio (CBR)

To assess the strength of subgrade soils, a CBR test was conducted on all subgrade and replacement soil specimens compacted (at 10, 30, and 60 blows per layer for five layers) and soaked for four days. Swelling was also measured using a dial gauge up to the end of the soaking period.

3.6.2.7 Triaxial Compression Test

The unconsolidated-undrained (UU) triaxial compression test was used to determine the shear strength parameters and secant stiffness modulus. Two sets of testing were carried out.

- Set 1 – UU-triaxial test was performed on undisturbed-unsaturated specimens at the geotechnical laboratory of ECDSWC. The test was conducted at the natural moisture content. However, for replacement material, remolded specimens were used and tested at optimum moisture content.
- Set 2 – UU-triaxial test was done on remolded-unsaturated specimens. The test was carried out at the saturation moisture content, and the moisture content at 100% saturation was determined using phase relationships.

3.6.2.8 One-dimensional Consolidation Test

To determine void ratio, compression/swelling indices, and tangent stiffness modulus, a one-dimensional consolidation test was carried out on undisturbed soil specimens of each subgrade soil (at the geotechnical laboratory of ECDSWC).

Further, swelling pressure was also measured using the loading-after-wetting method as per ASTM D 4546-14 in conjunction with the consolidation test.

3.6.2.9 Free Swell

To study the swelling properties, free swell test as per IS 2720 Part XL 1977 was conducted on oven dried specimens for all subgrade soils.

3.6.2.10 X-ray diffraction (XRD) Analysis

An XRD-7000 X-ray diffractometer, which is available at JiT's Material Science Laboratory, was used to identify the minerals present in each subgrade soil. Bragg-Brentano geometry is used by this device. The wavelength and voltage of the copper Ka X-ray source are 1.540598 Å and 30 kV, respectively. The filament emission is 25 mA. 2-theta angles between 10° and 80° were used to scan the samples. The soil specimens were sieved through a 0.075-mm screen prior to testing.

Mineral identification was done using the MACTH software in a semi-automated manner after obtaining the raw 2-theta and intensity data from the X-ray diffractometer.

3.6.2.11 Geochemical tests

In order to identify the degree of laterization by determining the silica-sesquioxide ratio and to study the major and minor oxides present, chemical tests were conducted at the geochemical laboratory of Geological Institute of Ethiopia.

Lyon Associates Inc. [17] states that the silica-sesquioxide ratio (S-S ratio) or, $SiO_2/(Fe_2O_3 + Al_2O_3)$, could be used to determine the degree of laterization. As a result, S-S ratios has been computed with data from chemical tests. S-S ratios of less than 1.33 are considered true laterites, those between 1.33 and 2.0 are lateritic soils, and those larger than 2.0 are non-lateritic tropically weathered soils.

3.6.3 In-situ Test Program

The test procedure and techniques outlined in Table 3-3 were utilized to determine the additional geotechnical characteristics of each category of unsuitable subgrade soil.

Table 3-3 Standard field test protocols

Test method or determination of	Standard designation
Dynamic cone penetrometer (DCP)	ERA PDM 2013
Field density (core cutter method)	IS 2720 Part XXIX 1975

3.6.3.1 Dynamic Cone Penetrometer (DCP) Test

A dynamic cone penetrometer (DCP) test was used to evaluate in situ strength and investigate the properties of subgrade soils under the formation level. In addition, the DCP data was utilized to validate the undercutting model and determine the suitability of in situ subgrade soil. An 8-kg dropping hammer was used to drive the cone into the ground to a depth of 1 meter.

3.6.3.2 Field Density Test

The core cutting procedure described in IS 2720 Part XXIX 1975 was used to determine in-situ density for modeling and preparing remolded specimens. The core cutter was hammered into the ground using a falling hammer. After determining the filed density, the unit weights were calculated using phase relationships.

3.7 Data Processing Methods

Succeeding the collection of adequate data on the geotechnical properties of the unsuitable subgrade soils for each category, the information was processed and analyzed to come up with conclusive approach. The following subsections provide a description of the procedure used to process and analyze the collected data.

3.7.1 Numerical Model

Using PLAXIS 2D version 8.6 software, FEM modeling of unsuitable subgrade soils was performed. Several approaches were used, as detailed in the section below, to shorten computing times without affecting the quality of analysis.

3.7.1.1 Materials Model

As shown in Table 3-4, the subgrade soils were modeled using the hardening-soil model with small-strain stiffness in order to obtain a more accurate deformation analysis; on the other hand, the replacement material, pavement materials up to the base course, and asphalt concrete layers were modeled using the Mohor-coulomb, linear-elastic, and hardening soil models, respectively.

Table 3-4 Flexible pavement materials and material models

Item Number	Materials	Material Model
1	Asphalt concrete	Linear-elastic
2	Base course	Mohr-Coulomb
3	Sub-base	Mohr-Coulomb
4	Capping	Mohr-Coulomb
5	Subgrade	Hardening-soil small
6	Replacement material	Hardening-soil

The flexible pavement composition is adopted from the project road design data as shown in Figure 3-10. The unit weights used in the models were also obtained from actual project data. In addition, the standard material properties given in the ERA manual [12] were adopted for elastic modulus and passion’s ratio parameters. Shear strength parameters, on the other hand, were obtained using the USCS correlation given by [60,61] for base course, subbase, and capping with classification of GW, GC-CL, and GM-CL, respectively.

Angle of dilatancy, ψ, was determined using reasonable approximation, $\psi = \varphi - 30°$, given by Obrzud and Andrzej [47]. As a result, the material property used to model flexible pavement layers is as presented in Table 4-18. Data from test programs outlined in subsections 3.6.2 and 3.6.3 were utilized to determine the model parameters of the unsuitable subgrade soil and replacement material, which would be used as input in the finite element model. In APPENDIX C the analysis and procedure used to determine the material model parameters are described.

3.7.1.2 Loading Model (Cyclic loading)

In Ethiopia, as per the ERA manual [12], for each class of vehicle, the initial traffic volume derived from traffic count data will be converted to cumulative traffic volumes for the duration of the design period. The number of equivalent standard axles (ESA) that correspond to the total vehicular loading will then be calculated from the cumulative traffic volumes. Equivalent standard axles for two tires on a single axle are units of 80 kN. However, to simplify the analysis in this study, a moving standard axle with an 80 kN load and a single tire with a 30 cm contact diameter was used to simulate vehicle loads.

According to the literature, a variety of formulas and assumptions are employed to simulate pavement loading generated by moving loads [42]. However, it is more common to represent stress pulses as triangle loading or haversine loading with six sub-steps [34,62]. Triangular load intensity, which requires only two sub-steps, was used in this study to save computation time. The load intensity was computed by using equation (3-2) given by Huang [42].

$$L(t) = q sin^2\left(\frac{\pi}{2} + \frac{\pi t}{d}\right) \tag{3-2}$$

Where, $L(t)$ is the load function with respect to time, q is the load intensity of the tire in kPa, t is time in seconds, and d is duration of the load in seconds. d depends on the vehicle speed s (m/s) and the tire contact radius a (m). As a result, d was calculated using equation (3-3) [42]. In addition, F, the frequency of the load was computed by the inverse of d, and the tire pressure, q, was calculated by dividing the standard axle load by the tire area, A.

$$d = \frac{12a}{s} \tag{3-3}$$

The design vehicle speed of the road project ranges from 50 to 85 km/hr, depending on the terrain classification and level of urbanization [63,64]. In their investigation on the impact of vehicle speed, Sebaaly and Tabatabaee [65] found that the most significant range of vehicle speed is 32 to 56 km/hr. Accordingly, load modeling in this study was performed at an average speed of 40 km/hr.

Table 3-5 Load intensity function variables

Parameter	a	A	s	d	F	q
Value	0.150	0.0707	11.111	0.162	6.173	565.88
Unit	m	m^2	m/s	S	Hz	kPa

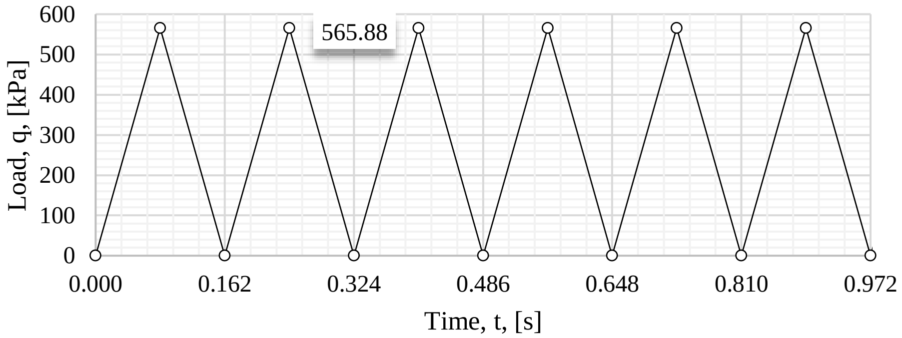

Figure 3-9 Multiple dynamic stress pulses

The cyclic load was applied as a circular distributed load with a radius of 0.15m at the top left corner, as shown in Figure 3-10.

3.7.1.3 Geometric Model

A two-dimensional axisymmetric model having dimensions as shown in Figure 3-10 was used for the numerical solution of the flexible pavement structure and subgrade. For every unsuitable subgrade category, a distinct deformation analysis was performed using the same geometry. The numerical model is 15 m high and 15 m wide. This would suggest that the model size in both directions is set to around 100 times the loading radius. These are ideal dimensions for minimizing the effects of boundary conditions, as recommended by earlier studies. Duncan et al. [66] demonstrated that model thickness and width had a substantial influence on the magnitude of deflections and proposed a minimum of 50 times the loading radius and 12 times the loading radius for the height and width of the flexible pavement model, respectively. Huang [42] adopted the same model dimension. In a more recent study, Karadag et al. [34] employed 100 times the loading diameter.

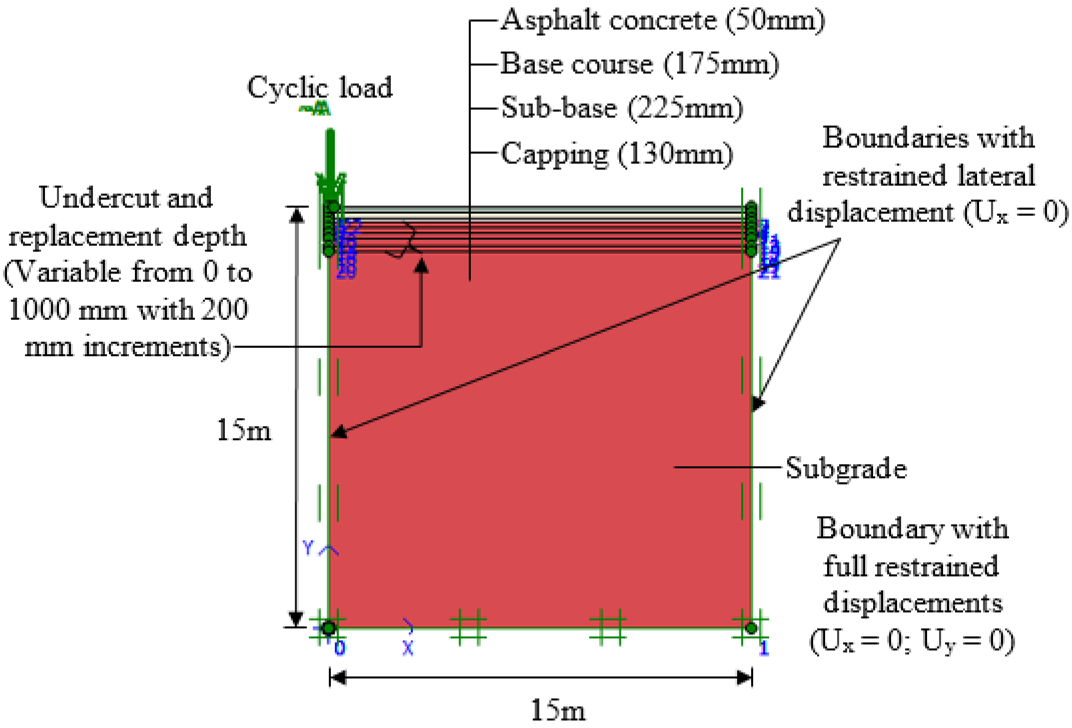

Figure 3-10 Geometry of finite element model

3.7.1.4 Mesh Generation and Boundary Condition

Fifteen node triangular elements were used to generate mesh. Boundary conditions were established using standard fixity as shown in Figure 3-10. There were a total of 1267 nodes and 149 elements in the model. To get reliable results, finer elements were introduced to the model near the upper left corner, where the wheel load was applied. To save calculation time, however, coarser elements were applied towards the other edges of the model.

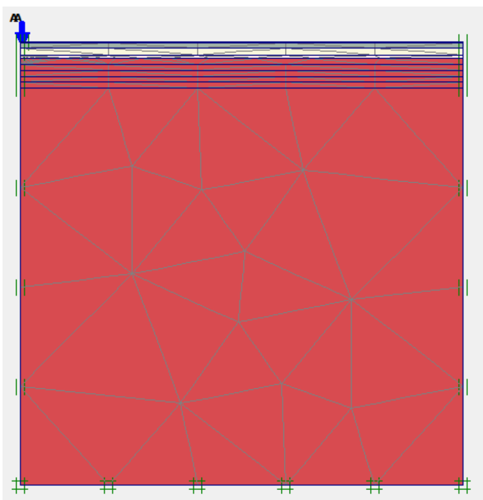

Figure 3-11 Generated mesh for the model

3.7.1.5 Model Analysis or Calculation

Dynamic analysis calculation type was used in this study to analyze the models established for each subgrade category. The cyclic load was activated by inputting 105 load cycles or 17 second load intensity data, as shown in Figure 3-9. The node chosen for deformation analysis was the one in the upper left corner, which was the center of the applied cyclic load.

3.7.2 Undercut Depth Analysis

The FEM study included modeling and analyzing unsuitable subgrade soil removal and replacement depth (referred to as undercutting depth). Hence, defining the minimum single-layer thickness of undercut and replacement is important, as it has a significant effect on the construction methods and finished work quality.

According to the ERA standard [9], fill or pavement lift thicknesses should not be less than 100 mm or greater than 200 mm. This study took the recommendation into consideration and used a minimum of 200 mm single-layer thickness for undercutting and replacement. Furthermore, only five layers, or 1000 mm, of undercutting depths were considered for the deformation analysis. In order to replace the unsuitable subgrade materials used in the FEM analysis, a suitable replacement material was used. Hence, the deformation analysis was performed on models with no undercutting (soil in its natural state) and with undercutting (after replacement by suitable material) at depths of 200 mm, 400 mm, 600 mm, 800mm, and 1000 mm.

To obtain the ultimate deformation, the 105 load cycles, or 17 second dynamic load analysis data, were projected onto the designed traffic load of the project, which is 4.5 million ESA [56]. Furthermore, the extent of undercutting depth was established using a maximum 1-inch or 25-mm total deformation criteria stated in the project's contract document. Thus, the ultimate deformation data was evaluated against the maximum 25 mm deformation criteria to determine an appropriate undercut depth for each subgrade category.

CHAPTER 4
RESULT AND DISCUSSION

In this study, appropriate geotechnical investigation, numerical modeling, and undercut depth treatment analysis were made for the unsuitable tropical red subgrade soils of the Merewa-Seka road project. This chapter presents the findings of the test programs in the laboratory and in the field, together with model parameters, numerical simulation results, and observation-based discussions. The detailed procedures for the geotechnical tests and the analysis of the necessary parameters for modeling are presented in APPENDIX B, APPENDIX C, and APPENDIX D.

4.1 Results of Test Programs (Geotechnical Properties)

Results derived from standard test protocols described in Table 3-2 and Table 3-3 are presented and discussed in the subsections below.

4.1.1 Natural Moisture Content

The effects of drying on sample preparation and testing have been studied with natural moisture content. As showed in Table 4-1, the moisture content differences between the two investigated methods (at 110 ^{o}C and 50 ^{o}C) are less than 4%, indicating that they are not significant. Additionally, it is noted that drying of all the subgrade soils using the standard method has no effect on structural water that may result in irreversible changes during drying. This is consistent with previous findings on similar soils [14,58]. As a result, the conventional moisture content determination approach (at 110 ^{o}C) is deemed appropriate and used in this study.

Table 4-1 Natural moisture content of each subgrade soil

	Natural moisture content using Method-1 (at 110 ^{o}C) [%]	Natural moisture content using Method-2 (at 50 ^{o}C) [%]	Moisture content difference [%]	Observation
Category-1	38.38	34.98	3.40	Insignificant
Category-2	38.78	36.21	2.57	Insignificant
Category-3	39.56	36.94	2.63	Insignificant

4.1.2 Specific Gravity

The specific gravity of the subgrade soils investigated ranged from 2.588 to 2.723, as illustrated in Table 4-2. Category-1 and 3 had specific gravity values larger than 2.6, which is consistent with earlier findings [15,27]. The higher result is due to the fact that the soil samples are rich in iron, as revealed in Table 4-14 of the geochemical study. According to [67], specific gravity of laterite soils is between 2.55 and 4.6.

Table 4-2 Specific gravity of each subgrade soil

	Category-1	Category-2	Category-3
Specific Gravity	2.723	2.588	2.620

4.1.3 Grain Size Distribution

The particle size distributions of the subgrade soils illustrated in Figure 4-1 were obtained using a combination of wet sieving and hydrometer analysis, whereas replacement material was determined only by wet sieving.

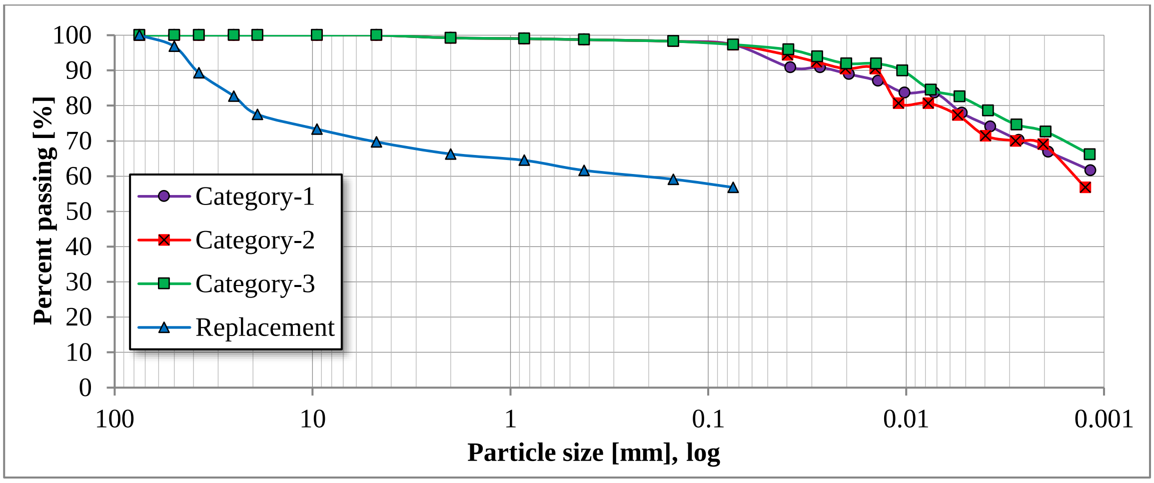

Figure 4-1 Combined grain size distribution curve for subgrade soils and replacement material

Furthermore, the fraction of each grain size has been determined and shown in Table 4-3. All subgrade soils contain a large proportion of clay, which exceeds 50%. These results support the findings of Teferi [15]. On the other hand, despite having a higher proportion of gravel and sand, the replacement material contains higher amount of silt and clay.

Table 4-3 Proportion of gravel, sand, silt and clay in each subgrade soil and replacement material

	Category-1	Category-2	Category-3	Replacement
Gravel (75 mm – 2mm) [%]	0.8	1.2	0.51	33.7
Sand (2 mm – 75 μm) [%]	1.9	2.6	1.03	9.5
Silt (75 μm – 2 μm) [%]	30.4	28.3	25.8	56.8
Clay (< 2 μm) [%]	66.9	69.0	72.6	

4.1.4 Atterberg limits

As shown in Table 4-4, using method-1 (standard), the liquid limit values for all subgrade categories are above 60%, defying the minimum requirement stipulated in the ERA standard [9].

Table 4-4 Atterberg limit values determined using method-1

	Category-1	Category-2	Category-3	Replacement
Liquid limit [%]	65	65	68	45
Plastic limit [%]	48	46	47	33
Plasticity index [%]	17	19	21	12
Shrinkage limit [%]	22	19	27	
Linear shrinkage [%]	16	15	16	7

These results were compared with liquid limit values determined using method-2 (recommended for tropical soils), as presented in Table 4-5. In addition, it was observed that the shrinkage limit and linear shrinkage values are higher as they are dependent on the liquid limit.

Table 4-5 Comparison of liquid limit value determination methods

	Liquid limit using method-1 (standard) [%]	Liquid limit using method-2 (recommended for tropical soils) [%]	Difference [%]	Observation
Category-1	65	64	1	Insignificant
Category-2	65	59	6	Significant
Category-3	68	62	6	Significant

Table 4-5 demonstrates that mixing duration and pretreatment significantly influence category-2 and category-3 subgrade soils, while not affecting category-1.

The differences between method-1 and method-2 are in agreement with earlier investigations conducted on comparable soils in various locations of Ethiopia [14,58]. Table 4-6 provides the recalculated and retested Atterberg limit values obtained using both methods for the respective subgrade soils.

Table 4-6 Atterberg limit values determined using method-2

	Category-1	Category-2	Category-3
Liquid limit [%]	64	59	62
Plastic limit [%]	48	46	47
Plasticity index [%]	16	13	15
Linear shrinkage [%]	16	13	14

Table 4-6 shows the Atterberg limits of category-2 and category-3 subgrade soils improved when method-2 was used; in fact, category-2 has satisfied the ERA standard requirements [9]. As a result, for this study, the subgrade soils were considered sensitive to mixing time, remolding, and pre-drying during liquid limit testing, and recommended procedures for tropical soils were followed.

4.1.5 Engineering Classification

Table 4-7, Figure 4-2, and Figure 4-3 show the soil classification based on Atterberg limits and grain sizes for subgrade soils and replacement material. A-7-5 materials are generally regarded as poor subgrade materials and very poor if the group index is more than 20. Further, as per the ERA manual [12], MH materials are valued as poor subgrades. On the other hand, all of the subgrade categories were observed to be inactive according to Skempton's recommendation, which specifies that soils are inactive if A is less than 0.75, normal if A is between 0.75 and 1.4, and active if A is greater than 1.4.

Table 4-7 Engineering classification based on AASHTO, USCS, and clay activity

	Category-1		Category-2		Category-3		Replacement
	method-1	method-2	method-1	method-2	method-1	method-2	
AASHTO	A-7-5 (26)	A-7-5 (25)	A-7-5 (27)	A-7-5 (21)	A-7-5 (30)	A-7-5 (24)	A-7-5 (6)
USCS	MH	MH	MH	MH	MH	MH	ML
Activity (A)	0.25	0.24	0.27	0.19	0.28	0.21	

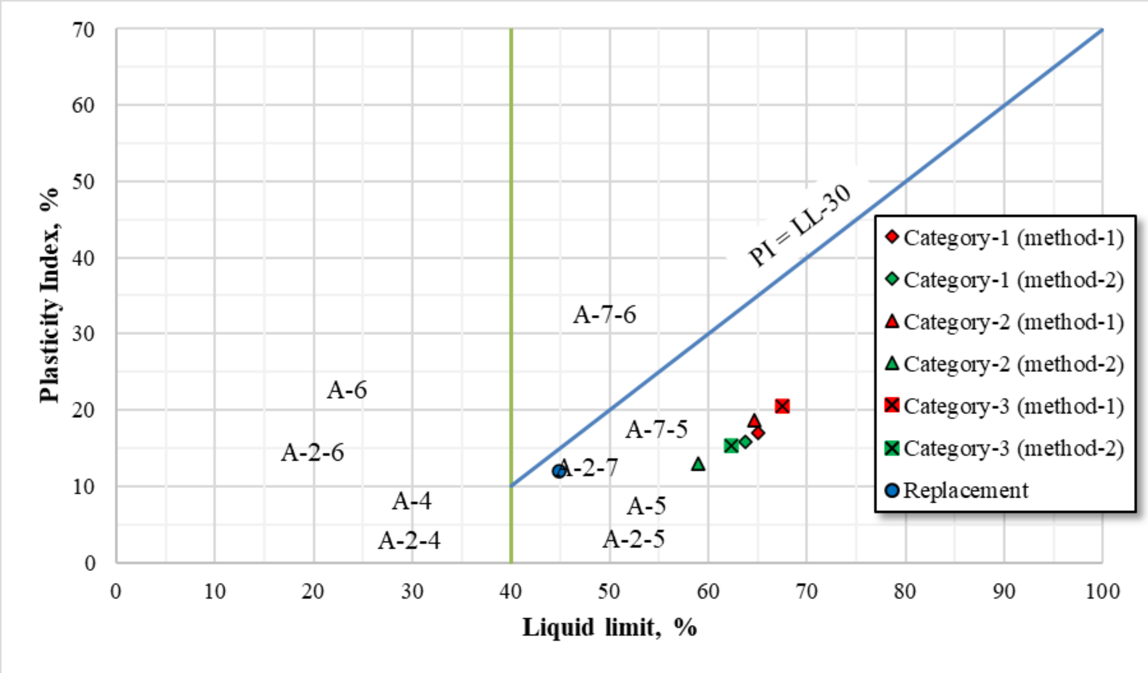

Figure 4-2 Classification according to AASHTO

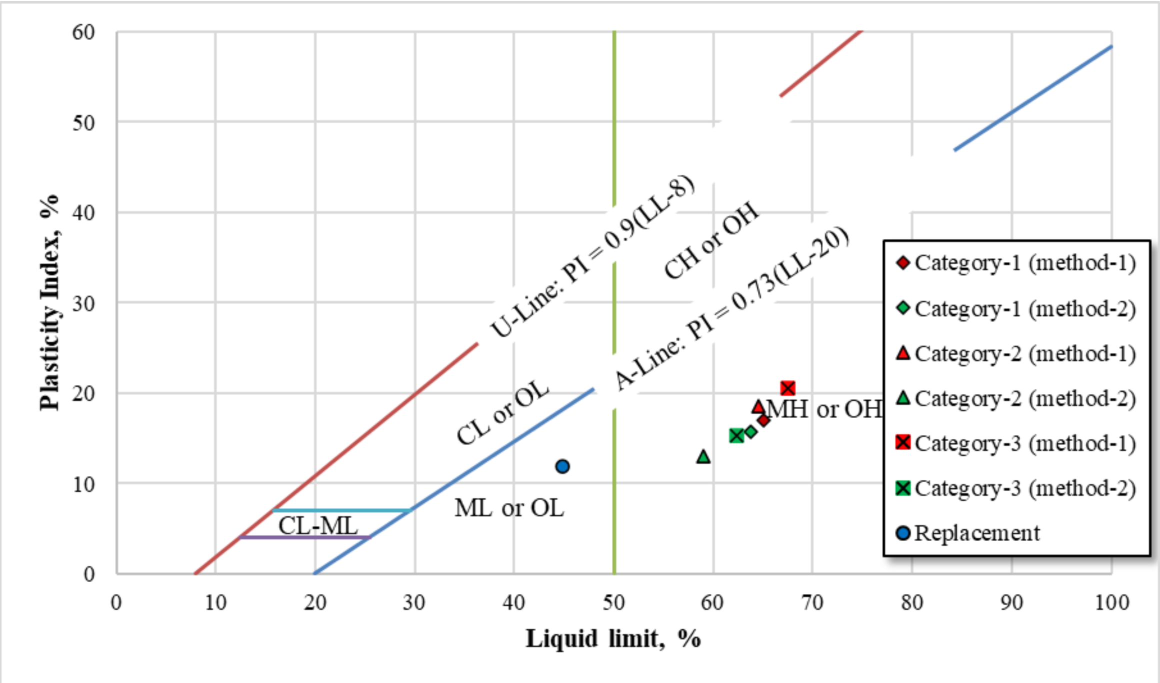

Figure 4-3 Classification according to USCS (plasticity chart)

It should be noted, however, that the goal of a soil classification system is to indicate a soil's characteristics and provide information on how it will behave as a construction material. It should not be utilized as a goal in itself; crucial geotechnical properties like as strength and compressibility must also be evaluated in order to reach a conclusion.

On the other hand, Wesely [19] emphasized that the classification of residual soils should be based on their location above or below the A-line of the plasticity chart (USCS), which is more important than liquid limit value assessment. Further, Wesely [68] suggested that soils that plot well below the A-line generally have good engineering properties.

4.1.6 Moisture-Density Relationship

Table 4-8 displays the OMC and MDD of the subgrade soils and replacement material determined with the modified compaction effort. The MDD ranged from 1424 to 1480 Kg/m^3, whereas the OMC varied from 30 to 31.2%. The MDD values are comparable with those of Muhammed et al. [27], which ranged from 1330 to 1540 Kg/m^3; however, the OMC results are slightly lower than reported, which varied between 32 and 36%.

Table 4-8 OMC and MDD data

	Category-1	Category-2	Category-3	Replacement
OMC [%]	31.2	30	30.7	13.2
MDD [Kg/m^3]	1480	1454	1424	1798

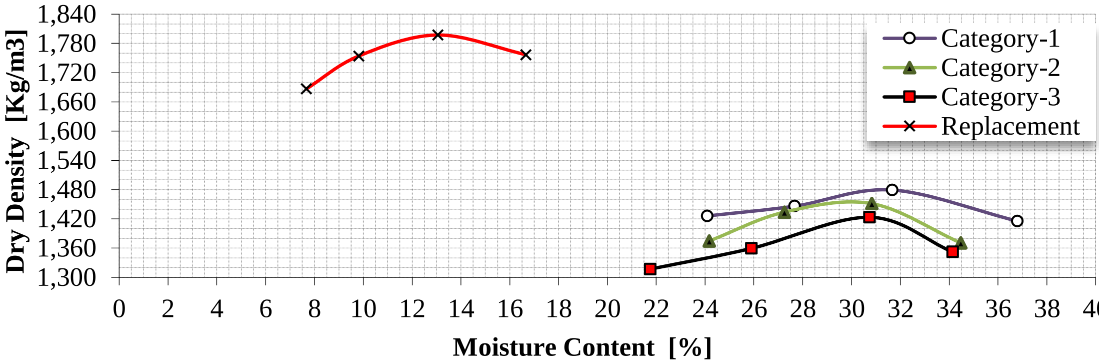

Figure 4-4 Moisture-Density relationship curves

4.1.7 California Bearing Ratio (CBR)

CBR values are most frequently applied to the assessment of subgrade strength. Table 4-9 presents the CBR and CBR-Swell values for each subgrade category and replacement material that were investigated. The results adhere to the already established average values for the corresponding subgrade category shown in Table 1-1. The CBR value of Category-3 exceeds the minimum requirement of the ERA standard [9] and the project specification for subgrade soil, which is 5% or higher. Whereas, Category-1 and 2 have acceptable CBR values for the required subgrade class. This increased strength is attributed to their self-hardening nature, as described by [20].

On the other hand, the CBR-Swell values for Category-2 and 3 surpass the ERA standard's maximum specification of 3%, necessitating treatment prior to use as a subgrade.

Table 4-9 CBR and CBR-Swell data

	Category-1	Category-2	Category-3	Replacement
CBR at 95 % MDD [%]	10.2	7.2	2.5	18
Swell at 95 % MDD [%]	1.9	4.5	6.3	0.9

4.1.8 Shear Strength Parameters

Table 4-10 presents the results of undrained triaxial tests that were used to examine the shear strength characteristics at natural moisture content (set-1) for subgrade soils, at OMC on remolded specimens (set-1) for replacement material, and at saturation moisture content (set-2) for replacement material. All subgrade soils have very high cohesion in their natural state, which is possibly attributed to their self-hardening characteristic, as stated by [20]. However, a subsequent study on remolded specimens with water added to the saturation level demonstrated a considerable loss in cohesion. These findings support the findings of [69], which showed that cohesion decreased from 144.65 kPa to 82.12 kPa as moisture increased up to saturation.

Table 4-10 Shear strength data for undisturbed and remolded specimens

	Category-1		Category-2		Category-3		Replacement
	Set 1[a]	Set 2[b]	Set 1[a]	Set 2[b]	Set 1[a]	Set 2[b]	Set 1[c]
C [kPa]	247.53	78.30	74.08	40.71	116.29	32.64	92.20
φ [Degree]	3.98	17.11	10.71	12.11	3.45	10.56	21.20
Moisture content [%]	38.38	46.64	38.78	55.14	39.56	55.04	19.4

[a] Undisturbed specimen (ECDSWC), [b] Remolded specimen, [c] Remolded specimen (ECDSWC)

4.1.9 Parameters Determined Using One-Dimensional Consolidation Test

Table 4-11 presents one-dimensional consolidation test results conducted on undisturbed specimens of each subgrade category. The subgrade soils were observed to have higher initial undisturbed void ratios, ranging between 1.27 and 1.442. This is in agreement with the value reported by Muhammed et al. [27], which is 1.29 for Jimma laterite soil. On the other hand, the swelling pressure for all subgrade soils is investigated to be below 11 kPa, indicating a low degree of expansion. As per Chen [70], swelling pressure of 48 kPa is a low degree of expansion.

Table 4-11 One-dimensional consolidation test data for undisturbed specimens

	Category-1	Category-2	Category-3
Pre-consolidation pressure [kPa]	240	230	118
Void ratio	1.27	1.427	1.442
Compression index	0.154	0.23	0.2
Swelling index	0.04	0.042	0.043
Swelling pressure [kPa]	Nil	3	11

4.1.10 Free Swell

Free swell test on oven dried speciemens for all subgrade soils was conducted to assess the swelling potential and the results were as shown in Table 4-12. The findings are consistent with the values published by Dilla et al. [14] for similar soils and lower than the values reported by Muhammed et al. [27] for Jimma soils. A free swell index value of 50% or below indicates that the soil has low expansion nature (as per IS 1498 1970).

Table 4-12 Free swell index test result

	Category-1	Category-2	Category-3
Free swell index [%]	15.0	18.9	20.9

4.1.11 Mineral Identification (XRD)

XRD analysis was performed on all subgrade soils and replacement material to determine the minerals present. As illustrated in Figure 4-5, quartz was found to be the most dominant mineral, followed by chloritoid, heulandite, kaolin, and anatase.

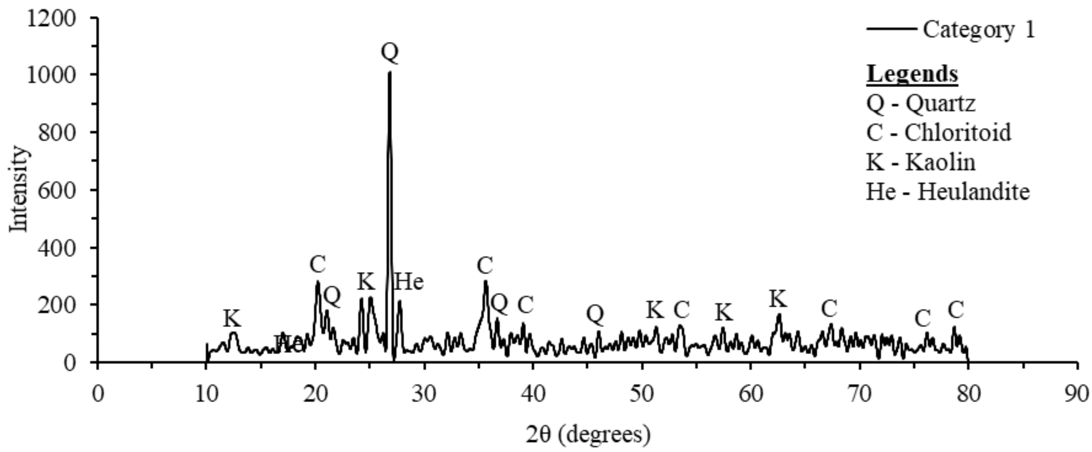

(a)

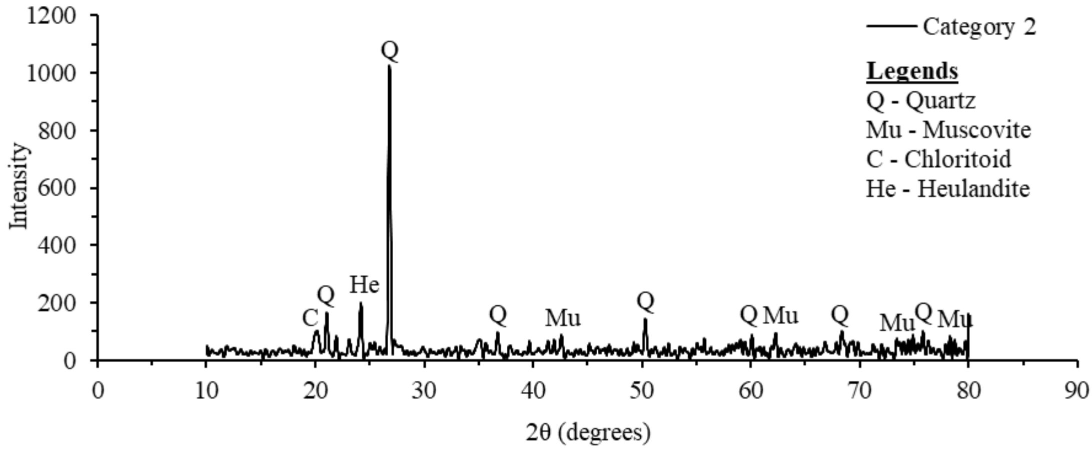

(b)

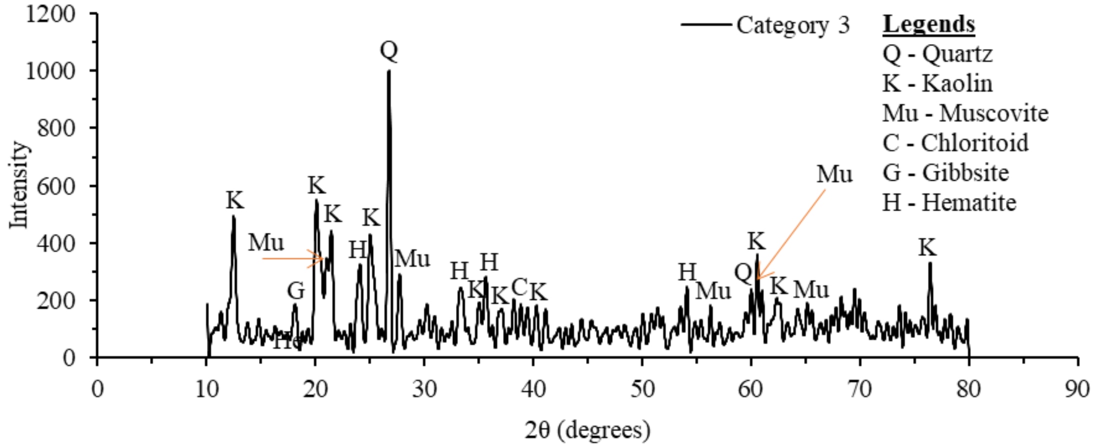

(c)

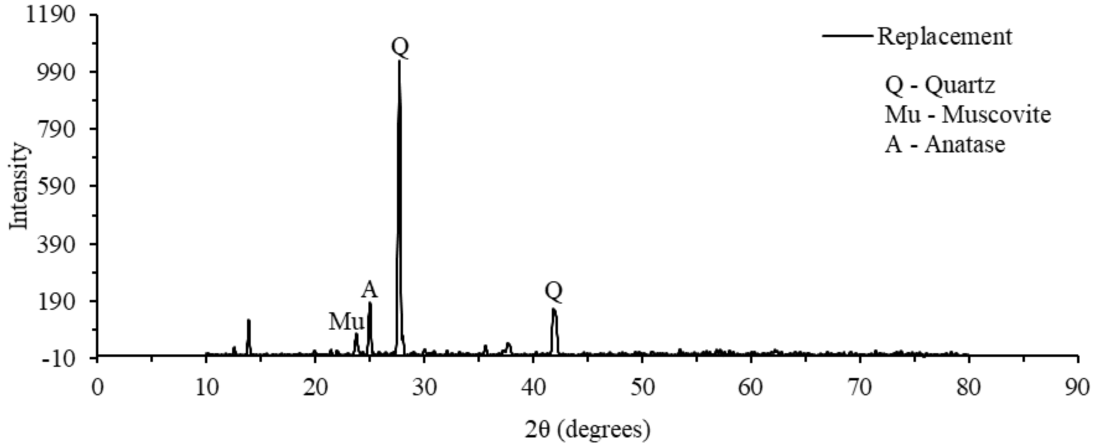

(d)

Figure 4-5 XRD pattern and minerals identified, (a) for category-1, (b) for category-2, (c) for category-3, and (d) for replacement material

Table 4-13 shows the most dominant minerals with the highest XRD peak for subgrade soils and replacement material. The primary minerals identified, quartz, kaolin, and muscovite, are inactive minerals, according to Skempton [59].

In addition, as reported by Kumari and Mohan [71], kaolinite, mica (muscovite), and chlorite have low or no swelling potential due to their interlayer space. On the other hand, problematic minerals with significant swelling potential, such as montmorillonite, bentonite, and vermiculite, were not found in any of the subgrade soils.

Table 4-13 The three strongest peaks of XRD data

	No.	Mineral	Intensity [Count per second]	2θ [Degree]	d-spacing [Å]
Category-1	1	Quartz	1000.00	26.82	3.32
	2	Chloritoid	255.68	35.66	2.52
	3	Chloritoid	248.17	20.24	4.38
Category-2	1	Quartz low	1000.00	26.82	3.32
	2	Heulandite	187.20	24.20	3.67
	3	Quartz low	149.30	21.06	4.22
Category-3	1	Quartz	1000.00	26.75	3.33
	2	Kaolin	564.81	20.09	4.42
	3	Kaolin	504.44	12.47	7.09
Replacement	1	Quartz	1000.00	27.70	3.22
	2	Anatase	173.45	25.00	3.56
	3	Quartz	155.65	41.88	2.16

4.1.12 Geochemical analysis

Geochemical analysis was conducted to determine the oxides present in each subgrade category. As shown in Table 4-14, the major oxides found are SiO_2, Al_2O_3, and Fe_2O_3. The results are in agreement with previous studies on soils from the Jimma zone [15,27] as well as similar soils in other regions of the country [14,25]. The degree of laterization was also assessed using the silica-sesquioxide ratio (S-S ratio) or $SiO_2/(Fe_2O_3 + Al_2O_3)$.

Table 4-14 Identified percentages of major and minor oxides

	SiO_2	Al_2O_3	Fe_2O_3	CaO	MgO	Na_2O	K_2O	MnO	P_2O_5	TiO_2	H_2O
Category-1	40.50	22.30	12.56	<0.01	<0.01	0.80	0.26	0.32	0.32	1.94	12.12
Category-2	41.76	20.42	11.16	<0.00	0.50	<0.01	0.50	0.38	0.30	0.12	14.30
Category-3	41.32	23.92	10.66	<0.01	<0.01	<0.01	0.24	0.20	0.24	1.60	10.71

As it can be seen from Table 4-15, all subgrade soils are true laterite, with an S-S ratio less than 1.33.

Table 4-15 Degree of laterization determined using soil chemical tests

	SiO_2	Al_2O_3	Fe_2O_3	S-S ratio	Remark
Category-1	40.50	22.30	12.56	1.16	Laterite
Category-2	41.76	20.42	11.16	1.32	Laterite
Category-3	41.32	23.92	10.66	1.19	Laterite

4.1.13 Dynamic Cone Penetrometer (DCP)

In addition to the laboratory examination, an in-situ test, DCP, was performed on each subgrade soil to evaluate the properties 100 cm below the subgrade level. As shown in Table 4-16, category-3 has a higher DCP value of 49 mm/blow, whereas categories 1 and 2 have nearly identical values (23 and 25 mm blow, respectively) at natural moisture. Borden et al. [52] discuss the NCDOT standard, which outlines that soils with blow rates greater than 38 mm/blow are deemed weak and require an undercut prior to treatment.

Table 4-16 DCP values of each subgrade category

	Category-1	Category-2	Category-3
Thickness [mm]	910	910	890
DCP [mm/blow]	23	25	49

4.1.14 In-situ Bulk Density and Unit Weight

As presented in Table 4-17, unsaturated and saturated unit weights were determined using specimens retrieved from coring mold. The unsaturated unit weight ranged from 15.24 to 16.54 kN/m^3, whereas the saturated unit weight varied from 17.26 to 16.23 kN/m^3. The bulk unit weights are somewhat lower than those found by Teklay et al. [58] for comparable soils, ranging from 17 to 19.2 kN/m^3.

Table 4-17 In-situ bulk density and unit weight of each subgrade category

	Category-1	Category-2	Category-3
Bulk density [g/cm^3]	1.686	1.651	1.553
Bulk unit weight [kN/m^3]	16.54	16.19	15.24
Saturated unit weight [kN/m^3]	17.26	16.23	16.32

4.2 Numerical Model Input Parameters

Model parameters determined for appropriate modeling are presented and discussed hereunder.

4.2.1 Model Parameters for Flexible Pavement Materials

Table 4-18 shows the model parameters determined for flexible pavements that were used for numerical analysis. The parameters are standard values obtained from [12] and correlation data. The stiffness and strength parameters are established in descending sequence, from the top asphalt concrete layer to the capping layer.

Table 4-18 Flexible pavement layers property used for the study

Properties	AC*	GBC*	GSB*	GC*
Thickness [mm]	50	175	225	130
γ, [kN/m^3]	24	23.3	21.5	18.3
E, [MPa]	3000	300	175	100
ν	0.3	0.3	0.3	0.3
c, [kPa]	-	0	0	0
φ, [^{o}]	-	40	35	29
ψ, [^{o}]	-	10	5	-

*AC – Asphalt concrete, GBC – Granular Base course, GSB – Granular Sub-base, and GC – Granular Capping.

γ - Unit weight, E - Elastic modulus, ν - Poisson's ratio, c - Cohesion, φ - Friction angle, and ψ – Dilatancy.

4.2.2 Model Parameters for Unsuitable Subgrade Soils and Replacement Material

The model parameters for the subgrade soils and replacement material were determined using the test program and correlations for a numerical study. Table 4-19 presents the required modeling parameters that were obtained from undisturbed specimens at natural moisture content. However, to study the effect of water at saturation levels, model parameters were determined using remolded specimens, as shown in Table 4-20. It was observed that adding water content to the saturation level drastically lowered the cohesion and stiffness module values of all subgrade soils.

Table 4-19 Unsuitable subgrade soils' and replacement material's property used in this study (for set 1)

Properties	Category-1	Category-2	Category-3	Replacement
γ, [kN/m^3]	16.54	16.19	15.24	20.3
γ_{sat}, [kN/m^3]	17.26	16.23	16.32	20.3
c, [kPa]	247.53	74.08	116.29	92.2
φ, [^{o}]	3.98	10.71	3.45	21.2
E_{50}^{ref}, [MPa]	12.78	4.79	5.42	18.1
E_{oed}^{ref}, [MPa]	12.78	4.79	5.42	18.1
E_{ur}^{ref}, [MPa]	38.34	14.36	16.26	54.29
G_0^{ref}, [MPa]	81.6	78.8	49.8	-
$\gamma_{0.7}$	0.00021	0.00023	0.00026	-

γ - Unit weight, γ_{sat} – Saturated unit weight, c - Cohesion, φ - Friction angle, E_{50}^{ref} – Reference secant stiffness modulus, E_{oed}^{ref} - Reference tangent stiffness modulus, E_{ur}^{ref} – Un-/reloading stiffness modulus, G_0^{ref} - Reference Shear Modulus at Very Small Strains, and $\gamma_{0.7}$ – Shear strain.

Table 4-20 Unsuitable subgrade soils' and replacement material's property used in this study (for set 2)

Properties	Category-1	Category-2	Category-3
c, [kPa]	78.30	40.71	32.64
φ, [^{o}]	17.11	12.11	10.56
E_{50}^{ref}, [MPa]	5.47	3.68	2.51
E_{oed}^{ref}, [MPa]	3.18	2.74	1.94
E_{ur}^{ref}, [MPa]	16.42	11.05	7.54

4.3 Results of Numerical Simulation

To investigate the deformation properties of flexible pavement under cyclic vehicular loads, a numerical simulation was done using PLAXIS 2D. Figure 4-6 shows the deformation-load cycle data from numerical simulation (using input data from Table 4-19) for the untreated subgrade condition (no undercut). After 105 load cycles, the top of the pavement deformed by 1.70 mm, 3.19 mm, and 2.53 mm for categories 1, 2, and 3, respectively.

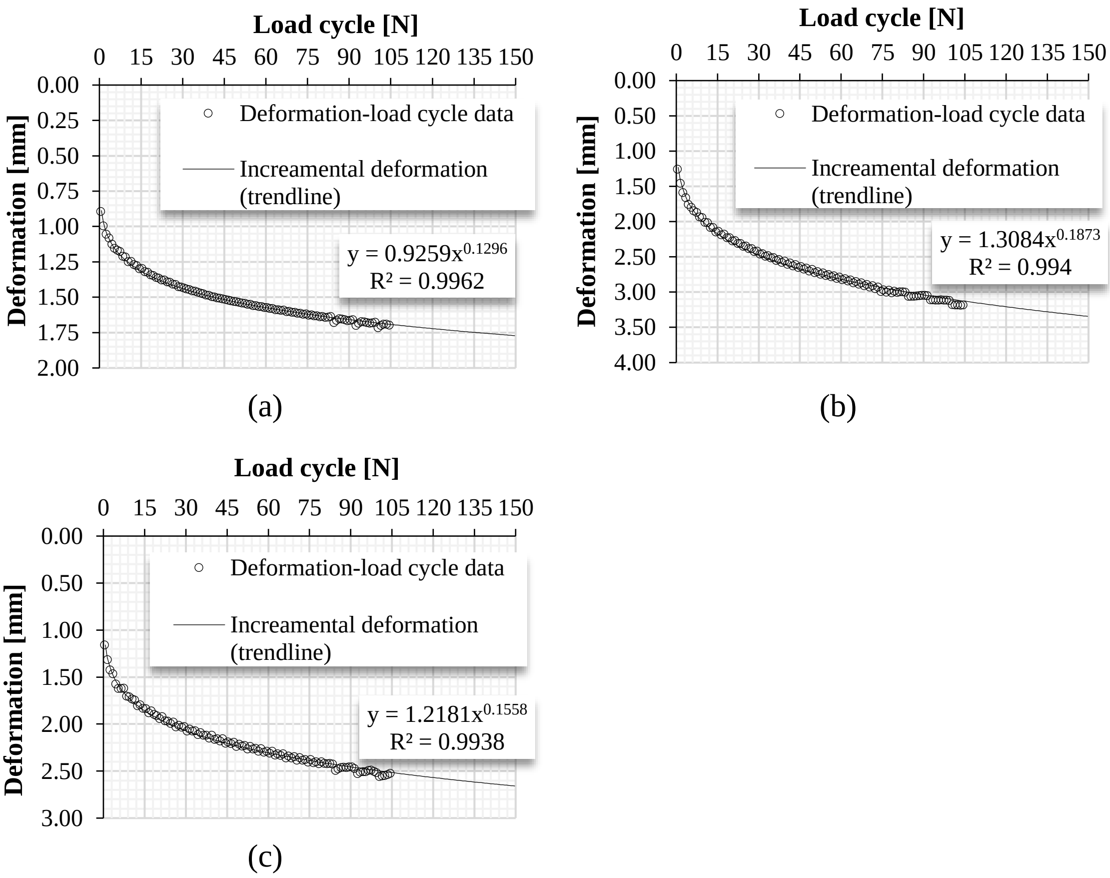

Figure 4-6 Deformation-Load cycle curve for set 1 input data with no undercut; (a) Category-1, (b) Category-2, and (c) Category-3

To assess the long-term performance, fitting curves (trendline equations) were used to project the deformation at the designed traffic (considering the traffic load expected at the end of the project design period) for 4.5 million load cycles, as shown in Table 4-21. The deformations were found to be 6.74 mm, 23.06 mm, and 13.25 mm in categories 1, 2, and 3, respectively. As a consequence, all subgrades with a natural moisture content were found to be appropriate for use as subgrade soils under flexible pavement since they met the 25 mm threshold deformation value. However, given that the study area has extended rainy weather, as shown in Figure 3-3, a further study was conducted by adding moisture content to the saturation level to analyze the worst-case scenario.

Figure 4-7 shows the deformation-load cycle data for numerical analysis at the saturation moisture content (using input data from Table 4-19 and Table 4-20) for category-1 subgrade. It was observed that after 105 load cycles, the top of the pavement overlaying category-1 subgrade soil deformed 2.78 mm, which is higher than the deformation at the natural moisture content of the subgrade (1.70 mm).

Similarly, it was found that the projected deformation after 4.5 million load cycles (from Table 4-21) was 19.99 mm, which is less than the 25 mm threshold deformation value. In this regard, category-1 subgrade soil is suitable for use as a subgrade soil beneath flexible pavement since it can sustain the stresses generated by vehicle loads at the end of the road project's design period, even when saturated.

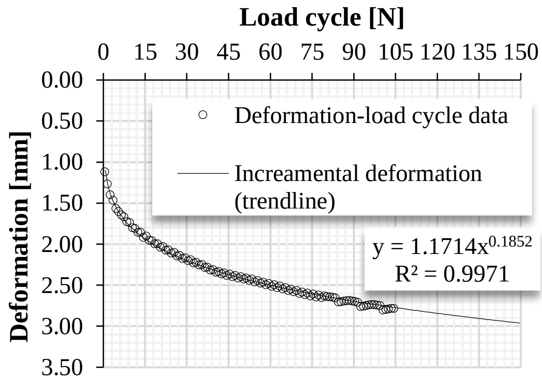

Figure 4-7 Deformation-Load cycle curve for set 2 input data with no undercut (Category-1)

Figure 4-8 shows the deformation-load cycle data for numerical analysis at the saturation moisture content (using input data from Table 4-19 and Table 4-20) for category-2 subgrade. After 105 load cycles, 3.80 mm deformation was noted, and the projected deformation after 4.5 million load cycles (from Table 4-21) was 45.25 mm, which is greater than the 25 mm threshold deformation value. This shows that category-2 subgrade soil is unsuitable for use as a subgrade soil under flexible pavement and requires undercut treatment when saturated. After the application of undercut treatments of 20 cm, 40 cm, and 60 cm, it was noted that the deformation had decreased to 32.54 mm, 27.90 mm, and 20.20 mm, respectively. At 60 cm depth undercut treatment, the deformation was found to be less than the 25 mm threshold deformation value, indicating a considerable reduction in deformation, as illustrated in Figure 4-10.

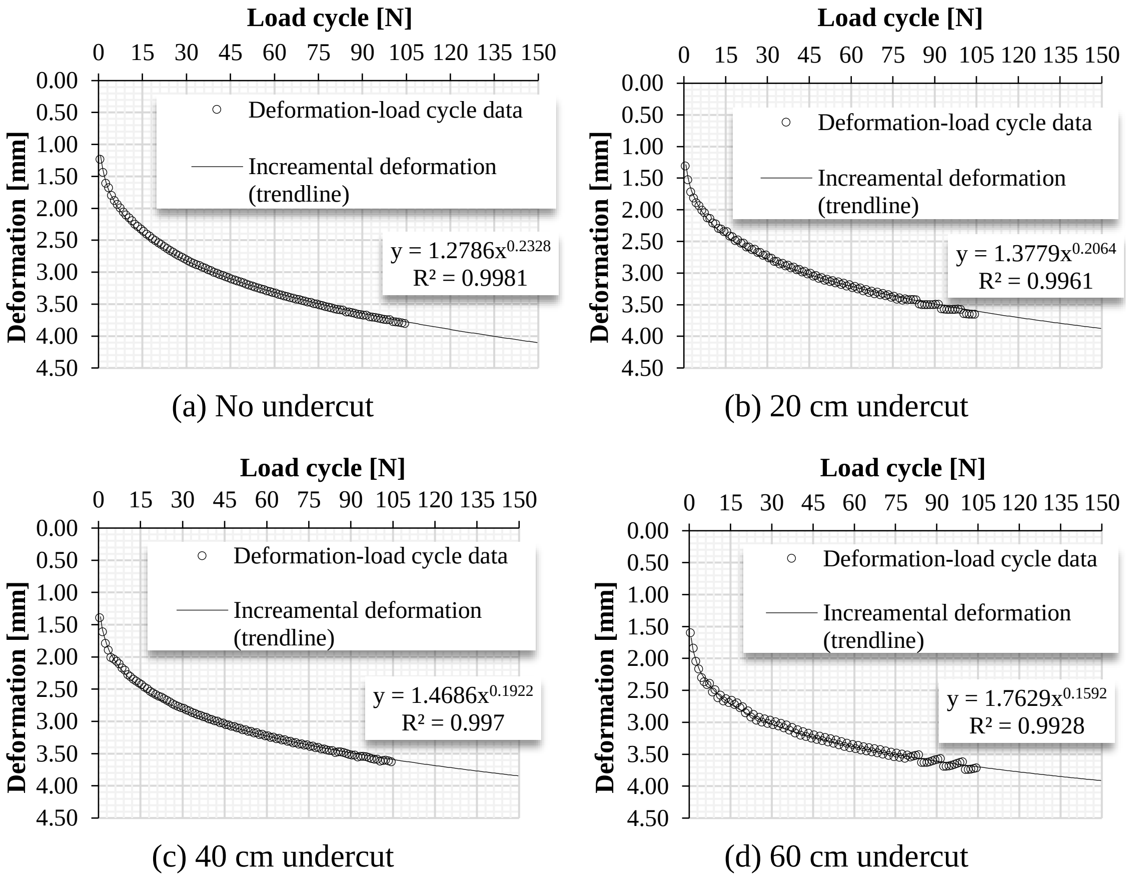

(a) No undercut (b) 20 cm undercut

(c) 40 cm undercut (d) 60 cm undercut

Figure 4-8 Deformation-Load cycle curve for set 2 input data (Category-2)

Figure 4-9 shows the deformation-load cycle data for numerical analysis at the saturation moisture content (using input data from Table 4-19 and Table 4-20) for category-3 subgrade. Following 105 load cycles, a deformation of 5.13 mm was recorded, with a projected deformation reaching 70.99 mm after 4.5 million load cycles (from Table 4-21), surpassing the threshold deformation value of 25 mm.

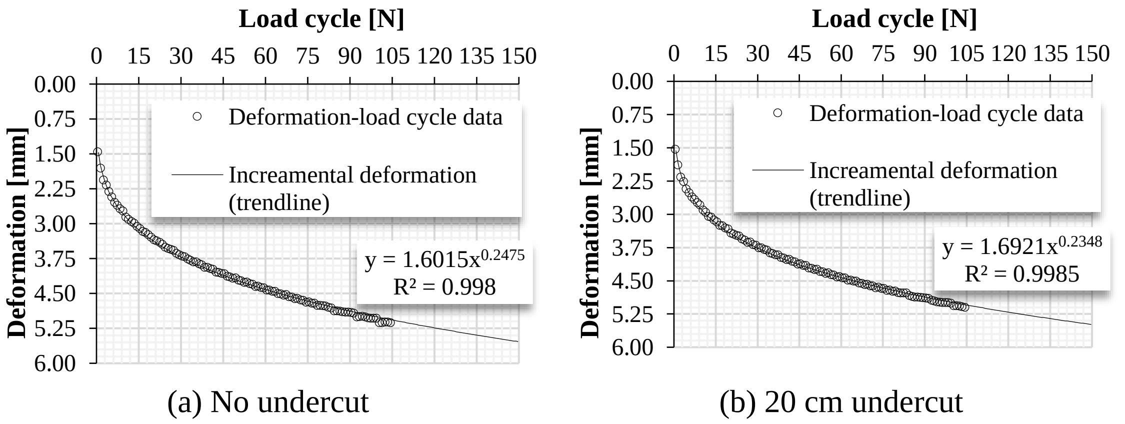

(a) No undercut (b) 20 cm undercut

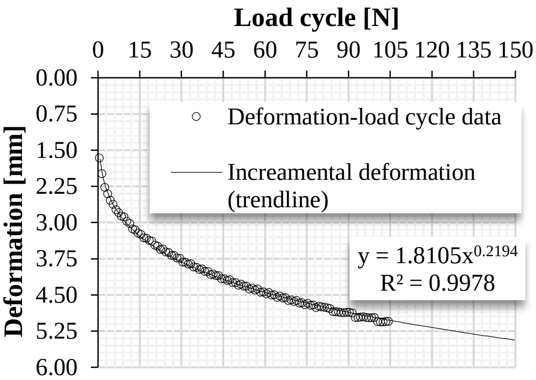

(c) 40 cm undercut

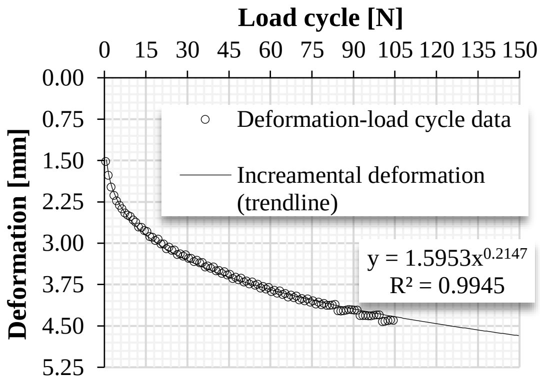

(d) 60 cm undercut

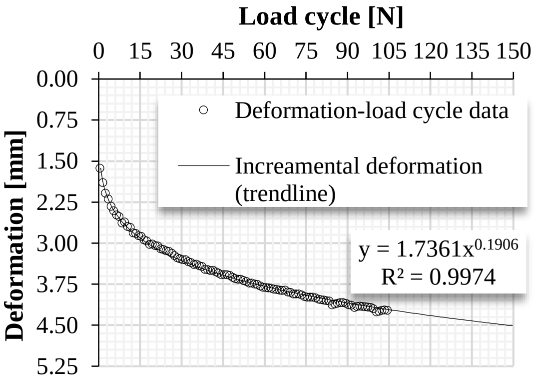

(e) 80 cm undercut

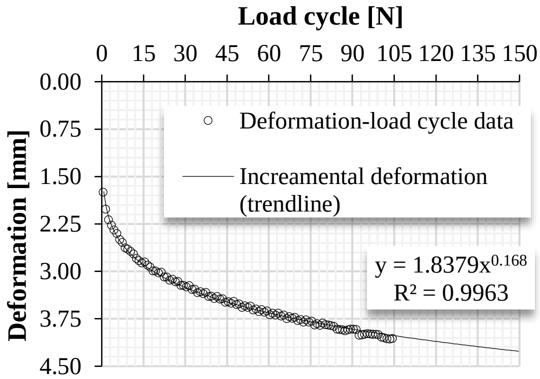

(f) 100 cm undercut

Figure 4-9 Deformation-Load cycle curve for set 2 input data (Category-3)

This indicates the unsuitability of category-3 subgrade soil for use as a subgrade beneath flexible pavement, necessitating undercut treatment when saturated. Upon implementing undercut treatments of 20 cm, 40 cm, 60 cm, 80 cm, and 100 cm, reductions in deformation were noted, with values decreasing to 61.74 mm, 52.18 mm, 42.78 mm, 32.19 mm, and 24.10 mm, respectively. Notably, at a depth of 100 cm undercut treatment, the deformation fell below the threshold of 25 mm, demonstrating a significant decrease in deformation as shown in Figure 4-10.

Table 4-21 Subgrade deformation data

Subgrade	Undercut depth	Deformation, δ,[mm]		Trendline equation to predict deformation
		After 105 load cycles	After 4.5x10^6 load cycles	
Category-1 (set 1)	0 cm	1.70	6.74	$\delta = 0.9259N^{0.1296}$
Category-2 (set 1)	0 cm	3.19	23.06	$\delta = 1.3084N^{0.1873}$
Category-3 (set 1)	0 cm	2.53	13.25	$\delta = 1.2181N^{0.1558}$
Category-1 (set 2)	0 cm	2.78	19.99	$\delta = 1.1714N^{0.1852}$

Subgrade	Undercut depth	Deformation, δ,[mm]		Trendline equation to predict deformation
		After 105 load cycles	After 4.5x10^6 load cycles	
Category-2 (set 2)	0 cm	3.80	45.25	$\delta = 1.2786N^{0.2328}$
	20 cm	3.65	32.54	$\delta = 1.3779N^{0.2064}$
	40 cm	3.63	27.90	$\delta = 1.4686N^{0.1922}$
	60 cm	3.72	20.20	$\delta = 1.7629N^{0.1592}$
Category-3 (set 2)	0 cm	5.13	70.99	$\delta = 1.6015N^{0.2475}$
	20 cm	5.10	61.74	$\delta = 1.6921N^{0.2348}$
	40 cm	5.05	52.18	$\delta = 1.8105N^{0.2194}$
	60 cm	4.40	42.78	$\delta = 1.5953N^{0.2147}$
	80 cm	4.23	32.19	$\delta = 1.7361N^{0.1906}$
	100 cm	4.06	24.10	$\delta = 1.8379N^{0.168}$

δ – Deformation [mm], N – Load cycle [in number]

Table 4-22 shows the deformation reduction; at 60 cm and 100 cm undercut treatment for categories 2 and 3, a 55.4% and 66.0% reduction in deformation from the original, respectively, was observed.

Table 4-22 Data on the effect of undercut treatment

Subgrade	Undercut depth	Deformation*, δ, [mm]	Effect of undercut**
Category-2 (set 2)	0 cm	45.25	-
	20 cm	32.54	28.1%
	40 cm	27.90	38.3%
	60 cm	20.20	55.4%
Category-3 (set 2)	0 cm	70.99	-
	20 cm	61.74	13.0%
	40 cm	52.18	26.5%
	60 cm	42.78	39.7%
	80 cm	32.19	54.7%
	100 cm	24.10	66.0%

*Deformation after 4.5x10^6 load cycles, **Percentage reduction in deformation relative to the model with no undercut (0 cm).

The relationship between deformation and incremental subgrade treatment was established, as presented in Figure 4-10. The results indicate that there is a linear relationship between the incremental undercut treatment and the deformation resulting from cyclic vehicle loads.

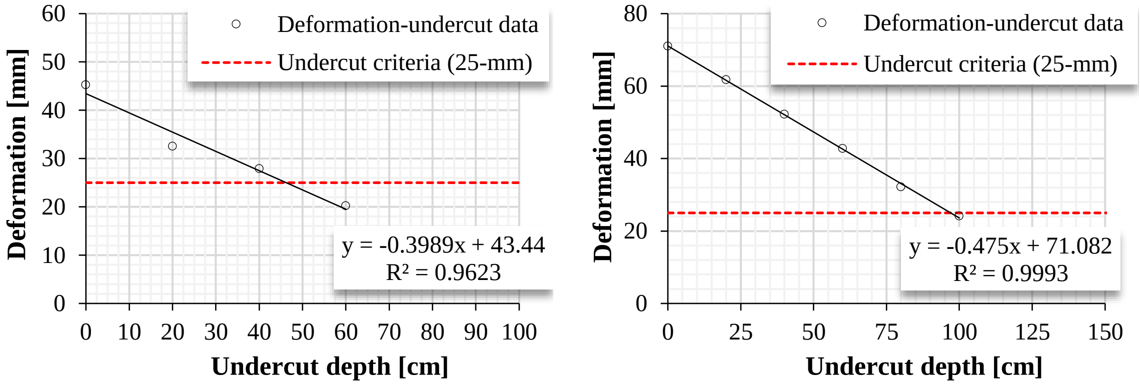

(a) Category-2 (set 2) (b) Category-3 (set 2)

Figure 4-10 Relationship between deformation and undercut depth

4.4 Optimum Undercut Depth

Table 4-23 presents the minimum undercut treatment required as per the findings of this study and practices on the project as per ERA standard [9] and project specification. The treatment of category-3 subgrade soil was found to be identical; however, the undercut requirements for categories 1 and 2 differed significantly. As a result, the findings of this study suggest that the actual practice is conservative.

Table 4-23 Undercut treatment required

	Minimum undercut required (cm)	
	This study	ERA standard and Project specification
Category-1	0	60
Category-2	60	100
Category-3	100	100

CHAPTER 5

CONCLUSION AND RECOMMENDATION

The study will be concluded in this chapter with a summary of the major research results and their significance and contribution in connection to the objectives and research questions. In addition, it will suggest directions for further investigation.

5.1 Conclusions

This study has investigated the essential geotechnical properties of unsuitable tropical red subgrade soils on the Merewa-Seka road project to better understand their inherent behavior. Further, the deformation characteristics of the subgrade soils under flexible pavement were assessed through numerical simulation. Finally, based on the data from the numerical simulation and its projected data, the optimum undercut depth was established for the corresponding subgrade category.

The laboratory and field tests carried out for the study were moisture content, specific gravity, grain size distribution, Atterberg limits, compaction test, CBR test, triaxial compression test, one-dimensional consolidation test, XRD, geochemical test, DCP test, and bulk density. The test methods fully adhered to ASTM, AASHTO, BS, and IS standards, with the exception of test protocols recommended for tropical soils under special conditions. PLAXIS 2D version 8.6 was utilized for numerical analysis, using model parameters determined from geotechnical investigation and correlation input data.

Summing up all the key aspects of the study, the following conclusions are drawn:

- The study intended to investigate the effect of drying and remolding on the characteristics of the unsuitable tropical red subgrade soils by performing natural moisture and Atterberg limit determination tests. The results showed that drying using conventional test procedures (at 110 ^oC) had no significant effect when compared to the recommended drying temperature of 50 ^oC, and standard drying methods could be utilized to determine the moisture content for the Merewa-Seka road project. However, the remolding of specimens for the determination of the liquid limit was shown to have significant effects on the majority of subgrade soils (categories 2 and 3).

As a result, the Atterberg limits should be determined immediately upon receipt without drying, with a mixing period of under five minutes and fresh soil specimens used for each test water content point.

- The engineering classifications of the unsuitable tropical red subgrade soils using common classification systems were evaluated. Despite the fact that subgrade soils are classified as fine grained, it was found that soils plotted below the A-line of the plasticity chart (USCS) have good engineering properties, as evidenced by their CBR, DCP, and shear strength values. Thus, the project's subgrade soils should be evaluated primarily based on their plasticity chart plot and strength performance.
- The swelling potential of the unsuitable tropical red subgrade soils on undisturbed, disturbed, and remolded samples in connection with their activity, mineralogical composition, and swelling pressure were studied. The results showed that all of the subgrade soils investigated had low activity (between 0.19 and 0.28) and contained inactive minerals with low swelling potential, a low free swell index value, and low swelling pressure. However, under remolded and soaked conditions, categories 2 and 3 had a greater CBR-Swell value, which was reflected in a drop in shear strength (triaxial test) at saturated moisture content. Therefore, the subgrade soils of the project studied generally have low swelling potential (non-expansive nature) but could have swelling character under remolded and soaked conditions.
- The study aimed at numerical modeling and model parameter determination for two conditions of subgrade soils, which are at natural moisture content and at saturation moisture content. From the results, it is revealed that the subgrades have higher shear strength (cohesion) and higher stiffness modules at natural moisture content, attributed to their hardening properties. However, when remolded specimens were studied at saturation moisture content, there was a significant loss in shear strength and stiffness modules.
- The deformation analysis using numerical simulation revealed that the subgrades at natural moisture content under flexible pavement have lower deformation (ranging from 6.74 to 23.06 mm) after 4.5 million load cycles, affirming that the subgrades are suitable to be used without treatment. However, significantly higher deformations (ranging from 19.99 to 70.99 mm) were noted at saturation moisture content.

As a result, categories 2 and 3 (with deformations of 45.25 and 70.99 mm, respectively) were found to be weak, requiring treatment.

- This research sought to establish the optimum undercut depth for unsuitable tropical red subgrade soils in the Merewa-Seka project. The outcomes suggested that category-1 subgrade required no undercut treatment, while categories 2 and 3 needed 60 cm and 100 cm of undercut and replacement treatments, respectively, before being used under flexible pavement. This finding significantly deviates from the current practice suggested by the ERA standard as well as the project specification.

Finally, from the study's results, it can be concluded that the tropical red subgrade soils of the project under study have different engineering characteristics, even at the same classification and visual description. The subgrade soils ranged from suitable (category-1) to unsuitable (categories 2 and 3) after vehicular cyclic loading at saturation condition. Despite the subgrade soils have a non-expansive nature and are true laterites, at saturation moisture content, a significant strength reduction was noted. Furthermore, more economical undercut treatment than practiced by the ERA standard was the outcome of this research, suggesting appropriate in-depth investigations be made for the project's subgrade soils before applying treatments recommended for expansive soils. This is vital for maintaining the wellbeing of the environment around the project corridor as well as practicing economical road construction.

5.2 Recommendations

This study revealed the optimum undercut depth treatment of unsuitable tropical red subgrade soils using numerical analysis. Also, the study has presented a comprehensive geotechnical investigation. Based on the findings and conclusions presented, the following recommendations are suggested:

- Additional geotechnical investigations and numerical analysis should be carried out on a large number of unsuitable tropical red subgrade soils in order to obtain reliable and comprehensive information on how they behave.
- Since the optimum undercut depth treatment was selected based on one replacement material, cheaper but suitable materials, possibly category 1 subgrade soil, should be analyzed as a replacement material for categories 2 and 3 subgrade soils for more economical and environmentally-friendly road construction.

REFERENCES

[1] Baligar V. C., Fageria N. K., Eswaran H., Wilson M. J., and He Z. Nature and Properties of Red Soils of the World. In: *The Red Soils of China*. Springer Netherlands; 2004:7-27. doi:10.1007/978-1-4020-2138-1_2

[2] Northmore K. J., Culshaw M. G., Hobbs P. R. N., Hallam J. R., and Entwisle D. C. *Engineering Geology of Tropical Red Clay Soils: Summary Findings and Their Application for Engineering Purposes*.; 1992.

[3] Gidigasu M. D. Degree of Weathering in the Identification of Laterite Materials for Engineering Purposes - A Review. *Eng Geol*. 1974;8(3):213-266. doi:10.1016/0013-7952(74)90001-5

[4] Brink G. A Brief Overview of the Typical Engineering Characteristics of Tropical Red Soils. In: *Engineering Geology for Society and Territory - Volume 6*. Springer International Publishing; 2015:211-214. doi:10.1007/978-3-319-09060-3_33

[5] Catt J. A. Tropical Residual Soils. Geological Society Engineering Group Working Party Report. *Quarterly Journal of Engineering Geology*. 1990;23(1):4-101. doi:10.1144/GSL.QJEG.1990.023.001.01

[6] Burland J., Chapman T., Skinner H., and Brown M. *ICE Manual of Geotechnical Engineering Volume 1: Geotechnical Engineering Principles, Problematic Soils and Site Investigation*. (Chapman T, Skinner HD, Brown M, Burland J, eds.). Thomas Telford Ltd; 2012. doi:10.1680/moge.57074

[7] Fookes P. G. A Review: Genesis and Classification of Tropical Residual Soils for Engineers. *Geotechnics in the African Environment*. 1994;2:423-442.

[8] Fruhauf B., and Willis E. A. A Study of Lateritic Soils. *Proceedings of the Twenty-Sixth Annual Meeting of the Highway Research Board*. 1946;26:579-593. https://onlinepubs.trb.org/Onlinepubs/hrbproceedings/26/26-046.pdf

[9] Ethiopian Roads Authority. *Standard Technical Specifications and Method of Measurement for Roads*. The Federal Democratic Republic of Ethiopia, Ethiopian Roads Authority; 2013. https://www.era.gov.et

[10] China Tiesiju Civil Engineering Group Co. Ltd. *Final Soils and Materials Investigation Report*.; 2020.

[11] Ethiopian Roads Authority. *Design Manual for Low Volume Roads*. Vol Part B. The Federal Democratic Republic of Ethiopia, Ethiopian Roads Authority; 2011. Accessed December 11, 2023. https://www.era.gov.et

[12] Ethiopian Roads Authority. *Pavement Design Manual*. Vol 1. Flexible pavements. The Federal Democratic Republic of Ethiopia, Ethiopian Roads Authority ; 2013. https://www.era.gov.et

[13] Ethiopian Roads Authority. *Design Manual for Low Volume Roads*. Vol Part D. The Federal Democratic Republic of Ethiopia, Ethiopian Roads Authority; 2011. https://www.era.gov.et

[14] Dilla D., and Rao V. P. Index and Engineering Properties of Residual Tropical Soils of Southwestern Ethiopia. *International Research Journal of Engineering and Technology (IRJET)*. Published online 2019:2214-2222. https://www.irjet.net/archives/V6/i5/IRJET-V6I5427.pdf

[15] Teferi L. *Evaluation of the Suitability of Lateritic Soil of Jimma Zone as Road Construction Materials*. Jimma University, Jimma Institute of Technology; 2016. doi:http://10.140.5.162//handle/123456789/570

[16] Morin W. J., and Todor P. C. *Laterite and Lateritic Soils and Other Problem Soils of the Tropics: An Engineering Evaluation and Highway Design Study for United States Agency for International Development: Instruction Manual*. Vol 2. Lyon Associates Inc. & Road Research Institute Brazilian National Highway Department; 1975. https://trid.trb.org/view/50988

[17] Lyon Associates Inc. *Laterite and Lateritic Soils and Other Problem Soils of Africa: Development of Engineering Standards and Criteria for the Usage of Laterite, Lateritic Soils, and Other Problem Soils in Connection with the Construction of Roads, Highways and Airfields: An Engineering Study for Agency for International Development*. Lyon Associates Inc. & Building & Road Research Institute ; 1971. https://trid.trb.org/view/124606

[18] Gidigasu M. D. Identification of Problem Laterite Soils in Highway Engineering: A Review. *53rd Annual Meeting of the Highway Research Board*. 1974;(497):96-111. http://onlinepubs.trb.org/Onlinepubs/trr/1974/497/497-010.pdf

[19] Wesley L. D. *Geotechnical Engineering in Residual Soils*. Wiley; 2010. doi:https://doi.org/10.1002/9780470943113

[20] Ethiopian Roads Authority. *Site Investigation Manual*. The Federal Democratic Republic of Ethiopia, Ethiopian Roads Authority; 2013. Accessed December 1, 2023. https://www.era.gov.et

[21] Catt J. A. Tropical residual soils. Geological society engineering group working party report. *QJ Eng Geol Hydrogeol*. 1990;23(1):4-101.

[22] Hassan S. A., Shitote S. M., and Thuo J. N. Investigation of the Impact of Tropical Red Clay Soils' Mineralogical Composition on their Physical and Mechanical Properties– a Case Study Ruaka – Kenya. *The Open Civil Engineering Journal*. 2022;16(1). doi:10.2174/18741495-v16-e2209260

[23] *Laterite and Lateritic Soils, and Other Problem Soils of Africa: Development of Engineering Standards and Criteria for the Usage of Laterite, Lateritic Soils, and Other Problem Soils in Connection with the Construction of Roads, Highways and Airfields: An Engineering Study for Agency for International Development*. Lyon Associates; 1971.

[24] Proceedings of the ASCE Geotechnical Engineering Division Specialty Conference: Engineering and Construction in Tropical and Residual Soils. *GRS - Bericht (Gesellschaft fuer Reaktorsicherheit)*. Published online January 1, 2017.

[25] Akalu M. *Engineering Characteristics of Red Soil: A Case from Western Addis Ababa*. Addis Ababa University; 2017. http://etd.aau.edu.et/bitstream/handle/123456789/7130/Medhanit%20Akalu.pdf?isAllowed=y&sequence=1

[26] Chen F. H. *Foundations on Expansive Soils*. Elsevier Scientific Publishing Company; 1975.

[27] Muhammed J. J., and Teferra Prof. A. *In-Depth Investigation into Engineering Characteristics of Jimma Soils*. Addis Ababa University, Addis Ababa Institute of Technology ; 2014. https://www.researchgate.net/publication/321138070_In-depth_Investigation_into_Engineering_Characteristics_of_Jimma_Soils

[28] Brinkgreve R., Broere W., and Waterman D. *Plaxis 2D - Version 8.*; 2004. https://www.researchgate.net/publication/262012153_Plaxis_2D_-_Version_8

[29] Faheem H., and Hassan A. M. 2D PLAXIS finite element modeling of asphalt-concrete pavement reinforced with geogrid. *JES Journal of Engineering Sciences*. 2014;42(6):1336-1348. doi:10.21608/jesaun.2014.115106

[30] Ahirwar S. K., and Mandal J. N. Finite Element Analysis of Flexible Pavement with Geogrids. *Procedia Eng*. 2017;189:411-416. doi:10.1016/j.proeng.2017.05.065

[31] Carvajal E., and Romana M. Analysis of the influence of soft soil depth on the subgrade capacity for flexible pavements. *Proceedings of the 18th International Conference on Soil Mechanics and Geotechnical Engineering*. Published online 2013:1249-1253.

[32] Masood G. G., Mohammed H. A., Afaj H. A. H., and Fattah M. Y. Behavior of flexible pavement on swelling subgrade soil reinforced with geogrid. *Archives of Civil Engineering*. 2021;67(4):393-402. doi:http://dx.doi.org/10.24425/ace.2021.138507

[33] Djellali A., Ounis A., and Saghafi B. Behavior of flexible pavements on expansive soils. Published online 2012. doi:https://doi.org/10.22119/ijte.2013.2626

[34] Karadag H., Firat S., Isik N. S., and Yilmaz G. Determination of Permanent Deformation of Flexible Pavements Using Finite Element Model. Lakusic S, ed. *Journal of the Croatian Association of Civil Engineers*. 2022;74(06):471-480. doi:10.14256/JCE.2708.2019

[35] Nigade-Saha Sanjivani D., and Viswanadham B. V. S. Some Studies on Pavements on Flyash-Stabilized Expansive Subgrades. In: *Construction in Geotechnical Engineering: Proceedings of IGC 2018*. Springer; 2020:655-676. doi:10.1007/978-981-15-6090-3_49

[36] Djellali A., Houam A., Saghafi B., Hamdane A., and Benghazi Z. Static Analysis of Flexible Pavements over Expansive Soils. *International Journal of Civil Engineering*. 2017;15(3):391-400. doi:10.1007/s40999-016-0058-6

[37] Hashem M. D., Abu-Baker A. M., and Hashem M. D. Numerical modeling of flexible pavement constructed on expansive soils. *European International Journal*

of Science and Technology. 2013;2(10):19-34. https://dokumen.tips/documents/numerical-modeling-of-flexible-pavement-constructed-on-mostafa-deep-hashem-civil.html?page=1

[38] Kinetic Vision. Finite Element Modeling - Information Resources by Kinetic Vision. Published online December 2023. https://kinetic-vision.com/capabilities/finite-element-modeling/

[39] Yassenn O. M., Rohani I., Endut D., Ishak S. Z., Hafez M. A., and Yaseen H. M. Finite Element Modelling of Flexible Pavement. *Journal of Multidisciplinary Engineering Science and Technology*. 2015;2(1):115-120. https://www.jmest.org/wp-content/uploads/JMESTN42350341.pdf

[40] Van Vuuren J. D. Relationship Between Tire Inflation Pressure and Mean Tire Contact Pressure. *Transp Res Rec*. 1974;523:76-87. https://api.semanticscholar.org/CorpusID:113201389https://api.semanticscholar.org/CorpusID:113201389

[41] Yap P. Truck Tire Types and Road Contact Pressures. In: *Second International Symposium on Heavy Vehicle Weights and Dimensions*. ; 1989. https://api.semanticscholar.org/CorpusID:107248204

[42] Huang Y. H. *Pavement Analysis and Design*. 2nd ed. Pearson Prentice Hall Upper Saddle River, NJ; 2004. https://civilnode.com/download-book/10226743867698/pavement-analysis-and-design-2nd-edition

[43] Mousavi S. H., Gabr M. A., and Borden R. H. *Field Verification of Undercut Criteria and Alternatives for Subgrade Stabilization in the Piedmont Area*.; 2016. https://rosap.ntl.bts.gov/view/dot/31860

[44] Gouw Dr T. L. Common Mistakes on the Application of Plaxis 2D in Analyzing Excavation Problems. *International Journal of Applied Engineering Research*. 2014;9:8291-8311. https://www.researchgate.net/publication/282997310_Common_Mistakes_on_the_Application_of_Plaxis_2D_in_Analyzing_Excavation_Problems

[45] Mousavi S. H., Gabr M. A., and Borden R. H. *Field Verification of Undercut Criteria and Alternatives for Subgrade Stabilization in the Piedmont Area.* North Carolina State University. Dept. of Civil, Construction, and …; 2016.

[46] Schanz T., Vermeer P. A., and Bonnier P. G. The Hardening Soil Model: Formulation and Verification. *Beyond 2000 in Computational Geotechnics*. 1999;1:281-296. https://communities.bentley.com/cfs-file/__key/communityserver-wikis-components-files/00-00-00-01-05/The_5F00_Hardening_5F00_Soil_5F00_Model_5F002D005F00_Formulation_5F00_and_5F00_Verfication.pdf

[47] Obrzud R., and Andrzej T. *The Hardening Soil Model: A Practical Guidebook*. ZSoil 100701 report (revised 21.10.2018), Lausanne, Zace Services Ltd; 2018.

[48] Wu J. T. H., and Tung S. C. Y. Determination of Model Parameters for the Hardening Soil Model. *Transportation Infrastructure Geotechnology*. 2020;7(1):55-68. doi:10.1007/s40515-019-00085-8

[49] Benz T. *Small-Strain Stiffness of Soils and Its Numerical Consequences*. Inst. für Geotechnik; 2007. https://books.google.com.et/books?id=nzp5MwAACAAJ

[50] Ethiopian Roads Authority. *Geotechnical Design Manual*. The Federal Democratic Republic of Ethiopia, Ethiopian Roads Authority; 2013. https://www.era.gov.et

[51] Chou E., Fournier L., Wielinski J., Rao C., and Titus-Glover L. *Evaluation of Guidelines for Subgrade Treatments*. Ohio. Dept. of Transportation; 2005. https://rosap.ntl.bts.gov/view/dot/20519/dot_20519_DS1.pdf

[52] Borden R. H., Cote B. M., Gabr M. A., Park Y. J., Pyo S. C., and Robinson B. R. *Establishment of Subgrade Undercut Criteria and Performance of Alternative Stabilization Measures*.; 2010. https://rosap.ntl.bts.gov/view/dot/18455

[53] *ERA Geometric Design Manual*. Ethiopian Roads Authority; 2013. Accessed December 2, 2023. https://www.era.gov.et

[54] Alemu T., and Hageresalam Y. *Geology of Dinger, Dega and Parts of Arjo Subsheets of Arjo Map Sheet (NC37-13/A, G and B)*. GSE; 2005.

[55] Haro W., Besufikad A., Bulto D., Belete F., and Edris M. *Geology, Geochemistry, and Gravity Survey of Jima Area*. GSE; 2012.

[56] China Tiesiju Civil Engineering Group Co. Ltd. *Pavement Design Report*.; 2020.

[57] Blight G. E., and Leong E. C. *Mechanics of Residual Soils*. 2nd ed. CRC Press; 2012. doi:10.1201/b12014

[58] Teklay A., Haile M., Teferra A., and Murray E. J. The Effect of Sample Preparation and Testing Procedure on the Geotechnical Properties of Tropically Weathered Residual Laterite Soils of Ethiopia. *Zede Journal*. 2015;33:45-62. https://www.ajol.info/index.php/zj/article/view/142186

[59] Skempton A. W. The Colloidal Activity of Clays. *Proceedings of the 3rd International Conference of Soil Mechanics and Foundation Engineering*. 1953;1:57-60.

[60] Geotechdata.info. Angle of Friction. Published December 14, 2013. http://geotechdata.info/parameter/angle-of-friction.html

[61] ecorisQ.org. USCS Soil Classes, Cohesion, and Friction Angle. International EcorisQ Association. https://www.ecorisq.org/docs/USCS_soilclasses.pdf

[62] Al-Qadi I. L., Xie W., and Elseifi M. A. Frequency determination from vehicular loading time pulse to predict appropriate complex modulus in MEPDG. *Asphalt Paving Technology-Proceedings*. 2008;77:739. https://experts.illinois.edu/en/publications/frequency-determination-from-vehicular-loading-time-pulse-to-pred

[63] Ethiopian Roads Authority. *Geometric Design Manual*. The Federal Democratic Republic of Ethiopia, Ethiopian Roads Authority ; 2013. https://www.era.gov.et

[64] China Tiesiju Civil Engineering Group Co. Ltd. *Geometric Design Report*.; 2020.

[65] Sebaaly P. E., and Tabatabaee N. Influence of Vehicle Speed on Dynamic Loads and Pavement Response. *Transp Res Rec*. Published online 1993:107-114. https://api.semanticscholar.org/CorpusID:107784434

[66] Duncan J. M., Monismith C. L., and Wilson E. L. Finite Element Analyses of Pavements. *Highway Research Record*. Published online 1968:18-33. https://api.semanticscholar.org/CorpusID:61485611

[67] Specific Gravity of Solids in Laterite Soils. In: ; 1976:217-225. doi:10.1016/B978-0-444-41283-6.50016-2

[68] Wesley L. D. *Fundamentals of Soil Mechanics for Sedimentary and Residual Soils*. John Wiley & Sons; 2009. doi:10.1002/9780470549056

[69] Huang F., Zhuo L., and Zhang K. A Study on the Shear Strength Characteristic of Unsaturated Red Clay. *World Journal of Engineering and Technology*. 2022;10(04):714-727. doi:10.4236/wjet.2022.104046

[70] Chen F. H. *Foundations on Expansive Soils*. Elsevier; 1988. http://worldcat.org/isbn/0444430369

[71] Das B. M., and Sobhan K. *Principles of Geotechnical Engineering, SI Edition*. Cengage Learning; 2014. https://books.google.com.et/books?id=L925CgAAQBAJ

[72] Parry J. D., Brooks D. M., Jones T. E., and Hewitt N. C. *Overseas Road Note 9: A Design Manual for Small Bridges*. 2nd ed. Transport Research Laboratory and Department for International Development; 2000. https://www.gov.uk/research-for-development-outputs/orn9-a-guide-to-small-bridge-design-for-highway-engineers#citation

APPENDIX A
SECONDARY DATA

A.1 Subgrade Test Results

Table A-1 Subgrade soil suitability/unsuitability classification investigation at design phase of the project [10]

Description	ERA STS 2013 Criteria for Unsuitable Roadbed/Subgrade soils				Total Unsuitable Subgrade soils	Total Suitable Subgrade soils	Total
	LL > 60	PI > 30	CBR < 5	CBR-Swell > 3			
Number of tested soil samples	22	3	12	3	28	61	89
Percentage	24.7%	3.4%	13.5%	3.4%	31.5%	68.5%	100.0%

Table A-2 Subgrade soil suitability/unsuitability classification investigation during construction phase of the project (Source: Project site investigation data)

Description	ERA STS 2013 Criteria for Unsuitable Roadbed/Subgrade soils				Total Unsuitable Subgrade soils	Total Suitable Subgrade soils	Total
	LL > 60	PI > 30	CBR < 5	CBR-Swell > 3			
Length of tested road section [m]	27,410.0	6,460.0	7,500.0	20,384.0	34,024.0	52,440.0	86,464.0
Percentage	31.7%	7.5%	8.7%	23.6%	39.4%	60.6%	100.0%

Table 1-1 shows different subgrade soil category of the project for the purpose of this study. Based on [10], Category-1, Category-2 and Category-3 are unsuitable subgrade soils while Category-4 is suitable. The index properties of the subgrade soil categories are described below:

- **Category-1**: Has unacceptable Atterberg limit value, it could be Liquid limit (>60%) or Plasticity index (>30%) or both. But has acceptable CBR value (≥5%) and CBR-swell value (≤3%).
- **Category-2**: Regardless of Atterberg limit value, it has acceptable CBR value (≥5%) but unacceptable CBR-swell value (>3%). High swelling and the subgrade may exhibit volumetric change.
- **Category-3**: Regardless of Atterberg limit value and CBR-swell value, it has unacceptable CBR value (<5%). Bearing capacity is compromised and the subgrade under this category could be considered us weak subgrade soils.
- **Category-4**: Has acceptable Atterberg limit value (Liquid limit ≤60% and Plasticity index ≤30%), CBR value ≥5% and CBR-swell value ≤3%.

APPENDIX B

LABORATORY AND IN-SITU TEST RESULTS

B.1 Natural Moisture Content Determination

Table B-1 Moisture content test data in oven drying for 24 hours at 110 ± 5 ^oC

Subgrade category	Category - 1			Category - 2			Category - 3		
Test No	1	2	3	1	2	3	1	2	3
Container No	08	ML	41	ZC	C1	V	01	07	68
Mass of wet soil + container [gm]	73.92	74.77	76.87	78.81	75.76	75.73	74.78	72.14	73.97
Mass of dry soil + container [gm]	57.85	59.06	60.62	61.62	60.09	59.24	58.54	56.60	58.23
Mass of container [gm]	17.49	17.41	17.40	17.32	18.85	17.54	18.05	17.11	18.11
Mass of water [gm]	16.07	15.71	16.25	17.19	15.67	16.49	16.24	15.54	15.74
Mass of dry soil [gm]	40.36	41.65	43.22	44.3	41.24	41.7	40.49	39.49	40.12
Moisture content [%]	39.82	37.72	37.60	38.80	38.00	39.54	40.11	39.35	39.23
Average moisture content [%]	38.38			38.78			39.56		

Table B-2 Moisture content test data in oven drying for 48 hours at 50 ^oC

Subgrade category	Category - 1			Category - 2			Category - 3		
Test No	1	2	3	1	2	3	1	2	3
Container No	M2	S1	03	F8	H1	HT	E	84	02
Mass of wet soil + container [gm]	72.60	76.89	75.53	76.39	76.13	75.58	72.64	76.10	73.30
Mass of dry soil + container [gm]	58.43	61.10	60.73	60.62	60.76	59.95	58.22	60.16	58.35
Mass of container [gm]	17.56	16.65	18.12	17.64	17.05	17.45	18.75	17.22	18.12
Mass of water [gm]	14.17	15.79	14.80	15.77	15.37	15.63	14.42	15.94	14.95
Mass of dry soil [gm]	40.87	44.45	42.61	42.98	43.71	42.50	39.47	42.94	40.23
Moisture content [%]	34.67	35.52	34.73	36.69	35.16	36.78	36.53	37.12	37.16
Average moisture content [%]	34.98			36.21			36.94		

B.2 Specific Gravity Determination

Table B-3 Specific gravity test data using boiling method for oven dried specimens

Subgrade category	Category-1		Category-2		Category-3	
Test No	1	2	1	2	1	2
Mass of the dry pycnometer [gm]	159.3	159.3	159.3	159.3	159.3	159.3
Mass of the pycnometer and water [gm]	660.9	660.9	660.9	660.9	660.9	660.9
Mass of pycnometer, water and soil solids [gm]	692.4	692.6	691.3	691.5	691.5	692.2
Temperature of test water [^oC]	27	25	29	26	27	28
Mass of the oven dry soil solids [gm]	49.7	50.1	49.4	49.9	49.4	50.6
Specific gravity of soil solids	2.731	2.723	2.600	2.585	2.628	2.622
Correction factor	0.998	0.999	0.998	0.999	0.998	0.998
Corrected Specific Gravity of soil solids at 20^oC	2.726	2.720	2.594	2.582	2.623	2.617
Average Specific Gravity of soil solids at 20^oC	2.723		2.588		2.620	

B.3 Grain Size Distribution Analysis

The following definition given by AASHTO and Das and Sobhan [71] was used.

Gravel	Sand	Silt	Clay

75mm 2mm 0.075mm 0.002mm

B.3.1 Category-1 Subgrade Soil

Table B-4 Wet sieve analysis data for category-1

Sieve size [mm]	Mass retained [gm]	Percent retained [%]	Percent pass [%]	Mass retained [gm]	Percent retained [%]	Percent pass [%]	Average percent passing [%]
	Test No: 1			Test No: 2			
75	0	0	100	0	0	100	100
50	0	0	100	0	0	100	100
37.5	0	0	100	0	0	100	100
25	0	0	100	0	0	100	100
19	0	0	100	0	0	100	100
9.5	0	0	100	0	0	100	100
4.75	0	0	100	0.0	0.0	100.0	100
2	5.8	1.2	98.8	1.8	0.4	99.6	99.2
0.85	1.1	0.2	98.6	1.2	0.2	99.4	99.0
0.425	1.4	0.3	98.3	1.4	0.3	99.1	98.7

Sieve size [mm]	Mass retained [gm]	Percent retained [%]	Percent pass [%]	Mass retained [gm]	Percent retained [%]	Percent pass [%]	Average percent passing [%]
	Test No: 1			Test No: 2			
0.15	2.1	0.4	97.9	2.6	0.5	98.6	98.3
0.075	3.8	0.8	97.2	5.4	1.1	97.5	97.3
Pan	485.8	97.2		487.6	97.5		

Test No	1	2
Total mass of soil before washing [gm]	500.0	500.0
Total mass of soil after washing [gm]	14.2	12.4

Table B-5 Hydrometer analysis data for category-1

Mass of dry soil [gm]	50.0
Percent passing on sieve 0.075mm [%]	97.30
Specific gravity of solids	2.723
Correction factor, α	0.985

Elapsed Time [min]	Hydrometer reading	Composite Correction	Corrected Hydrometer	Temperature [^{o}C]	Effective Depth [cm]	Coefficient	Grain Size [mm]	Percentage Finer [%]	Percentage Finer Combined [%]
1	51	-3.6	47.4	21	8.5	0.01319	0.038	0.93	90.9
2	51	-3.6	47.4	21	8.5	0.01319	0.027	0.93	90.9
4	50	-3.6	46.4	21	8.7	0.01319	0.019	0.91	88.9
8	49	-3.6	45.4	21	8.8	0.01319	0.014	0.89	87.0
15	47	-3.4	43.7	22	9.1	0.01304	0.010	0.86	83.7
30	47	-3.4	43.7	22	9.1	0.01304	0.007	0.86	83.7
60	44	-3.4	40.7	22	9.6	0.01304	0.005	0.80	77.9
120	42	-3.4	38.7	22	10.0	0.01304	0.004	0.76	74.1
240	40	-3.4	36.7	22	10.3	0.01304	0.003	0.72	70.3
480	38	-3.1	34.9	23	10.6	0.01288	0.002	0.69	66.9
1440	36	-3.9	32.2	20	11.0	0.01336	0.001	0.63	61.6

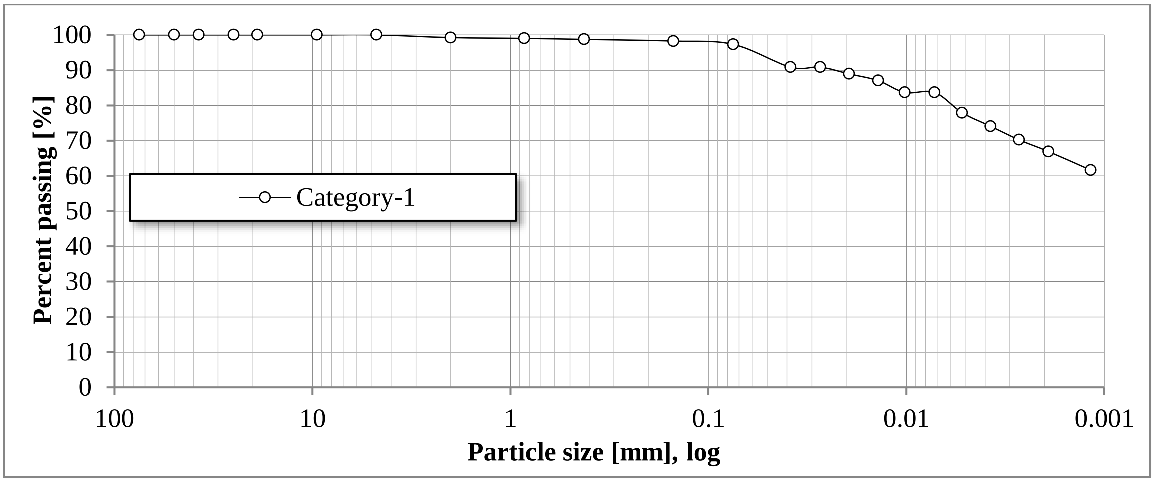

Figure B-1 Grain size distribution curve for category-1

B.3.2 Category-2 Subgrade Soil

Table B-6 Wet sieve analysis data for category-2

Sieve size [mm]	Mass retained [gm]	Percent retained [%]	Percent pass [%]	Mass retained [gm]	Percent retained [%]	Percent pass [%]	Average percent passing [%]
	Test No: 1			Test No: 2			
75	0	0	100	0	0	100	100
50	0	0	100	0	0	100	100
37.5	0	0	100	0	0	100	100
25	0	0	100	0	0	100	100
19	0	0	100	0	0	100	100
9.5	0	0	100	0	0	100	100
4.75	0.0	0.0	100.0	0.0	0.0	100.0	100.0
2	5.8	1.2	98.8	5.8	1.2	98.8	98.8
0.85	2.3	0.5	98.4	2.4	0.5	98.4	98.4
0.425	2.2	0.4	97.9	1.9	0.4	98.0	98.0
0.15	2.9	0.6	97.4	3.1	0.6	97.4	97.4
0.075	4.9	1.0	96.4	6.2	1.2	96.1	96.3
Pan	481.9	96.4		480.6	96.1		

Test No	1	2
Total mass of soil before washing [gm]	500.0	500.0
Total mass of soil after washing [gm]	18.1	19.4

Table B-7 Hydrometer analysis for category-2

Mass of dry soil [gm]	50.0
Percent passing on sieve 0.075mm [%]	96.30
Specific gravity of solids	2.588
Correction factor, α	1.012

Elapsed Time [min]	Hydrometer reading	Composite Correction	Corrected Hydrometer	Temperature [oC]	Effective Depth [cm]	Coefficient	Grain Size [mm]	Percentage Finer [%]	Percentage Finer Combined [%]
1	52	-3.6	48.4	21	8.4	0.01374	0.040	0.98	94.4
2	51	-3.6	47.4	21	8.5	0.01374	0.028	0.96	92.4
4	50	-3.6	46.4	21	8.7	0.01374	0.020	0.94	90.5
8	50	-3.6	46.4	21	8.7	0.01374	0.014	0.94	90.5
15	45	-3.6	41.4	21	9.5	0.01374	0.011	0.84	80.7
30	45	-3.6	41.4	21	9.5	0.01374	0.008	0.84	80.7
60	43	-3.4	39.7	22	9.8	0.01358	0.005	0.80	77.3
120	40	-3.4	36.7	22	10.3	0.01358	0.004	0.74	71.5
240	39	-3.1	35.9	23	10.4	0.01342	0.003	0.73	70.0
480	39	-3.6	35.4	21	10.5	0.01374	0.002	0.72	69.0
1440	33	-3.9	29.2	20	11.5	0.01391	0.001	0.59	56.8

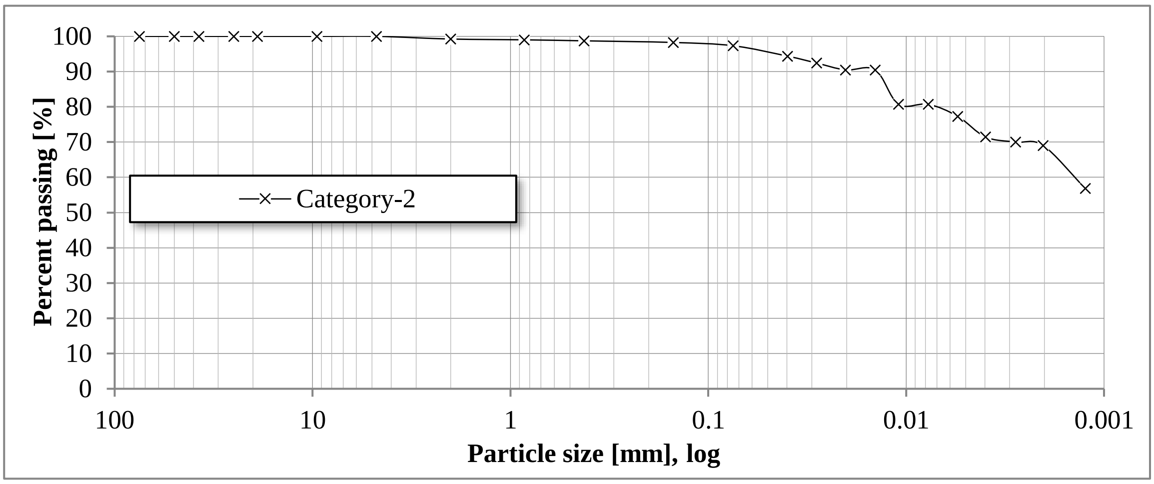

Figure B-2 Grain size distribution curve for category-2

B.3.3 Category-3 Subgrade Soil

Table B-8 Wet sieve analysis data for category-3

Sieve size [mm]	Mass retained [gm]	Percent retained [%]	Percent pass [%]	Mass retained [gm]	Percent retained [%]	Percent pass [%]	Average percent passing [%]
	Test No: 1			Test No: 2			
75	0	0	100	0	0	100	100
50	0	0	100	0	0	100	100
37.5	0	0	100	0	0	100	100
25	0	0	100	0	0	100	100
19	0	0	100	0	0	100	100
9.5	0	0	100	0	0	100	100
4.75	0.0	0.0	100.0	0.0	0.0	100.0	100.0
2	2.5	0.5	99.5	2.6	0.5	99.5	99.5
0.85	0.8	0.2	99.3	0.9	0.2	99.3	99.3
0.425	1.4	0.3	99.1	1.0	0.2	99.1	99.1
0.15	1.6	0.3	98.7	1.5	0.3	98.8	98.8
0.075	1.6	0.3	98.4	1.5	0.3	98.5	98.5
Pan	492.1	98.4		492.5	98.5		

Test No	1	2
Total mass of soil before washing [gm]	500.0	500.0
Total mass of soil after washing [gm]	7.9	7.5

Table B-9 Hydrometer analysis data for category-3

Mass of dry soil [gm]	50.0
Percent passing on sieve 0.075mm [%]	98.50
Specific gravity of solids	2.620
Correction factor, α	1.01

Elapsed Time [min]	Hydrometer reading	Composite Correction	Corrected Hydrometer	Temperature [ºC]	Effective Depth [cm]	Coefficient	Grain Size [mm]	Percentage Finer [%]	Percentage Finer Combined [%]
1	52	-3.6	48.4	21	8.4	0.01361	0.039	0.97	95.9
2	51	-3.6	47.4	21	8.5	0.01361	0.028	0.95	93.9
4	50	-3.6	46.4	21	8.7	0.01361	0.020	0.93	92.0
8	50	-3.6	46.4	21	8.7	0.01361	0.014	0.93	92.0
15	49	-3.6	45.4	21	8.8	0.01361	0.010	0.91	90.0
30	46	-3.4	42.7	22	9.3	0.01350	0.008	0.86	84.5
60	45	-3.4	41.7	22	9.5	0.01350	0.005	0.84	82.5

Elapsed Time [min]	Hydrometer reading	Composite Correction	Corrected Hydrometer	Temperature [oC]	Effective Depth [cm]	Coefficient	Grain Size [mm]	Percentage Finer [%]	Percentage Finer Combined [%]
120	43	-3.4	39.7	22	9.8	0.01350	0.004	0.80	78.6
240	41	-3.4	37.7	22	10.1	0.01350	0.003	0.76	74.6
480	40	-3.4	36.7	22	10.3	0.01350	0.002	0.74	72.6
1440	37	-3.6	33.4	21	10.8	0.01361	0.001	0.67	66.2

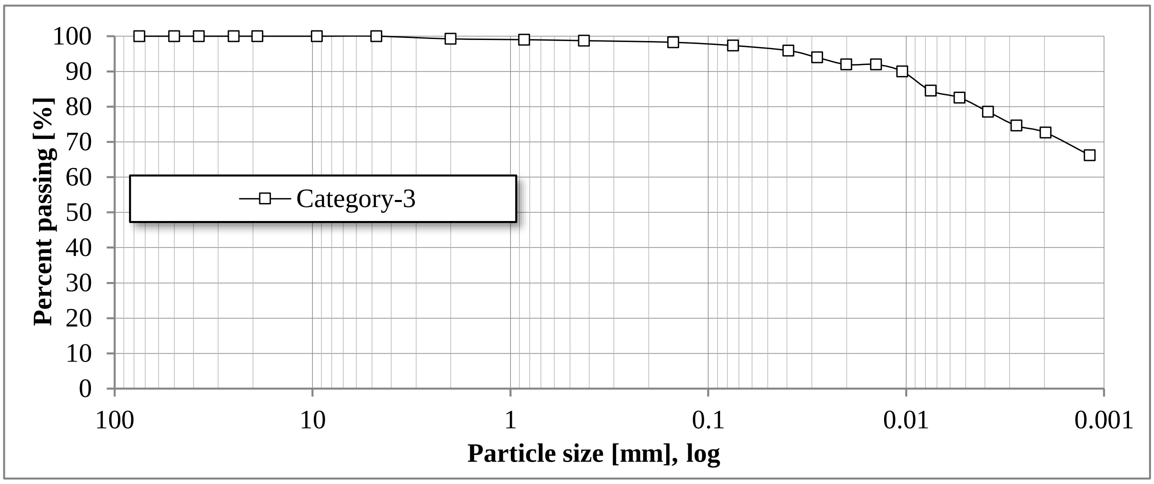

Figure B-3 Grain size distribution curve for category-3

B.3.4 Replacement Material

Table B-10 Wet sieve analysis data for replacement material

Sieve size [mm]	Mass retained [gm]	Percent retained [%]	Percent pass [%]	Mass retained [gm]	Percent retained [%]	Percent pass [%]	Average percent passing [%]
	Test No: 1			Test No: 2			
75	0	0	100	0	0	100	100
50	186.2	3.3	96.7	166.2	3.1	96.9	96.8
37.5	456.0	8.0	88.7	387.6	7.1	89.8	89.3
25	366.7	6.4	82.3	365.2	6.7	83.1	82.7
19	241.0	4.2	78.1	333.6	6.1	77.0	77.5
9.5	257.6	4.5	73.6	209.8	3.9	73.1	73.4
4.75	193.6	3.4	70.2	211.9	3.9	69.2	69.7
2	198.0	3.5	66.7	183.4	3.4	65.9	66.3
0.85	102.5	1.8	64.9	98.3	1.8	64.0	64.5
0.425	191.2	3.4	61.6	126.9	2.3	61.7	61.6
0.15	158.9	2.8	58.8	124.1	2.3	59.4	59.1
0.075	129.3	2.3	56.5	125.4	2.3	57.1	56.8
Pan	3225.9	56.5		3107.8	57.1		

Test No	1	2
Total mass of soil before washing [gm]	5706.9	5440.2
Total mass of soil after washing [gm]	2481.0	2332.4

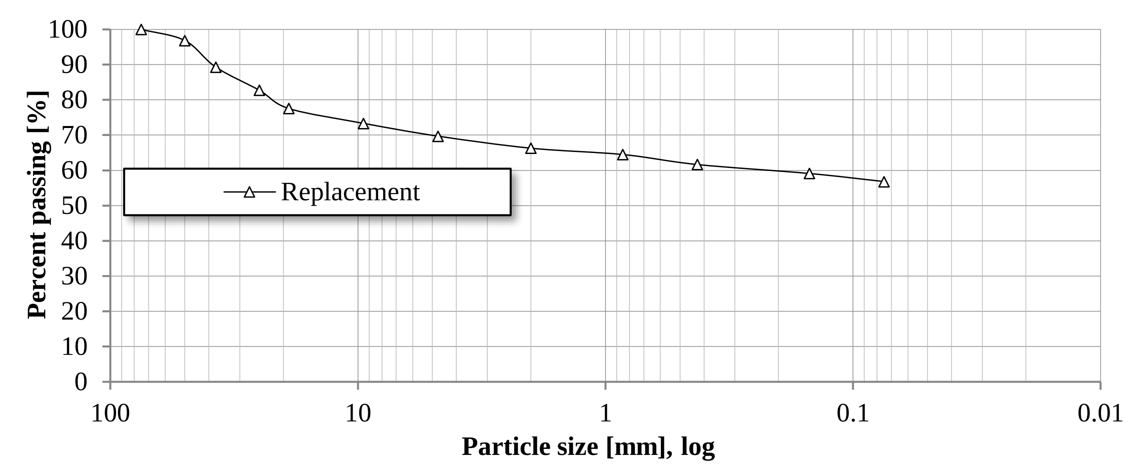

Figure B-4 Grain size distribution curve for replacement material

B.4 Atterberg Limits Determination

B.4.1 Category-1 Subgrade Soil

Table B-11 Liquid limit, plastic limit, plasticity index, and linear shrinkage test data using method-1

Liquid Limit				Plastic Limit	
Trial No	1	2	3	1	2
Container No	z1	8	v	md	3
Mass of wet soil + container [gm]	48.19	48.33	48.58	10.19	10.16
Mass of dry soil + container [gm]	36.51	36.54	35.94	9.02	9.05
Mass of container [gm]	17.46	18.17	17.55	6.57	6.71
Mass of water [gm]	11.68	11.79	12.64	1.17	1.11
Mass of dry soil [gm]	19.05	18.37	18.39	2.45	2.34
Moisture content [%]	61.3	64.2	68.7	47.8	47.4
Number of blows [N]	32	27	18	47.6	

Liquid Limit (LL), [%]	65
Average Plastic Limit (PL), [%]	48
Plasticity Index, PI = (LL - PL), [%]	17

Linear Shrinkage		
Test No	1	2
Specimen reference	A	A
Initial length, [mm]	140	140
Oven-dried length, [mm]	118	118.2
Linear Shrinkage, [%]	15.7	15.6
Average, [%]	15.65	

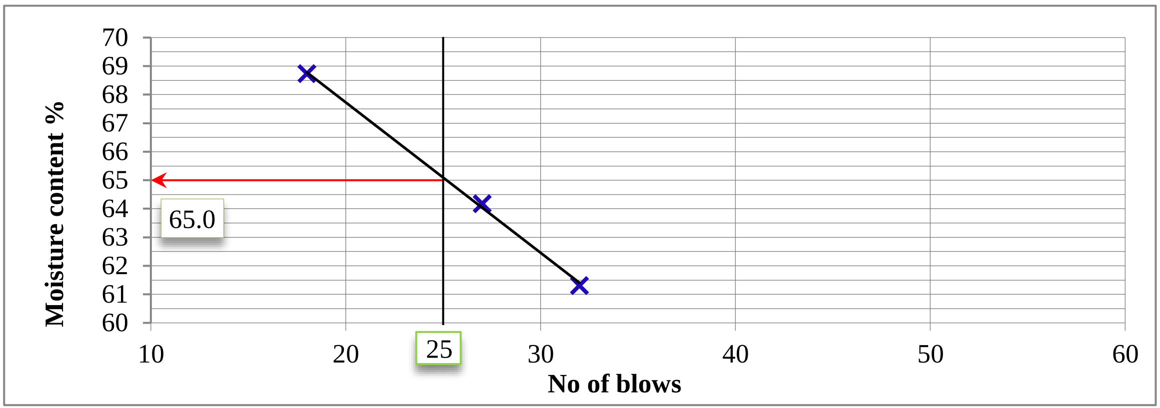

Figure B-5 Flow curve for liquid limit determination at 25 blows using method-1

Table B-12 Classification for results obtained using method-1

Group Index (GI)	26
AASHTO Classification (AASHTO M 145-91)	A-7-5 (26)
Unified Soil Classification System (ASTM D 2487-11)	MH
Activity (A)	0.25

Table B-13 Liquid limit test data using method-2

Liquid Limit			
Trial No	1	2	3
Container No	1	2	A4
Mass of wet soil + container [gm]	50.46	51.20	51.73
Mass of dry soil + container [gm]	38.00	38.42	38.41
Mass of container [gm]	18.04	18.36	17.85
Mass of water [gm]	12.46	12.78	13.32
Mass of dry soil [gm]	19.96	20.06	20.56
Moisture content [%]	62.4	63.7	64.8
Number of blows [N]	33	27	19

Liquid Limit (LL), [%]	64

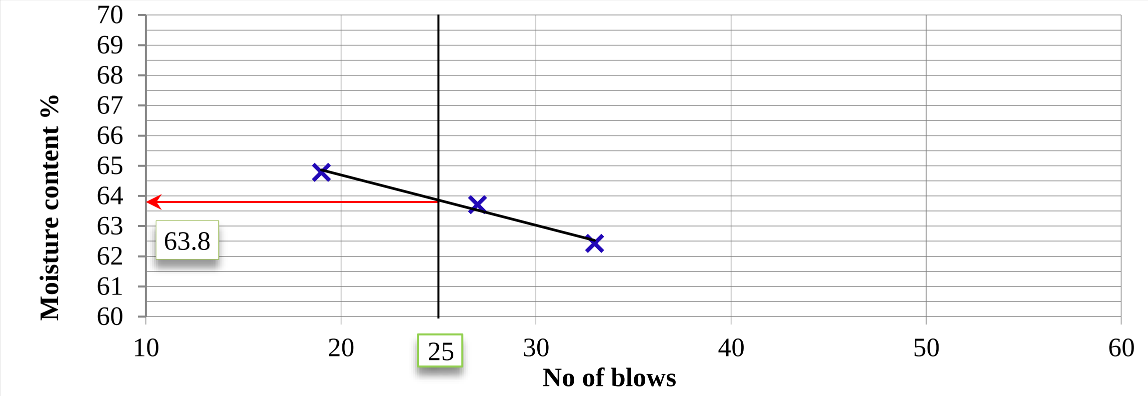

Figure B-6 Flow curve for liquid limit determination at 25 blows using method-2

Table B-14 Classification for results obtained using method-2

Group Index (GI)	25
AASHTO Classification (AASHTO M 145-91)	A-7-5 (25)
Unified Soil Classification System (ASTM D 2487-11)	MH
Activity (A)	0.24

B.4.2 Category-2 Subgrade Soil

Table B- 15 Liquid limit, plastic limit, plasticity index, and linear shrinkage test data using method-1

	Liquid Limit			Plastic Limit	
Trial No	1	2	3	1	2
Container No	B	1	8	NO	CH
Mass of wet soil + container [gm]	50.66	51.64	50.05	10.21	10.21
Mass of dry soil + container [gm]	38.56	38.50	36.67	9.06	9.11
Mass of container [gm]	18.57	18.30	17.3	6.58	6.75
Mass of water [gm]	12.10	13.14	13.38	1.15	1.1
Mass of dry soil [gm]	19.99	20.20	19.37	2.48	2.36
Moisture content [%]	60.5	65.0	69.1	46.4	46.6
Number of blows [N]	31	26	17	46.5	

Liquid Limit (LL), [%]	65
Average Plastic Limit (PL), [%]	46
Plasticity Index, PI = (LL - PL), [%]	19

Linear Shrinkage		
Test No	1	2
Specimen reference	A	A
Initial length, [mm]	140	140
Oven-dried length, [mm]	119	118.8
Linear Shrinkage, [%]	15	15.1
Average, [%]	15.05	

Figure B-7 Flow curve for liquid limit determination at 25 blows using method-1

Table B-16 Classification for results obtained using method-1

Group Index (GI)	27
AASHTO Classification (AASHTO M 145-91)	A-7-5 (27)
Unified Soil Classification System (ASTM D 2487-11)	MH
Activity (A)	0.27

Table B-17 Liquid limit determination test data using method-2

Liquid Limit			
Trial No	1	2	3
Container No	B	C1	41
Mass of wet soil + container [gm]	48.41	49.24	49.18
Mass of dry soil + container [gm]	37.46	37.99	37.15
Mass of container [gm]	18.04	18.87	17.43
Mass of water [gm]	10.95	11.25	12.03
Mass of dry soil [gm]	19.42	19.12	19.72
Moisture content [%]	56.4	58.8	61.0
Number of blows [N]	34	27	17

Liquid Limit (LL), [%]	59

Linear Shrinkage		
Test No	1	2
Specimen reference	A	A
Initial length, [mm]	140	140
Oven-dried length, [mm]	121.5	121
Linear Shrinkage, [%]	13.2	13.6
Average, [%]	13.4	

Figure B-8 Flow curve for liquid limit determination at 25 blows using method-2

Table B-18 Classification for results obtained using method-2

Group Index (GI)	21
AASHTO Classification (AASHTO M 145-91)	A-7-5 (21)
Unified Soil Classification System (ASTM D 2487-11)	MH
Activity (A)	0.19

B.4.3 Category-3 Subgrade Soil

Table B-19 Liquid limit, plastic limit, plasticity index, and linear shrinkage test data using method-1

Liquid Limit				Plastic Limit	
Trial No	1	2	3	1	2
Container No	H1	A1	S1	M1	C3
Mass of wet soil + container [gm]	47.90	48.23	48.37	11.55	11.53
Mass of dry soil + container [gm]	35.76	35.77	35.5	9.92	9.99
Mass of container [gm]	17.09	17.41	16.69	6.44	6.7
Mass of water [gm]	12.14	12.46	12.87	1.63	1.54
Mass of dry soil [gm]	18.67	18.36	18.81	3.48	3.29
Moisture content [%]	65.0	67.9	68.4	46.8	46.8
Number of blows [N]	33	28	20	46.8	

Liquid Limit (LL), [%]	68
Average Plastic Limit (PL), [%]	47
Plasticity Index, PI = (LL - PL), [%]	21

Linear Shrinkage		
Test No	1	2
Specimen reference	A	A
Initial length, [mm]	140	140
Oven-dried length, [mm]	117	118
Linear Shrinkage, [%]	16.4	15.7
Average, [%]	16.05	

Figure B-9 Flow curve for liquid limit determination at 25 blows using method-1

Table B-20 Classification for results obtained using method-1

Group Index (GI)	30
AASHTO Classification (AASHTO M 145-91)	A-7-5 (30)
Unified Soil Classification System (ASTM D 2487-11)	MH
Activity (A)	0.28

Table B-21 Liquid limit determination test data using method-2

Liquid Limit			
Trial No	1	2	3
Container No	68	m1	7
Mass of wet soil + container [gm]	48.64	48.43	47.53
Mass of dry soil + container [gm]	36.84	36.72	35.75
Mass of container [gm]	17.43	18.11	17.11
Mass of water [gm]	11.80	11.71	11.78
Mass of dry soil [gm]	19.41	18.61	18.64
Moisture content [%]	60.8	62.9	63.2
Number of blows [N]	33	26	16

Liquid Limit (LL), [%]	62.3

Linear Shrinkage		
Test No	1	2
Specimen reference	A	A
Initial length, [mm]	140	140
Oven-dried length, [mm]	120	120
Linear Shrinkage, [%]	14.3	14.3
Average, [%]	14.3	

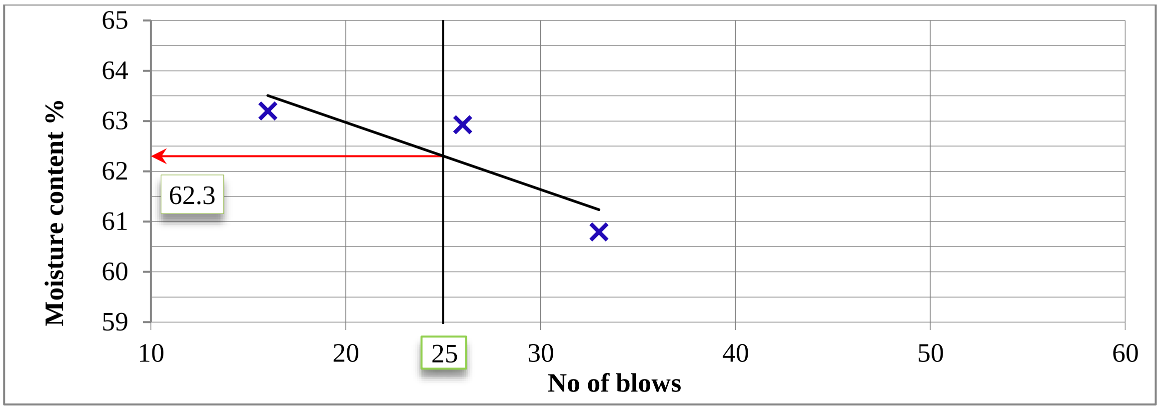

Figure B-10 Flow curve for liquid limit determination at 25 blows using method-2

Table B-22 Classification for results obtained using method-2

Group Index (GI)	24
AASHTO Classification (AASHTO M 145-91)	A-7-5 (24)
Unified Soil Classification System (ASTM D 2487-11)	MH
Activity (A)	0.21

B.4.4 Replacement Material

Table B- 23 Liquid limit, plastic limit, plasticity index, and linear shrinkage test data using method-1

Liquid Limit				Plastic Limit	
Trial No	1	2	3	1	2
Container No	c1	2	E	A1	L
Mass of wet soil + container [gm]	48.63	48.24	47.24	9.16	9.29
Mass of dry soil + container [gm]	39.85	39.09	37.94	8.57	8.69
Mass of container [gm]	18.83	18.14	18.77	6.75	6.9
Mass of water [gm]	8.78	9.15	9.3	0.59	0.6
Mass of dry soil [gm]	21.02	20.95	19.17	1.82	1.79
Moisture content [%]	41.8	43.7	48.5	32.4	33.5
Number of blows [N]	32	28	17	33.0	

Liquid Limit (LL), [%]	45
Average Plastic Limit (PL), [%]	33
Plasticity Index, PI = (LL - PL), [%]	12

Linear Shrinkage		
Test No	1	2
Initial length, [mm]	A	A
Oven-dried length, [mm]	140	140
Linear Shrinkage, [%]	131	130.5
Linear Shrinkage	6.4	6.8
Average, [%]	6.6	

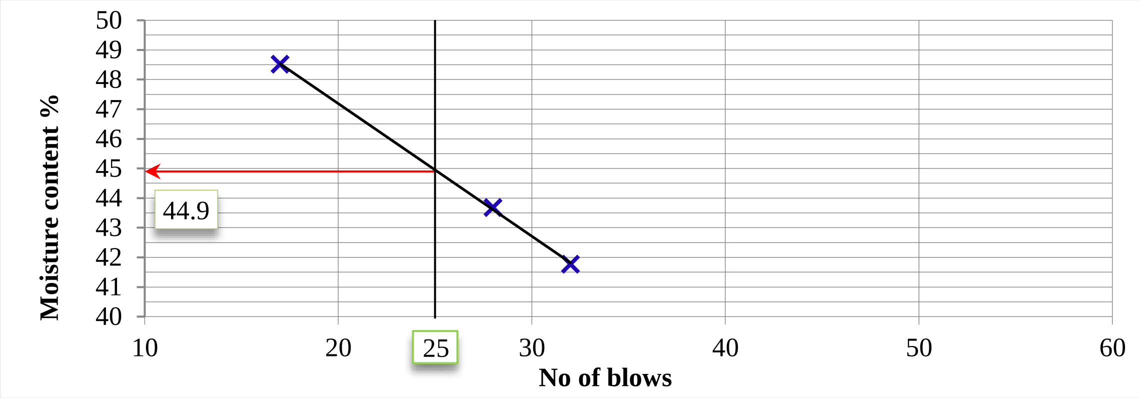

Figure B-11 Flow curve for liquid limit determination at 25 blows using method-1

Table B-24 Classification for results obtained using method-1

Group Index (GI)	6
AASHTO Classification (AASHTO M 145-91)	A-7-5 (6)
Unified Soil Classification System (ASTM D 2487-11)	ML

B.5 Moisture-Density Relationship Determination

B.5.1 Category-1 Subgrade Soil

Table B-25 Moisture-density relationship data for category-1

Bulk density determination

Trial Number	1	2	3	4
Mass of dry soil before adding water [gm]	3000	3000	3000	3000
Amount of water added [gm]	300	450	600	750
Mass of mold + base [gm]	4404	4404	4404	4404
Mass of soil + mold [gm]	6063.6	6135.6	6230.7	6219.9
Mass of soil [gm]	1659.6	1731.6	1826.7	1815.9
Bulk density of soil [Kg/m3]	1769.5	1846.3	1947.7	1936.2

Moisture and dry density determination

Container No	W	LM	D8	F
Mass of wet soil + container [gm]	475.5	453.8	402.8	406.4
Mass of dry soil + container [gm]	407.4	381.8	336.1	330.0
Mass of container [gm]	124.7	121.6	125.5	122.4
Mass of water [gm]	68.1	72.0	66.7	76.4
Mass of dry soil [gm]	282.7	260.2	210.6	207.6
Moisture content [%]	24.09	27.67	31.67	36.80
Dry density of soil [Kg/m3]	1426.0	1446.1	1479.2	1415.3

Optimum Moisture Content (OMC) [%]	31.2
Maximum Dry Density (MDD) [Kg/m3]	1480

Note: The volume of mold is 937.9 cm^3 and each trial had five layers of compaction, with 25 blows per layer.

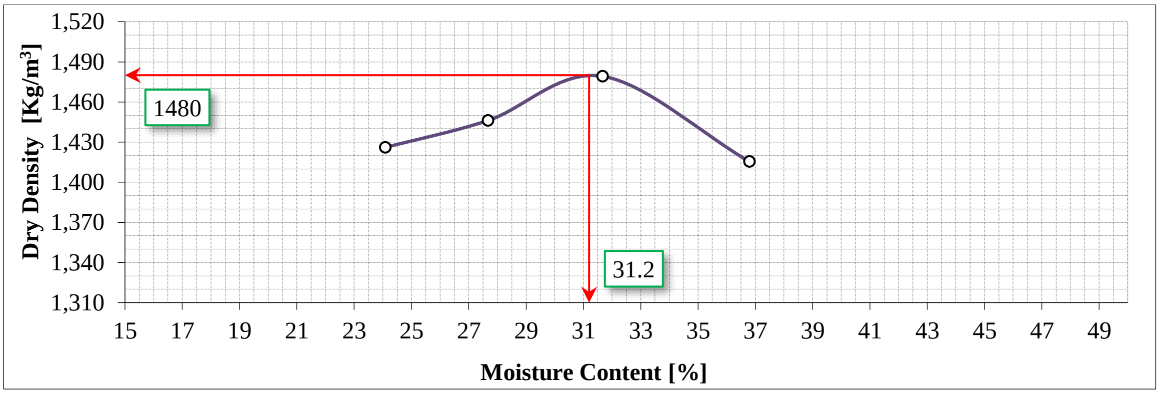

Figure B-12 Moisture-density curve for category-1

B.5.2 Category-2 Subgrade Soil

Table B-26 Moisture-density relationship data for category-2

Bulk density determination

Trial Number	1	2	3	4
Mass of dry soil before adding water [gm]	3000	3000	3000	3000
Amount of water added [gm]	240	420	600	780
Mass of mold + base [gm]	4404	4404	4404	4404
Mass of soil + mold [gm]	6005.1	6115.5	6184.8	6132.8
Mass of soil [gm]	1601.1	1711.5	1780.8	1728.8
Bulk density of soil [Kg/m3]	1707.1	1824.9	1898.7	1843.3

Moisture and dry density determination

Container No	H	A	K	MD
Mass of wet soil + container [gm]	512.6	505.0	507.0	505.4
Mass of dry soil + container [gm]	435.8	425.6	415.5	405.3
Mass of container [gm]	118.1	134.3	118.7	114.9
Mass of water [gm]	76.8	79.4	91.5	100.1
Mass of dry soil [gm]	317.7	291.3	296.8	290.4
Moisture content [%]	24.17	27.26	30.83	34.47
Dry density of soil [Kg/m3]	1374.8	1434.0	1451.3	1370.8

Optimum Moisture Content (OMC)	30
Maximum Dry Density (MDD)	1454

Note: The volume of mold is 937.9 cm^3 and each trial had five layers of compaction, with 25 blows per layer.

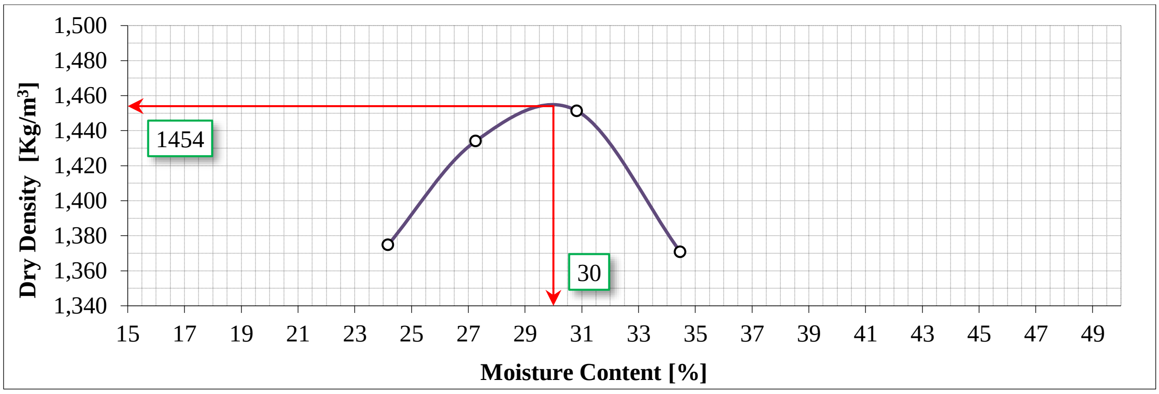

Figure B-13 Moisture-density curve for category-2

B.5.3 Category-3 Subgrade Soil

Table B-27 Moisture-density relationship data for category-3

Bulk density determination

Trial Number	1	2	3	4
Mass of dry soil before adding water [gm]	3000	3000	3000	3000
Amount of water added [gm]	360	480	600	720
Mass of mold + base [gm]	4404	4404	4404	4404
Mass of soil + mold [gm]	5908	6009.2	6149.2	6105.1
Mass of soil [gm]	1504	1605.2	1745.2	1701.1
Bulk density of soil [Kg/m3]	1603.6	1711.5	1860.8	1813.8

Moisture and dry density determination

Container No	B	V8	NS	P
Mass of wet soil + container [gm]	481.9	490.9	452.4	422.4
Mass of dry soil + container [gm]	418.4	415.3	377.5	345.2
Mass of container [gm]	126.6	123.4	133.8	119.1
Mass of water [gm]	63.5	75.6	74.9	77.2
Mass of dry soil [gm]	291.8	291.9	243.7	226.1
Moisture content [%]	21.76	25.90	30.73	34.14
Dry density of soil [Kg/m3]	1317.0	1359.4	1423.3	1352.1

Optimum Moisture Content (OMC)	30.7
Maximum Dry Density (MDD)	1424

Note: The volume of mold is 937.9 cm^3 and each trial had five layers of compaction, with 25 blows per layer.

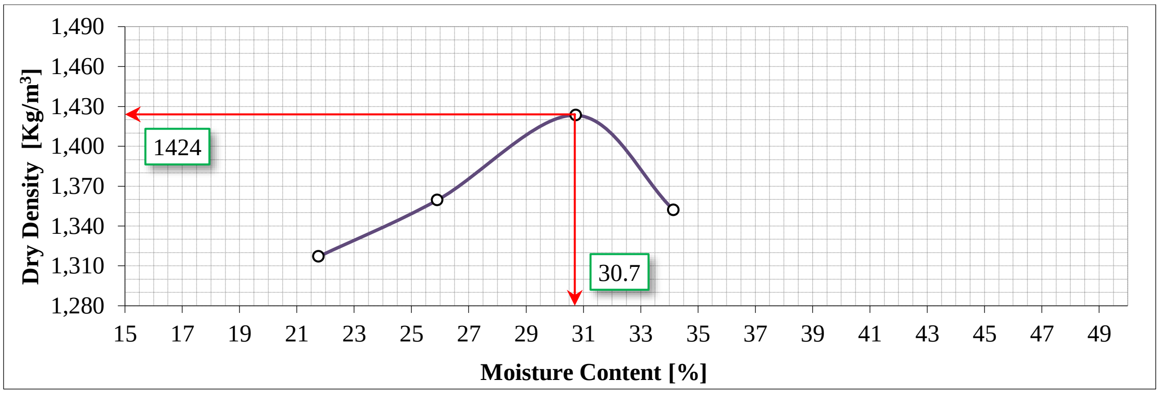

Figure B-14 Moisture-density curve for category-3

B.5.4 Replacement Material

Table B-28 Moisture-density relationship data for replacement material

Bulk density determination

Trial Number	1	2	3	4
Mass of dry soil before adding water [gm]	6000	6000	6000	6000
Amount of water added [gm]	120	240	360	480
Mass of mold + base [gm]	4898.8	4898.8	4898.8	4898.8
Mass of soil + mold [gm]	8763.9	8998	9222.5	9260.3
Mass of soil [gm]	3865.1	4099.2	4323.7	4361.5
Bulk density of soil [Kg/m3]	1816.3	1926.3	2031.8	2049.6

Moisture and dry density determination

Container No	D	CC	MD	EC
Mass of wet soil + container [gm]	560.0	547.9	569.5	567.4
Mass of dry soil + container [gm]	528.5	509.2	518.6	503.3
Mass of container [gm]	118.0	114.9	128.6	118.6
Mass of water [gm]	31.5	38.7	50.9	64.1
Mass of dry soil [gm]	410.5	394.3	390.0	384.7
Moisture content [%]	7.67	9.81	13.05	16.66
Dry density of soil [Kg/m3]	1686.9	1754.1	1797.2	1756.8

Optimum Moisture Content (OMC)	13.2
Maximum Dry Density (MDD)	1798

Note: The volume of mold is 2128 cm^3 and each trial had five layers of compaction, with 56 blows per layer.

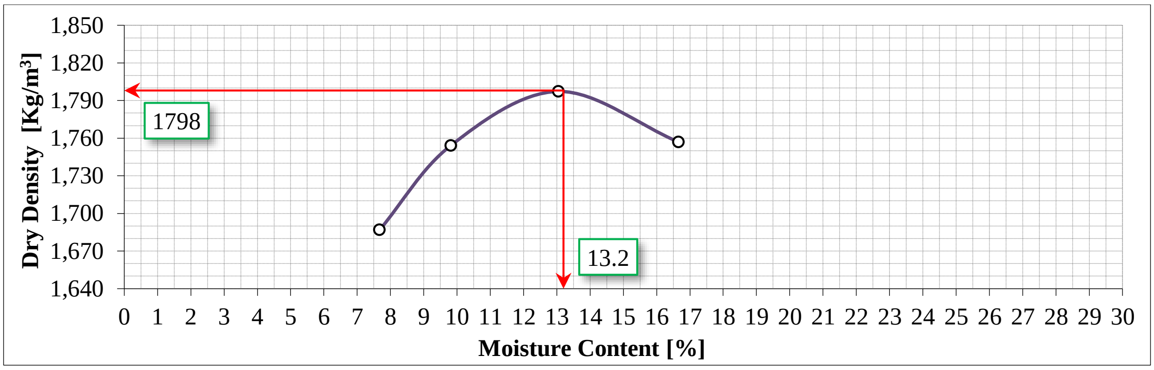

Figure B-15 Moisture-density curve for replacement material

B.6 CBR Value Determination

B.6.1 Category-1 Subgrade Soil

Table B-29 CBR test data for category-1

Determination of wet-density

Mold No.	7		AZ		CD	
No. of Layers	5		5		5	
No. of Blows per Layer	10		30		65	
Condition of sample (Before / After Soaking)	Before	After	Before	After	Before	After
Wt. of Wet Soil + Mold [gm]	11294.8	11483.8	11747.3	12019.8	11926.7	12044.8
Wt. of Mold [gm]	7687.7	7687.7	7743.3	7743.3	7682.5	7682.5
Wt. of Wet Soil [gm]	3607.1	3796.1	4004.0	4276.5	4244.2	4362.3
Wet Density [Kg/m^3]	1682.9	1771.1	1868.1	1995.2	1980.2	2035.3

Determination of moisture content and dry-density

Condition of sample (Before / After Soaking)	Before	After	Before	After	Before	After
Container No.	N	V8	EC	L	DU	T
Wt. of Container + Wet Soil [gm]	457.8	430.0	447.3	423.6	432.1	436.8
Wt. of Container + Dry Soil [gm]	380.3	336.0	370.7	339.8	358.0	351.7
Wt. of Container [gm]	134.2	123.7	118.9	125.9	118.5	127.2
Wt. of Moisture [gm]	77.5	94.0	76.6	83.8	74.1	85.1
Wt. of Dry Soil [gm]	246.1	212.3	251.8	213.9	239.5	224.5
Moisture Content [%]	31.49	44.28	30.42	39.18	30.94	37.91
Dry Unit Weight [Kg/m^3]	1279.9	1227.6	1432.3	1433.6	1512.3	1475.8

Note: The volume of mold is 2143 cm^3.

Penetration and CBR data

Penetration [mm]	Standard stress [Mpa]	10 Blows			30 Blows			65 Blows		
		Gauge Reading	Stress [Mpa]	CBR [%]	Gauge Reading	Stress [Mpa]	CBR [%]	Gauge Reading	Stress [Mpa]	CBR [%]
0		0	0		0	0		0	0	
0.64		5	0.14		6	0.16		6	0.16	
1.27		8	0.22		13	0.35		16	0.43	
1.91		11	0.30		21	0.57		27	0.73	
2.54	6.9	13	0.35	5.10	29	0.79	11.39	38	1.03	14.92
3.81		15	0.41		38	1.03		51	1.38	
5.08	10.3	17	0.46	4.47	42	1.14	11.05	56	1.52	14.73

Note: The penetration rate was 1.27 min/minutes.

Swell data

No. of Blows per Layer		10			30			65		
Condition	Elapse time [Hours]	Gauge reading	Swell		Gauge reading	Swell		Gauge reading	Swell	
			mm	%		mm	%		mm	%
Soaked	0	0.00	2.76	2.37	0.00	2.08	1.79	0.00	1.82	1.56
Tested	96	2.76			2.08			1.82		

Note: Initial height of sample is 116.43 mm.

95 % of MDD [Kg/m^3]	1406
CBR at 95 % MDD [%]	10.2
Swell at 95 % MDD [%]	1.9

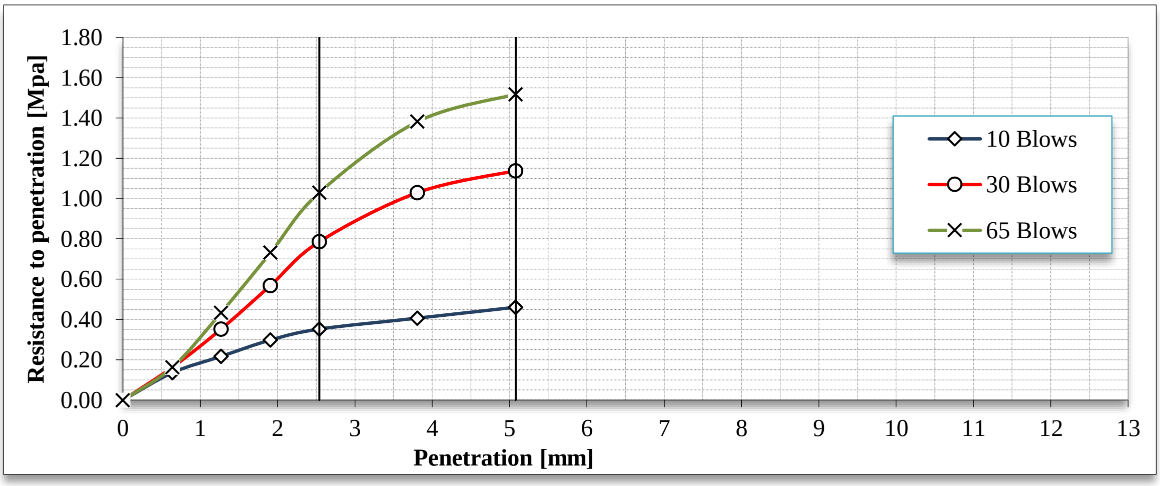

Figure B-16 Stress-Strain (penetration) curve for category-1

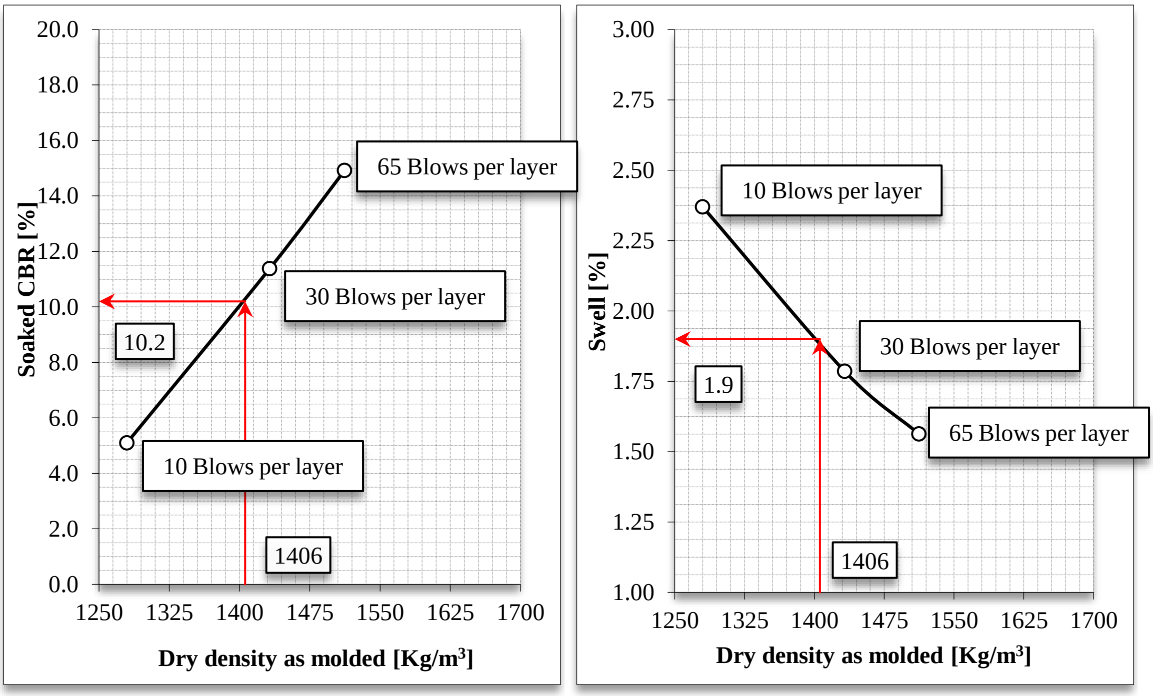

(a) (b)

Figure B-17 (a) Soaked CBR-Dry density & (b) Swell-Dry density curves for category-1

B.6.2 Category-2 Subgrade Soil

Table B-30 CBR test data for category-2

Determination of wet-density

Mold No.	4		9		B	
No. of Layers	5		5		5	
No. of Blows per Layer	10		30		65	
Condition of sample (Before / After Soaking)	Before	After	Before	After	Before	After
Wt. of Wet Soil + Mold [gm]	10486.6	10912.4	11857.7	12155.8	11589.0	11782.7
Wt. of Mold [gm]	7084.3	7084.3	8002.5	8002.5	7401.2	7401.2
Wt. of Wet Soil [gm]	3402.3	3828.1	3855.2	4153.3	4187.8	4381.5
Wet Density [Kg/m^3]	1587.4	1786.0	1798.7	1937.7	1953.8	2044.2

Determination of moisture content and dry-density

Condition of sample (Before / After Soaking)	Before	After	Before	After	Before	After
Container No.	TM	K	CR	O	B	A
Wt. of Container + Wet Soil [gm]	464.4	439.3	457.3	463.4	421.1	459.3
Wt. of Container + Dry Soil [gm]	384.8	345.2	380.0	368.1	352.9	366.8
Wt. of Container [gm]	130.1	116.8	128.0	128.0	127.1	126.6
Wt. of Moisture [gm]	79.6	94.1	77.3	95.3	68.2	92.5
Wt. of Dry Soil [gm]	254.7	228.4	252.0	240.1	225.8	240.2
Moisture Content [%]	31.25	41.20	30.67	39.69	30.20	38.51
Dry Unit Weight [Kg/m^3]	1209.4	1264.9	1376.4	1387.2	1500.6	1475.9

Note: The volume of mold is 2143 cm^3

Penetration and CBR data

Penetration [mm]	Standard stress [Mpa]	10 Blows			30 Blows			65 Blows		
		Gauge Reading	Stress [Mpa]	CBR [%]	Gauge Reading	Stress [Mpa]	CBR [%]	Gauge Reading	Stress [Mpa]	CBR [%]
0		0	0.00		0	0.00		0	0.00	
0.64		3	0.08		6	0.16		9	0.24	
1.27		6	0.16		10	0.27		14	0.38	
1.91		8	0.22		14	0.38		18	0.49	
2.54	6.9	10	0.27	3.93	18	0.49	7.07	22	0.60	8.64
3.81		13	0.35		23	0.62		28	0.76	
5.08	10.3	16	0.43	4.21	28	0.76	7.37	35	0.95	9.21

Note: The penetration rate was 1.27 min/minutes.

Swell data

No. of Blows per Layer		10			30			65		
Condition	Elapse time [Hours]	Gauge reading	Swell		Gauge reading	Swell		Gauge reading	Swell	
			mm	%		mm	%		mm	%
Soaked	0	0.00	7.40	6.36	0.00	5.24	4.50	0.00	3.89	3.34
Tested	96	7.40			5.24			3.89		

Note: Initial height of sample is 116.43 mm.

95 % of MDD [Kg/m^3]	1381.3
CBR at 95 % MDD [%]	7.2
Swell at 95 % MDD [%]	4.5

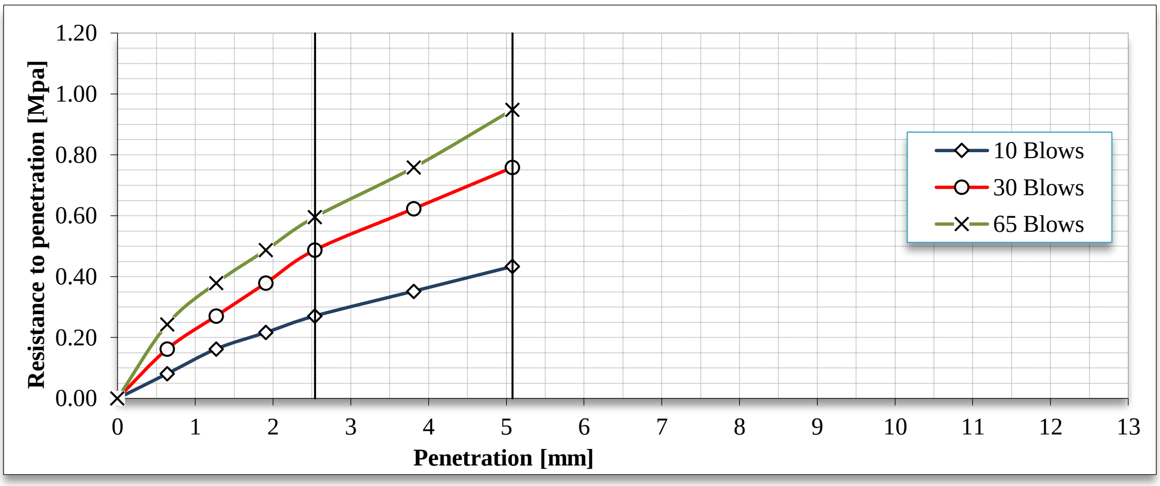

Figure B-18 Stress-Strain (penetration) curve for category-2

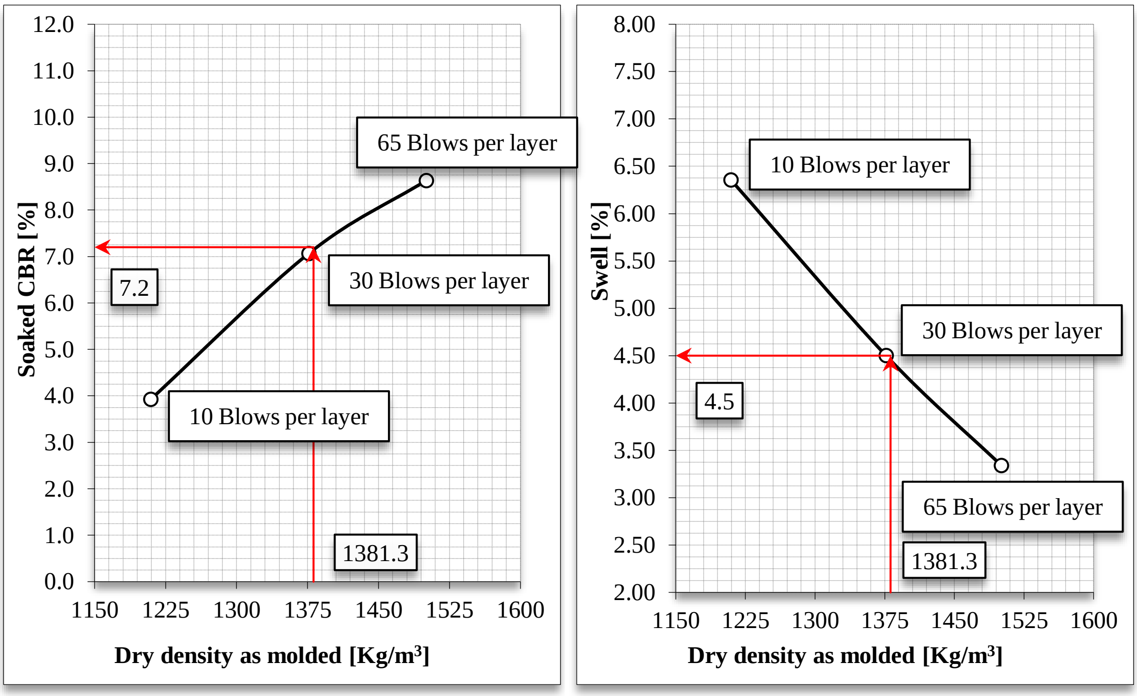

(a) (b)

Figure B-19 (a) Soaked CBR-Dry density & (b) Swell-Dry density curves for category-2

B.6.3 Category-3 Subgrade Soil

Table B-31 CBR test data for category-3

Determination of wet-density

Mold No.	8		65		CD	
No. of Layers	5		5		5	
No. of Blows per Layer	10		30		65	
Condition of sample (Before / After Soaking)	Before	After	Before	After	Before	After
Wt. of Wet Soil + Mold [gm]	10140.8	10691.8	11496.2	11874.3	11377.3	11702.9
Wt. of Mold [gm]	6916.8	6916.8	7775.3	7775.3	7357.0	7357.0
Wt. of Wet Soil [gm]	3224.0	3775.0	3720.9	4099.0	4020.3	4345.9
Wet Density [Kg/m3]	1504.2	1761.2	1736.0	1912.4	1875.7	2027.6

Determination of moisture content and dry-density

Condition of sample (Before / After Soaking)	Before	After	Before	After	Before	After
Container No.	L	V8	SM	TM	U8	I
Wt. of Container + Wet Soil [gm]	528.1	532.0	525.6	559.1	569.8	492.8
Wt. of Container + Dry Soil [gm]	437.3	408.8	432.7	431.9	465.1	386.2
Wt. of Container [gm]	125.3	123.0	129.7	129.3	123.4	126.1
Wt. of Moisture [gm]	90.8	123.2	92.9	127.2	104.7	106.6
Wt. of Dry Soil [gm]	312.0	285.8	303.0	302.6	341.7	260.1
Moisture Content [%]	29.10	43.11	30.66	42.04	30.64	40.98
Dry Unit Weight [Kg/m3]	1165.1	1230.7	1328.6	1346.4	1435.8	1438.2

Note: The volume of mold is 2143 cm^3

Penetration and CBR data

Penetration [mm]	Standard stress [Mpa]	10 Blows			30 Blows			65 Blows		
		Gauge Reading	Stress [Mpa]	CBR [%]	Gauge Reading	Stress [Mpa]	CBR [%]	Gauge Reading	Stress [Mpa]	CBR [%]
0		0	0.00		0	0.00		0	0.00	
0.64		1	0.03		3	0.08		4	0.11	
1.27		2	0.05		4	0.11		5	0.14	
1.91		3	0.08		5	0.14		6	0.16	
2.54	6.9	4	0.11	1.57	6	0.16	2.36	7	0.19	2.75
3.81		6	0.16		8	0.22		9	0.24	
5.08	10.3	8	0.22	2.10	10	0.27	2.63	11	0.30	2.89

Note: The penetration rate was 1.27 min/minutes.

Swell data

No. of Blows per Layer		10			30			65		
Condition	Elapse time [Hours]	Gauge reading	Swell		Gauge reading	Swell		Gauge reading	Swell	
			mm	%		mm	%		mm	%
Soaked	0	0.00	8.63	7.41	0.00	7.58	6.51	0.00	6.32	5.43
Tested	96	8.63			7.58			6.32		

Note: Initial height of sample is 116.43 mm.

95 % of MDD [Kg/m3]	1352.8
CBR at 95 % MDD [%]	2.5
Swell at 95 % MDD [%]	6.3

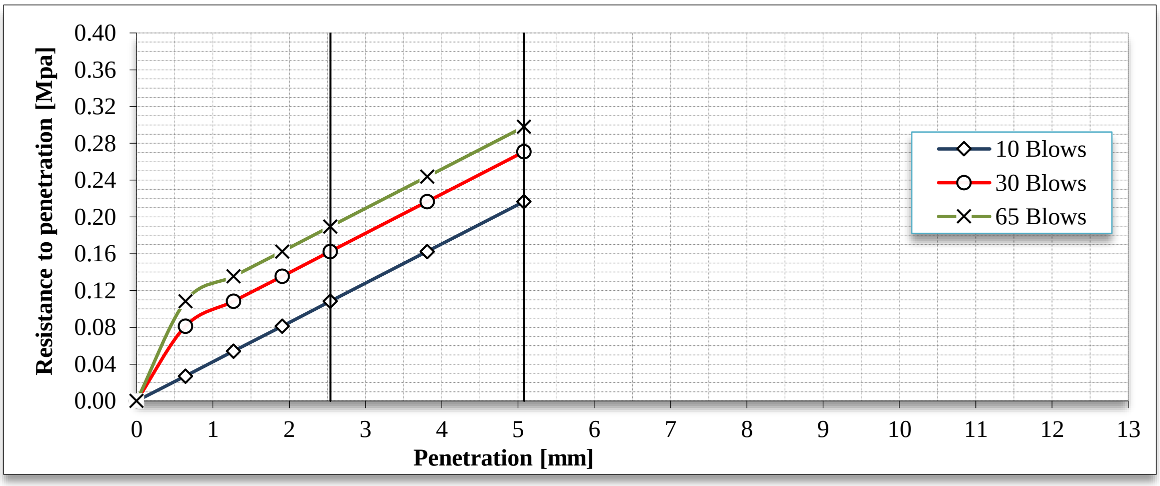

Figure B-20 Stress-Strain (penetration) curve for category-3

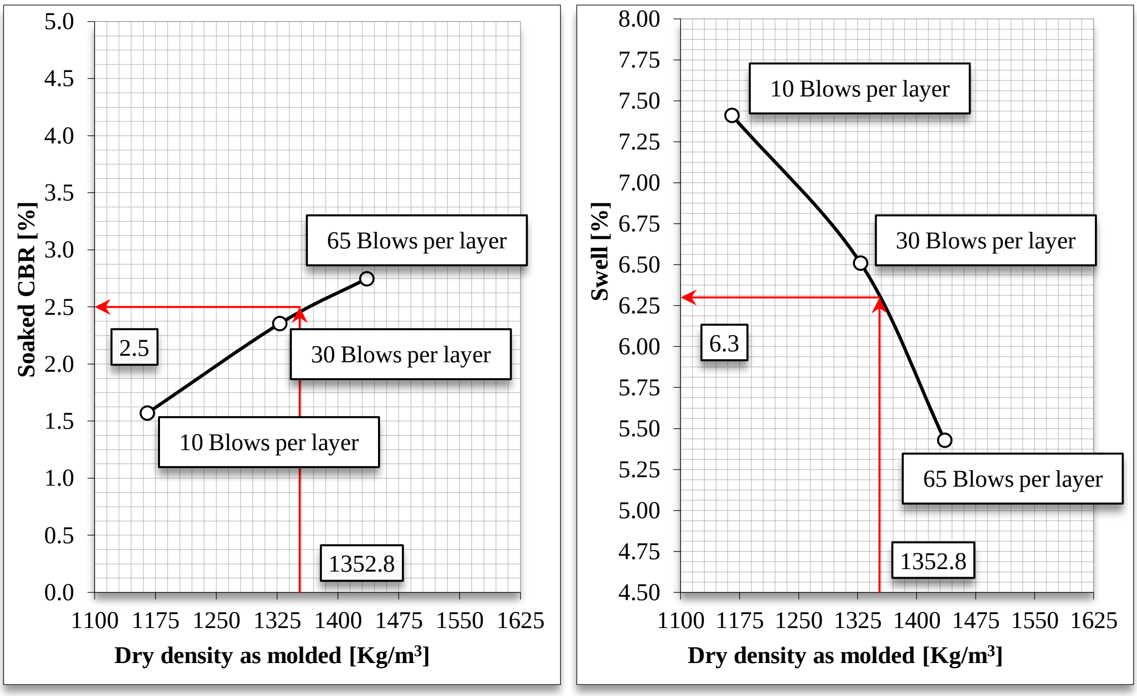

(a) (b)

Figure B-21 (a) Soaked CBR-Dry density & (b) Swell-Dry density curves for category-3

B.6.4 Replacement Material

Table B-32 CBR test data for replacement material

Determination of wet-density

Mold No.	M		5		M(6)	
No. of Layers	5		5		5	
No. of Blows per Layer	10		30		65	
Condition of sample (Before / After Soaking)	Before	After	Before	After	Before	After
Wt. of Wet Soil + Mold [gm]	12252.3	12924.0	11810.3	12145.8	11747.8	11986.1
Wt. of Mold [gm]	8520.9	8520.9	7657.1	7657.1	7360.1	7360.1
Wt. of Wet Soil [gm]	3731.4	4403.1	4153.2	4488.7	4387.7	4626.0
Wet Density [Kg/m3]	1740.9	2054.3	1937.7	2094.2	2047.1	2158.3

Determination of moisture content and dry-density

Condition of sample (Before / After Soaking)	Before	After	Before	After	Before	After
Container No.	8	BD	O	9	NA	X
Wt. of Container + Wet Soil [gm]	542.4	500.0	532.3	489.9	541.4	512.9
Wt. of Container + Dry Soil [gm]	491.4	421.4	482.2	416.5	493.0	451.1
Wt. of Container [gm]	109.0	123.2	127.1	108.9	122.4	128.1
Wt. of Moisture [gm]	51.0	78.6	50.1	73.4	48.4	61.8
Wt. of Dry Soil [gm]	382.4	298.2	355.1	307.6	370.6	323.0
Moisture Content [%]	13.34	26.36	14.11	23.86	13.06	19.13
Dry Unit Weight [Kg/m3]	1536.0	1625.8	1698.1	1690.8	1810.6	1811.7

Note: The volume of mold is 2143 cm^3

Penetration and CBR data

Penetration [mm]	Standard stress [Mpa]	10 Blows			30 Blows			65 Blows		
		Gauge Reading	Stress [Mpa]	CBR [%]	Gauge Reading	Stress [Mpa]	CBR [%]	Gauge Reading	Stress [Mpa]	CBR [%]
0		0	0.00		0	0.00		0	0.00	
0.64		2	0.13		5	0.33		6	0.39	
1.27		4	0.26		9	0.59		14	0.91	
1.91		5	0.33		14	0.91		25	1.63	
2.54	6.9	7	0.46	6.61	18	1.17	16.99	36	2.34	33.98
3.81		9	0.59		23	1.50		56	3.65	
5.08	10.3	12	0.78	7.59	28	1.82	17.70	71	4.62	44.89

Note: The penetration rate was 1.27 min/minutes.

Swell data

No. of Blows per Layer		10			30			65		
Condition	Elapse time [Hours]	Gauge reading	Swell mm	Swell %	Gauge reading	Swell mm	Swell %	Gauge reading	Swell mm	Swell %
Soaked	0	0.00	1.17	1.00	0.00	1.03	0.88	0.00	0.65	0.56
Tested	96	1.17			1.03			0.65		

Note: Initial height of sample is 116.43 mm.

95 % of MDD [Kg/m3]	1708.1
CBR at 95 % MDD [%]	18
Swell at 95 % MDD [%]	0.87

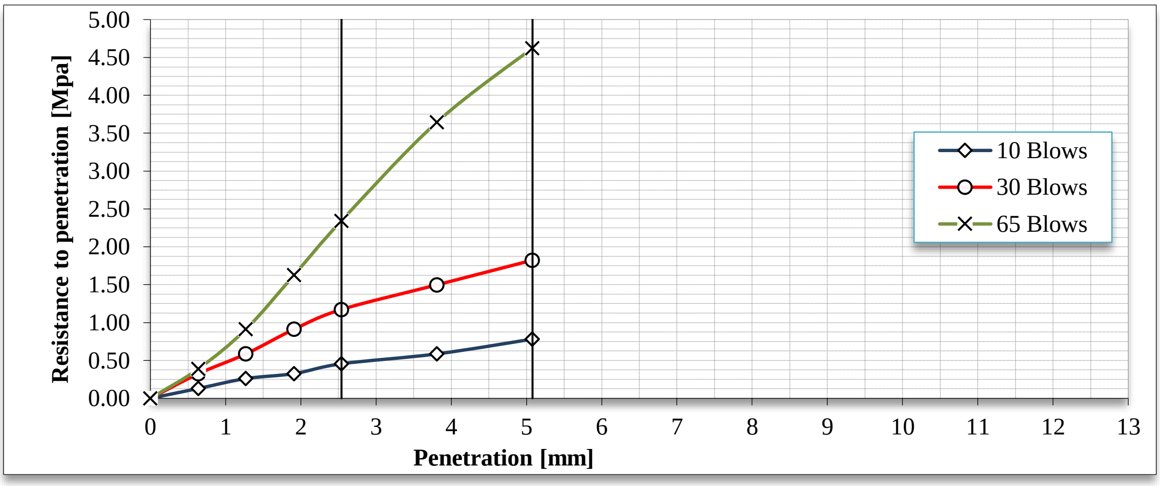

Figure B-22 Stress-Strain (penetration) curve for replacement material

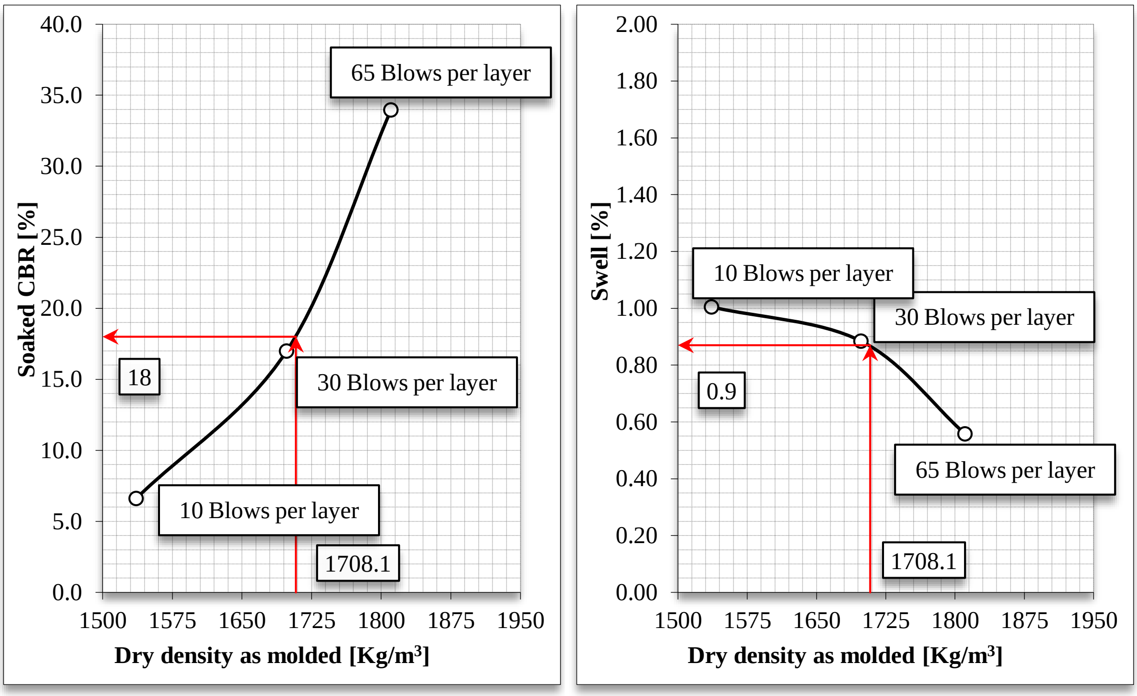

(a) (b)

Figure B-23 (a) Soaked CBR-Dry density & (b) Swell-Dry density curves for replacement material

B.7 Shear Strength Parameters Determination

B.7.1 Category-1 Subgrade Soil

Company Name:
በኢትዮጵያ የኮንስትራክሽን ዲዛይንና ሱፐርቪዥን ሥራዎች ኮርፖሬሽን
Ethiopian Construction Design & Supervision Works Corporation

Title	Document No:	Issue No.	Page No.
Triaxial Test (UU)	OF/ECDSWC/0816	1	2 of 11

Project :- MSc thesis
Client :- Binyam Gezahegn
Location :- -
Sample ID :- Categoory-1
Depth (m) :- -

SPECIMEN DATA

Lab No.	1642/16
Initial height (cm)	7.60
Initial Area (cm²)	11.34
Initial Wet Weight (gm)	166.00
Final Dry Weight (gm)	120.50
Moisture content (%)	37.76

Test Type	TRIAXIAL TEST
Sample condition	Undisturbed
Initial diameter (cm)	3.8
Initial volume (cm³)	86.20
Bulk density (gm/cm³)	1.926
Dry density (gm/cm³)	1.398

$P = 1/2\ (\sigma_1 + \sigma_3)$
$q = 1/2\ (\sigma 1 - \sigma 3)$

					C (KN/m²)	Ø (Degrees)
Chamber press. (KN/m²)	(σ_3)	100	200	300	247.53	3.98
Deviator Stress, (KN/m²)	$(\sigma_1 - \sigma_3)$	547	563	577		

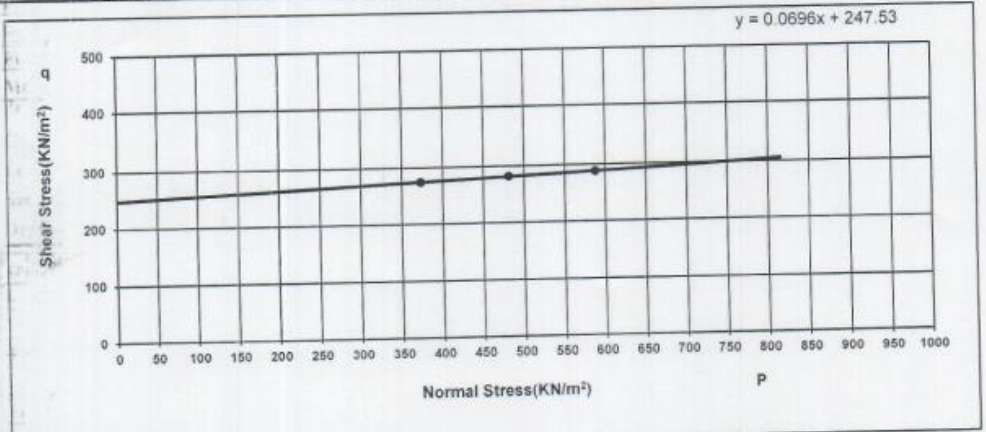

Tested by : Mammo.H
Lab Expert

Processed by : Getu.M
Geotechnical Engineer

Checked by : Biruk A.
Senior Geotechnical Engineer

Approved Bethlehem B.
Geotechnical Lab S/P Manager

Please make sure that this document is the correct version before use

Figure B-24 Snapshot of triaxial test result for category-1 (set 1)

Table B-33 Triaxial test data for category-1 (set 2)

Determination of degree of saturation

Void ratio	1.27	Natural moisture content [%]	38.38
Specific Gravity	2.723	Degree of Saturation [%]	82.29
Determination of moisture content at 100% saturation			
Moisture content [%]			46.64
Determination of remolding water content at 100% saturation			
Volume of mold [cm^3]	91.85	Total mass of wet soil (Remolding) [gm]	164.11
Bulk density (in situ) [g/cm3]	1.686	Total mass of wet soil (in situ) [gm]	154.87
Dry density [g/cm3]	1.218	Mass of total water (Remolding) [gm]	52.20
Mass of dry soil [gm]	111.9	Additional water for remolding [gm]	9.24
Remolding density [g/cm3]	1.787	Natural moisture [gm]	42.95

Initial specimen height [mm]	81
Diameter [mm]	38
Initial area [mm2]	1134

Chamber pressure = σ3

Deviatoric stress = Δσf

Deviatoric stress + Chamber stress = σ1

Test - 1		Test - 2		Test - 3	
Δσf [kPa]	284.6	Δσf [kPa]	379.0	Δσf [kPa]	453.0
σ3 [kPa]	100.0	σ3 [kPa]	200.0	σ3 [kPa]	300.0
σ1=σ3+Δσf [kPa]	384.6	σ1=σ3+Δσf [kPa]	579.0	σ1=σ3+Δσf [kPa]	753.0
p=1/2(σ1+σ3) [kPa]	242.3	p=1/2(σ1+σ3) [kPa]	389.5	p=1/2(σ1+σ3) [kPa]	526.5
q=1/2(σ1-σ3) [kPa]	142.3	q=1/2(σ1-σ3) [kPa]	189.5	q=1/2(σ1-σ3) [kPa]	226.5

C [kPa]	78.3
φ [Degree]	17.1

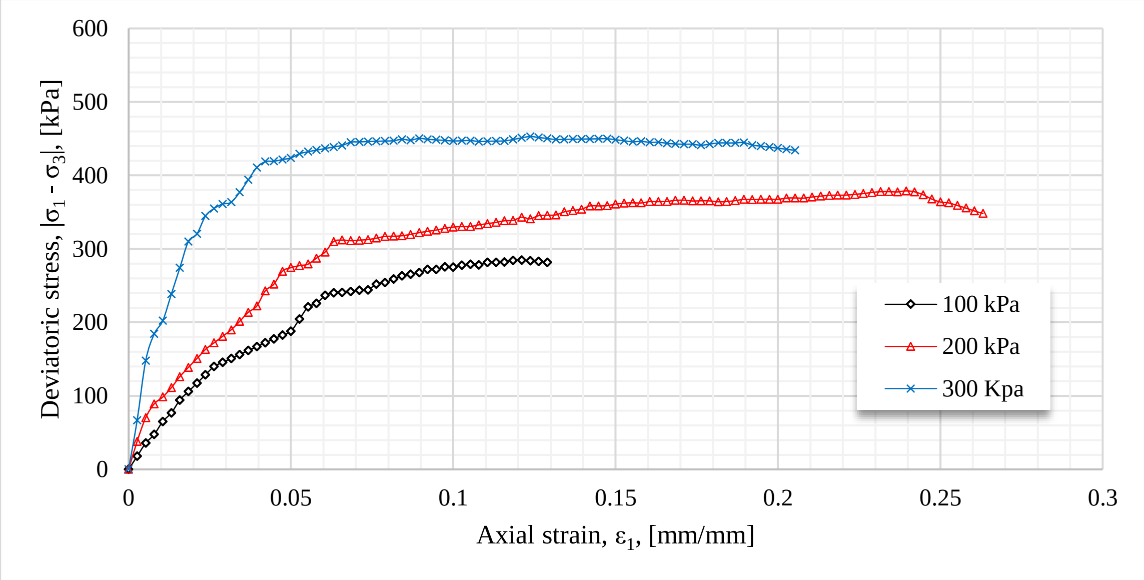

Figure B-25 Stress-strain curve for category-1 (set 2)

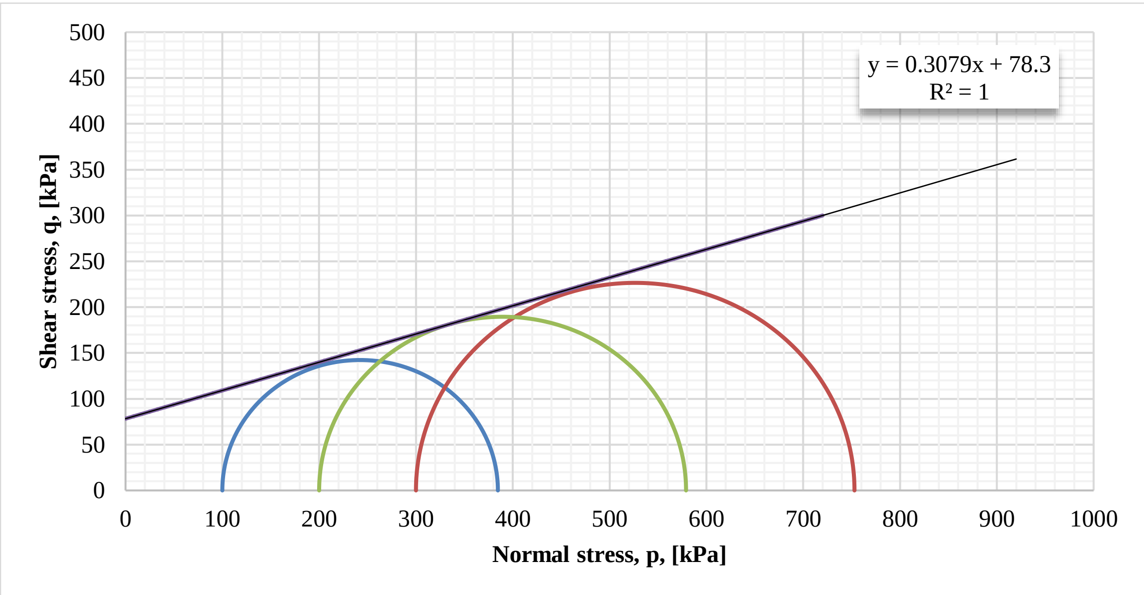

Figure B-26 p-q diagram and Mohr-coulomb failure for category-1 (set 2)

B.7.2 Category-2 Subgrade Soil

Company Name:
በኢትዮጵያ የኮንስትራክሽን ዲዛይንና ሱፐርቪዥን ሥራዎች ኮርፖሬሽን
Ethiopian Construction Design & Supervision Works Corporation

Title	Document No:	Issue No.	Page No.
Triaxial Test (UU)	OF/ECDSWC/0816	1	3 of 11

Project :- MSc thesis
Client :- Binyam Gezahegn
Location :- -
Sample ID :- Categoory-2
Depth (m) :- -

SPECIMEN DATA

Lab No.	1643/16
Initial height (cm)	7.60
Initial Area (cm^2)	11.34
Initial Wet Weight (gm)	165.00
Final Dry Weight (gm)	117.50
Moisture content (%)	40.43

Test Type	TRIAXIAL TEST
Sample condition	Undisturbed
Initial diameter (cm)	3.8
Initial volume (cm^3)	86.20
Bulk density (gm/cm^3)	1.914
Dry density (gm/cm^3)	1.363

P =	$1/2\ (\sigma_1 + \sigma_3)$
q =	$1/2\ (\sigma1 - \sigma3)$

					C (KN/m^2)	Ø (Degrees)
Chamber press. (KN/m^2)	(σ_3)	100	200	300	74.08	10.71
Deviator Stress , (KN/m^2)	($\sigma_1 - \sigma_3$)	229	276	323		

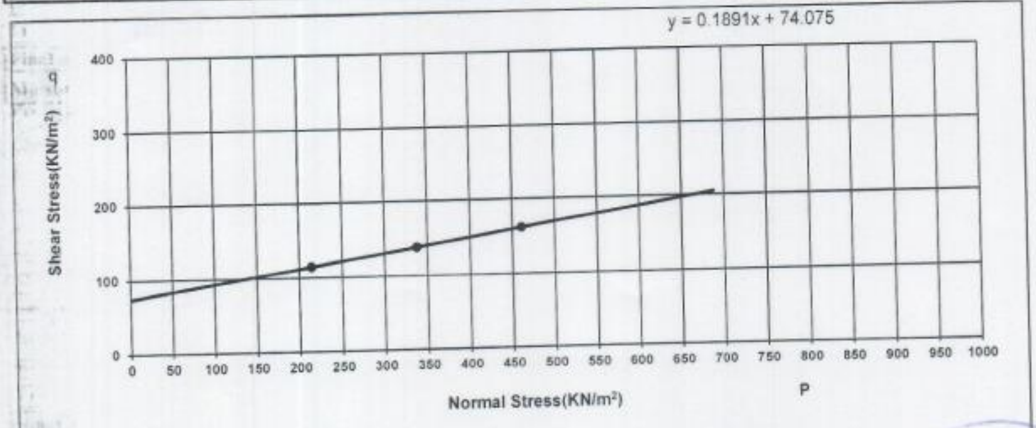

Tested by : Mammo.H
Lab Expert

Processed by : Getu.M
Geotechnical Engineer

Checked by : Biruk A.
Senior Geotechnical Engineer

Approved Bethlehem B.
Geotechnical Lab S/P Manager

Please make sure that this document is the correct version before use

Figure B-27 Snapshot of triaxial test result for category-2 (set 1)

Table B-34 Triaxial test data for category-2 (set 2)

Determination of degree of saturation

Void ratio	1.427	Natural moisture content [%]	38.78
Specific Gravity	2.588	Degree of Saturation [%]	70.33
Determination of moisture content at 100% saturation			
Moisture content [%]			55.14
Determination of remolding water content at 100% saturation			
Volume of mold [cm^3]	91.85	Total mass of wet soil (Remolding) [gm]	169.53
Bulk density (in situ) [g/cm3]	1.651	Total mass of wet soil (in situ) [gm]	151.65
Dry density [g/cm3]	1.190	Mass of total water (Remolding) [gm]	60.25
Mass of dry soil [gm]	109.3	Additional water for remolding [gm]	17.88
Remolding density [g/cm3]	1.846	Natural moisture [gm]	42.38

Initial specimen height [mm]	81
Diameter [mm]	38
Initial area [mm2]	1134

Chamber pressure = σ3

Deviatoric stress = Δσf

Deviatoric stress + Chamber stress = σ1

Test - 1		Test - 2		Test - 3	
Δσf [kPa]	158.4	Δσf [kPa]	212.6	Δσf [kPa]	267.7
σ3 [kPa]	100.0	σ3 [kPa]	200.0	σ3 [kPa]	300.0
σ1=σ3+Δσf [kPa]	258.4	σ1=σ3+Δσf [kPa]	412.6	σ1=σ3+Δσf [kPa]	567.7
p=1/2(σ1+σ3) [kPa]	179.2	p=1/2(σ1+σ3) [kPa]	306.3	p=1/2(σ1+σ3) [kPa]	433.8
q=1/2(σ1-σ3) [kPa]	79.2	q=1/2(σ1-σ3) [kPa]	106.3	q=1/2(σ1-σ3) [kPa]	133.8

C =	40.7
φ =	12.1

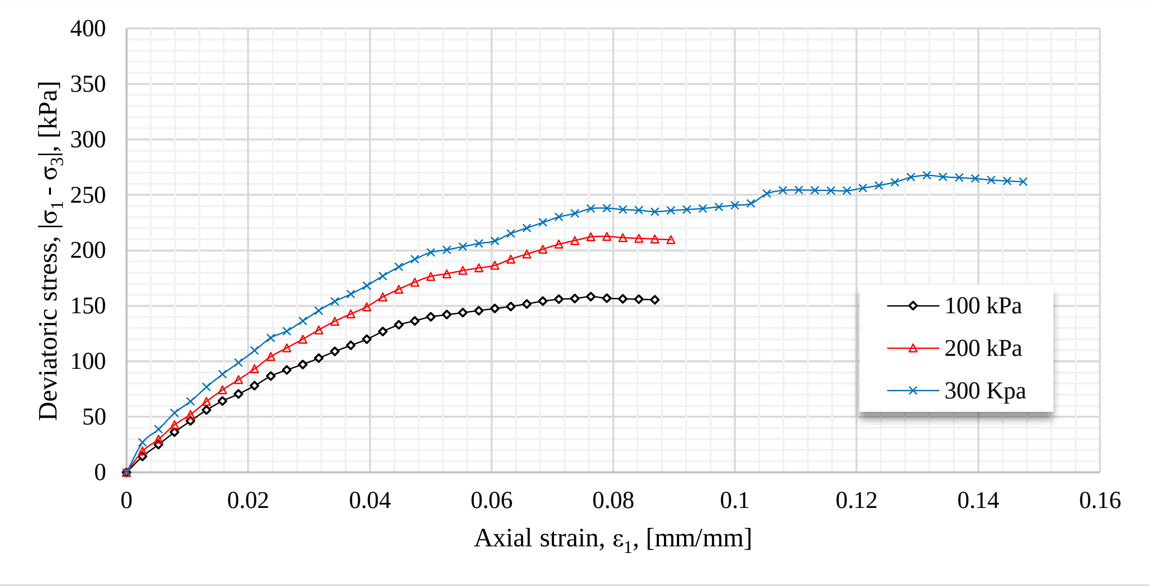

Figure B-28 Stress-strain curve for category-2 (set 2)

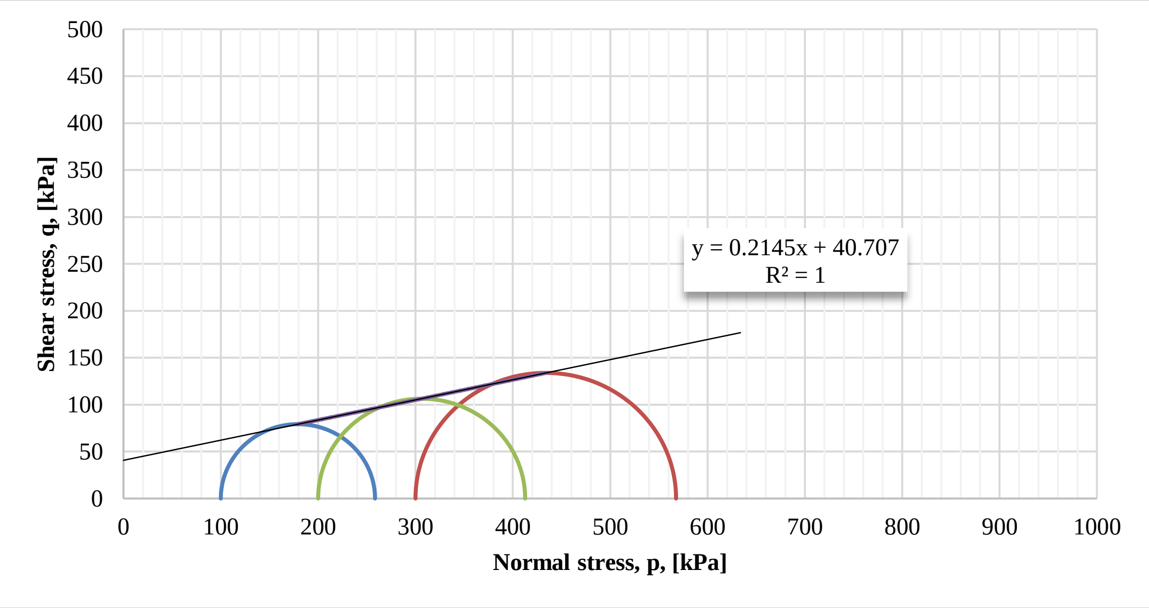

Figure B-29 p-q diagram and Mohr-coulomb failure for category-2 (set 2)

B.7.3 Category-3 Subgrade Soil

Company Name:

በኢትዮጵያ የኮንስትራክሽን ዲዛይንና ሱፐርቪዥን ሥራዎች ኮርፖሬሽን

Ethiopian Construction Design & Supervision Works Corporation

Title:	Document No:	Issue No.	Page No.
Triaxial Test (UU)	OF/ECDSWC/0816	1	4 of 11

Project :- MSc thesis
Client :- Binyam Gezahegn
Location :- -
Sample ID :- Categoory-3
Depth (m) :- -

SPECIMEN DATA

Lab No.	1644/16'
Initial height (cm)	7.60
Initial Area (cm²)	11.34
Initial Wet Weight (gm)	160.75
Final Dry Weight (gm)	111.75
Moisture content (%)	43.85

Test Type	TRIAXIAL TEST
Sample condition	Undisturbed
Initial diameter (cm)	3.8
Initial volume (cm³)	86.20
Bulk density (gm/cm³)	1.865
Dry density (gm/cm³)	1.296

P =	$1/2(\sigma_1+\sigma_3)$
q =	$1/2(\sigma1-\sigma3)$

					C (KN/m²)	Ø (Degrees)
Chamber press. (KN/m²)	(σ_3)	100	200	300		
Deviator Stress, (KN/m²)	$(\sigma_1-\sigma_3)$	260	274	286	116.29	3.45

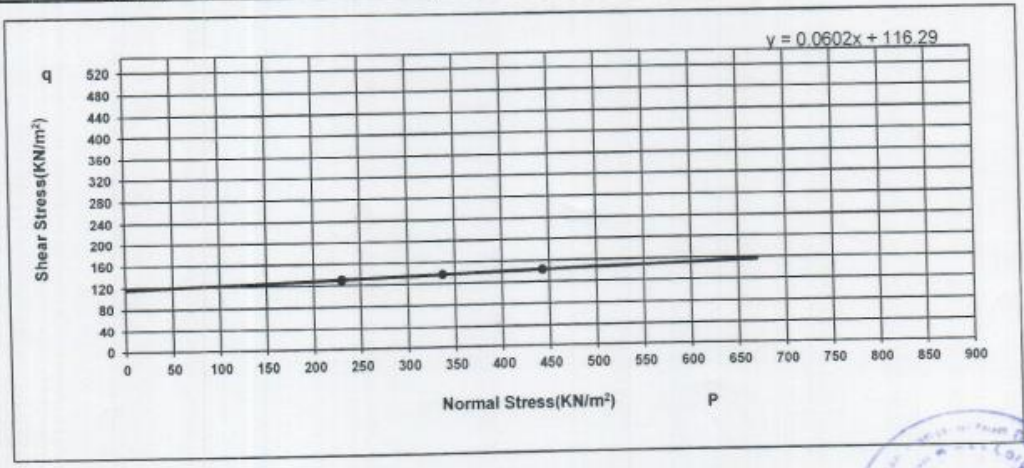

Tested by : Mammo.H
Lab Expert

Processed by : Getu.M
Geotechnical Engineer

Checked by : Biruk. A
Senior Geotechnical Engineer

Approved by : Bethlehem B.
Geotechnical Lab S/P Manager

Please make sure that this document is the correct version before use

Figure B-30 Snapshot of triaxial test result for category-3 (set 1)

Table B-35 Triaxial test data for category-3 (set 2)

Determination of degree of saturation			
Void ratio	1.442	Natural moisture content [%]	39.56
Specific Gravity	2.620	Degree of Saturation [%]	71.88
Determination of moisture content at 100% saturation			
Moisture content [%]			55.04
Determination of remolding water content at 100% saturation			
Volume of mold [cm^3]	91.85	Total mass of wet soil (Remolding) [gm]	158.47
Bulk density (in situ) [g/cm3]	1.553	Total mass of wet soil (in situ) [gm]	142.65
Dry density [g/cm3]	1.113	Mass of total water (Remolding) [gm]	56.26
Mass of dry soil [gm]	102.2	Additional water for remolding [gm]	15.82
Remolding density [g/cm3]	1.725	Natural moisture [gm]	40.44

Initial specimen height [mm]	81
Diameter [mm]	38
Initial area [mm2]	1134

Chamber pressure = σ3

Deviatoric stress = Δσf

Deviatoric stress + Chamber stress = σ1

Test - 1		Test - 2		Test - 3	
Δσf [kPa]	130.7	Δσf [kPa]	173.7	Δσf [kPa]	207.8
σ3 [kPa]	100.0	σ3 [kPa]	200.0	σ3 [kPa]	300.0
σ1=σ3+Δσf [kPa]	230.7	σ1=σ3+Δσf [kPa]	373.7	σ1=σ3+Δσf [kPa]	507.8
p=1/2(σ1+σ3) [kPa]	165.4	p=1/2(σ1+σ3) [kPa]	286.9	p=1/2(σ1+σ3) [kPa]	403.9
q=1/2(σ1-σ3) [kPa]	65.4	q=1/2(σ1-σ3) [kPa]	86.9	q=1/2(σ1-σ3) [kPa]	103.9

C =	32.6
φ =	10.6

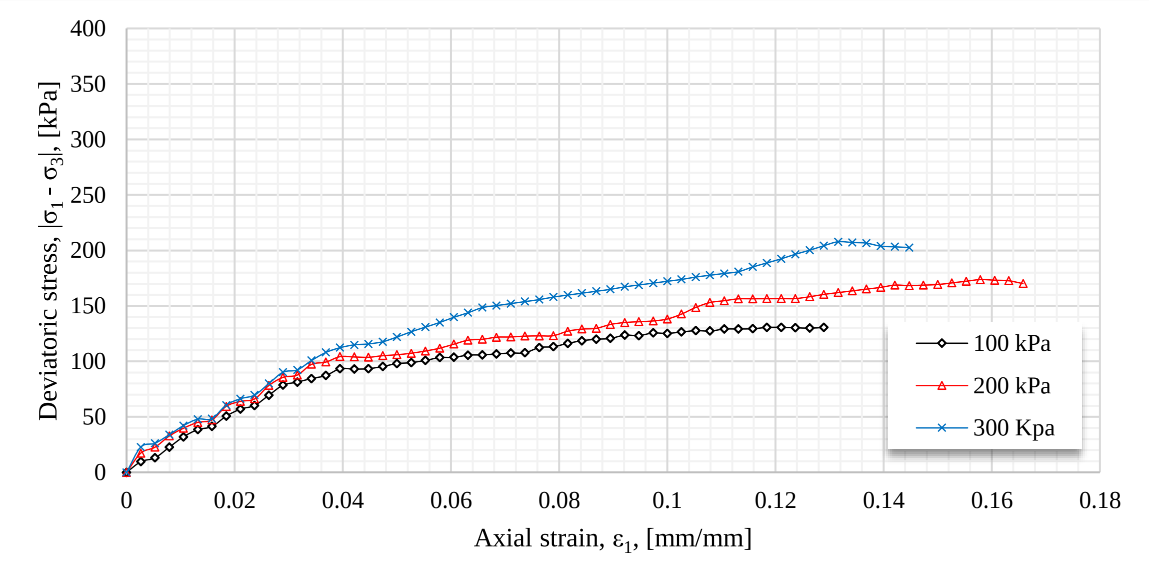

Figure B-31 Stress-strain curve for category-3 (set 2)

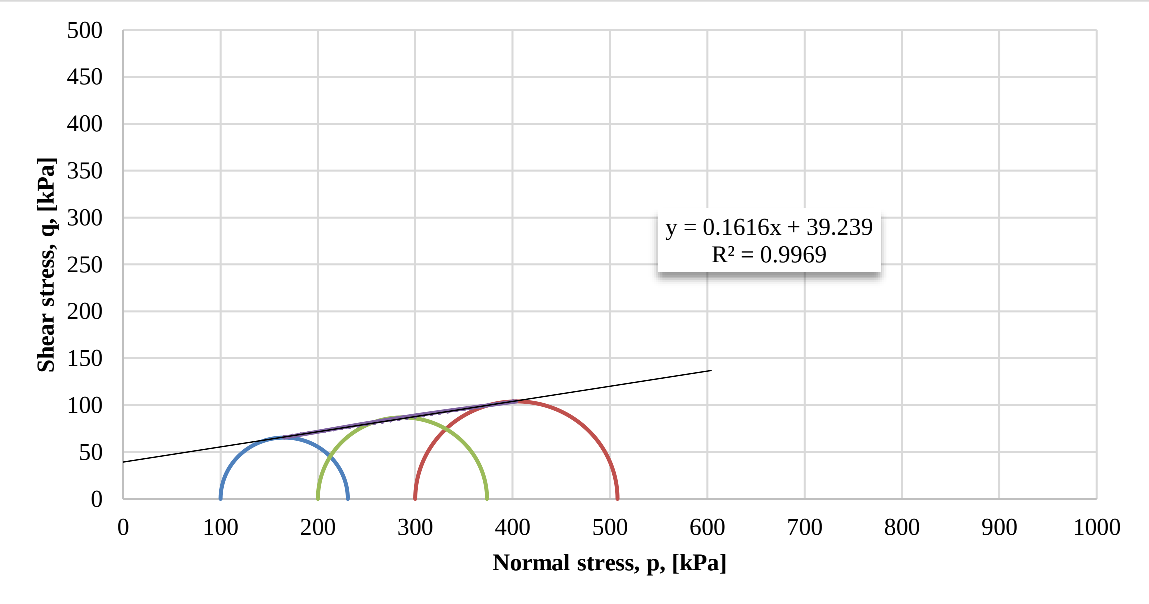

Figure B-32 p-q diagram and Mohr-coulomb failure for category-3 (set 2)

B.7.4 Replacement Material

Company Name:
በኢትዮጵያ የኮንስትራክሽን ዲዛይንና ሱፐርቪዥን ሥራዎች ኮርፖሬሽን
Ethiopian Construction Design & Supervision Works Corporation

Title:	Document No:	Issue No.	Page No.
Triaxial Test (UU)	OF/ECDSWC/0816	1	5 of 11

Project :- MSc thesis
Client :- Binyam Gezahegn
Location :- -
Sample ID :- Replacement Material
Depth (m) :- -

SPECIMEN DATA

Lab No.	1645/16'
Initial height (cm)	7.60
Initial Area (cm²)	11.34
Initial Wet Weight (gm)	160.25
Final Dry Weight (gm)	134.20
Moisture content (%)	19.41

Test Type	TRIAXIAL TEST
Sample condition	Remolded
Initial diameter (cm)	3.8
Initial volume (cm³)	86.20
Bulk density (gm/cm³)	1.859
Dry density (gm/cm³)	1.557

$P = 1/2\,(\sigma_1 + \sigma_3)$
$q = 1/2\,(\sigma 1 - \sigma 3)$

					C	Ø
Chamber press. (KN/m²)	(σ_3)	100	200	300	(KN/m²)	(Degrees)
Deviator Stress, (KN/m²)	($\sigma_1 - \sigma_3$)	427	558	680	92.20	21.20

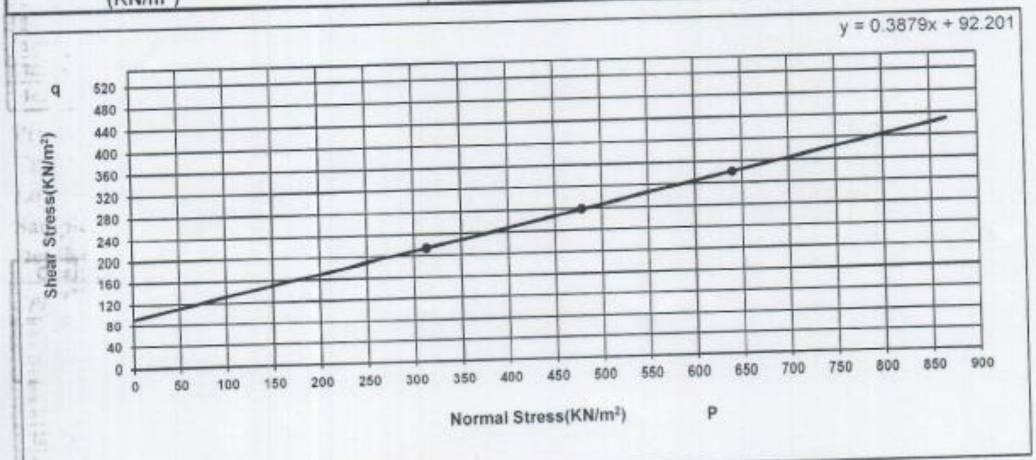

Tested by : Mammo.H
Lab Expert

Processed by : Getu.M
Geotechnical Engineer

Checked by : Biruk. A
Senior Geotechnical Engineer

Approved by : Bethlehem B.
Geotechnical Lab S/P Manager

Please make sure that this document is the correct version before use

Figure B-33 Snapshot of triaxial test result for replacement material (set 1)

B.8 Parameter Determination Using One-Dimensional Consolidation Test

B.8.1 Category-1 Subgrade Soil

በኢትዮጵያ የኮንስትራክሽን ዲዛይንና ሱፐርቪዥን ሥራዎች ኮርፖሬሽን
ምርምር፣ ላቦራቶሪና ስልጠና ማዕከል
Ethiopian Construction Design & Supervision Works Corporation
Research, Laboratory and Training Center

Title	Document No:	Issue No.	Page No.
Consolidation Test	OF/ECDSWC/0797A	1	6 of 11

Project :- MSc thesis
Client :- Binyam Gezahegn
Location :- -
BH / TP :- Category -
DEPTH (m) :- -

Lab No.	1642/16
Sample Type	Undisturbed
Test Type	Consolidation

Specimen data

BEFORE TEST

Weight of sample & Ring (gm)	248.30
Weight of Ring (gm)	108.40
Weight of sample (gm)	206.00
Weight of Dry Sample (gm)	101.60
Weight of Initial Moisture (gm)	104.40
Initial Moisture content (M_o) (%)	102.76
Initial Void Ratio : $e_o = (G_s/r_d)-1$	1.270
Height of Solids : $H_s = H_o/(1+e_o)$ (mm)	8.810
Initial Saturation : $S_o = (M_o*G_s)/e_o$ (%)	211.16

Specific Gravity (G_s)	2.61
Sample Diameter (D) (mm)	75.00
Sample Thickness (H_o) (mm)	20.00
Area (A) (cm^2)	44.18
Volume (V) (cm^3)	88.37
Bulk Density (r_b) (gm/cm^3)	2.331
Dry Density (r_d) (gm/cm^3)	1.150

AFTER TEST

Weight of Sample + Ring (gm)	250.40
Weight of Dry Sample + Ring (gm)	210.00
Weight of Ring (gm)	108.40
Weight of Wet Sample (gm)	142.00
Weight of Dry Sample (gm)	101.60
Final Moisture Content (M_f) (%)	39.76

Over all settlement (mm)	1.600
Volume change (cm^3)	7.07
Final Volume (cm^3)	81.30
Final Bulk Density (gm/cm^3)	1.747
Final Dry Denssity (gm/cm^3)	1.250

ONE - DIMENSIONAL CONSOLIDATION TEST CALCULATION SHEET

Sample diameter (D)	75.00 mm	Height H_O	20.0 mm
Height of solids H_S =	8.810	Initial Voids ratio e_o =	1.27

Voids Ratio					COMPRESSIBILITY			COEFFICIENT OF CONSOLIDATION			
					Incremental						C_v
Increment N°	Pressure Kpa	Cumulative compression (ΔH) mm	Consolidated height H = H_O-DH mm	Voids Ratio e=H-HS/Hs	Height change δH mm	Pressure change δp Kpa	m_v = (δH/H_1)*(1000 / δp) m^2/MN	t_{50} min	t_{90} min	H = 1/2(H_1+ H_2)	(0.848*H^2)/t_{90} m^2/year
								-	-		-
1	0	0.000	20.000	1.270							
					0.449	49.972	0.449	-	14.44	19.776	22.97
2	50	0.449	19.551	1.219							
					0.338	49.972	0.346	-	5.76	19.382	55.31
3	100	0.787	19.213	1.181							
					0.304	99.9439	0.158	-	7.84	19.061	39.30
4	200	1.091	18.909	1.146							
					0.409	199.888	0.108	-	9.00	18.705	32.96
5	400	1.500	18.500	1.100							
					0.558	399.776	0.075	-	9.00	18.221	31.28
6	800	2.058	17.942	1.037							
7	200	1.820	18.180	1.064							
8	50	1.600	18.400	1.088							

Tested by : Daneal.G
Lab Expert

Processed by : Getu.M
Geotechnical Engineer

Checked by :- Biruk A.
Senior Geotechnical Engineer

Approved by :- Bethlehem B.
Geotechnical Lab S/P Manager

Please make sure that this document is the correct version before use

Figure B-34 Snapshot of consolidation test data for category-1

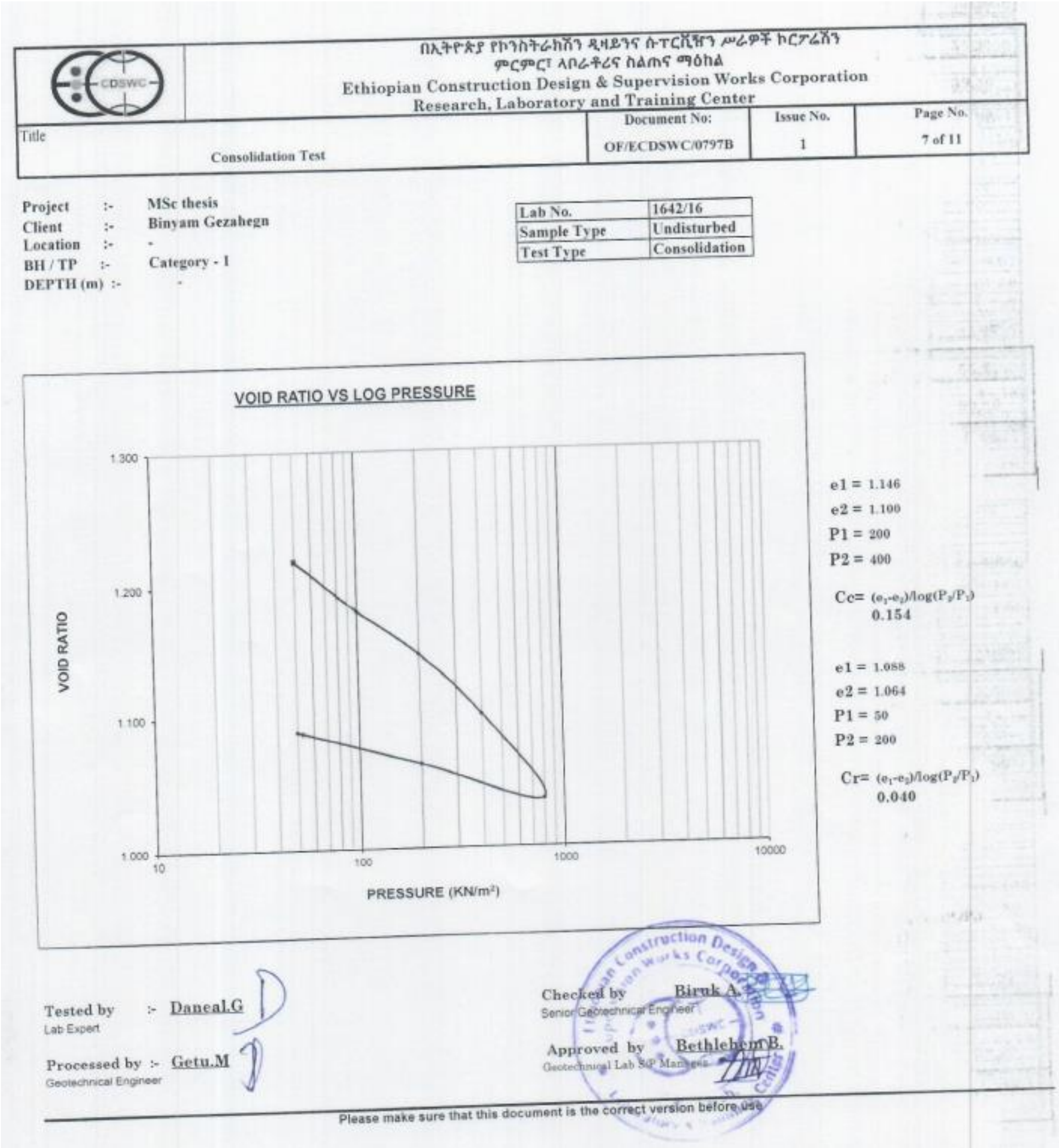

በኢትዮጵያ የኮንስትራክሽን ዲዛይንና ሱፐርቪዥን ሥራዎች ኮርፖሬሽን
ምርምር፣ ላቦራቶሪና ስልጠና ማዕከል
Ethiopian Construction Design & Supervision Works Corporation
Research, Laboratory and Training Center

Title	Document No:	Issue No.	Page No.
Consolidation Test	OF/ECDSWC/0797B	1	7 of 11

Project :- MSc thesis
Client :- Binyam Gezahegn
Location :- -
BH / TP :- Category - 1
DEPTH (m) :- -

Lab No.	1642/16
Sample Type	Undisturbed
Test Type	Consolidation

e1 = 1.146
e2 = 1.100
P1 = 200
P2 = 400

Cc= $(e_1-e_2)/\log(P_2/P_1)$
0.154

e1 = 1.088
e2 = 1.064
P1 = 50
P2 = 200

Cr= $(e_1-e_2)/\log(P_2/P_1)$
0.040

Tested by :- Daneal.G
Lab Expert

Processed by :- Getu.M
Geotechnical Engineer

Checked by Biruk A.
Senior Geotechnical Engineer

Approved by Bethlehem B.
Geotechnical Lab S&P Manager

Please make sure that this document is the correct version before use

Figure B-35 Snapshot of void ratio-pressure plot for category-1

B.8.2 Category-2 Subgrade Soil

CDSWC

በኢትዮጵያ የኮንስትራክሽን ዲዛይንና ሱፐርቪዥን ሥራዎች ኮርፖሬሽን
ምርምር፣ ላቦራቶሪና ስልጠና ማዕከል
Ethiopian Construction Design & Supervision Works Corporation
Research, Laboratory and Training Center

Title	Document No:	Issue No.	Page No.
Consolidation Test	OF/ECDSWC/0797A	1	8 of 11

Project :- MSc thesis
Client :- Binyam Gezahegn
Location :- -
BH / TP :- Category - 2
DEPTH (m) :- -

Lab No.	1643/16
Sample Type	Undisturbed
Test Type	Consolidation

Specimen data

BEFORE TEST

Weight of sample & Ring (gm)	238.80
Weight of Ring (gm)	106.90
Weight of sample (gm)	206.00
Weight of Dry Sample (gm)	94.30
Weight of Initial Moisture (gm)	111.70
Initial Moisture content (M_o) (%)	118.45
Initial Void Ratio : $e_o = (G_s/r_d)-1$	1.427
Height of Solids : $H_s = H_o/(1+e_o)$ (mm)	8.240
Initial Saturation : $S_o = (M_o*G_s)/e_o$ (%)	214.98

Specific Gravity (G_s)	2.59
Sample Diameter (D) (mm)	75.00
Sample Thickness (H_o) (mm)	20.00
Area (A) (cm^2)	44.18
Volume (V) (cm^3)	88.37
Bulk Density (r_b) (gm/cm^3)	2.331
Dry Density (r_d) (gm/cm^3)	1.067

AFTER TEST

Weight of Sample + Ring (gm)	241.00
Weight of Dry Sample + Ring (gm)	201.20
Weight of Ring (gm)	106.90
Weight of Wet Sample (gm)	134.10
Weight of Dry Sample (gm)	94.30
Final Moisture Content (M_f) (%)	42.21

Over all settlement (mm)	2.085
Volume change (cm^3)	9.21
Final Volume (cm^3)	79.16
Final Bulk Density (gm/cm^3)	1.694
Final Dry Denssity (gm/cm^3)	1.191

ONE - DIMENSIONAL CONSOLIDATION TEST CALCULATION SHEET

Sample diameter (D)	75.00 mm	Height H_O	20.0 mm
Height of solids H_S =	8.240	Initial Voids ratio e_o =	1.43

Voids Ratio					COMPRESSIBILITY			COEFFICIENT OF CONSOLIDATION			
					Incremental						C_v
Increment N°	Pressure Kpa	Cumulative compression (ΔH) mm	Consolidated height H = H_O-DH mm	Voids Ratio e=H-HS/Hs	Height change δH mm	Pressure change δp Kpa	m_v = (δH/H_1)*(1000 / δp) m^2/MN	t_{50} min	t_{90} min	H = 1/2(H_1+ H_2)	(0.848*H^2)/t_{90} m^2/year
1	0	0.000	20.000	1.427				-	-		
					0.458	49.972	0.458				
								-	4.00	19.771	82.87
2	50	0.458	19.542	1.372							
					0.220	49.972	0.225				
								-	1.96	19.432	163.37
3	100	0.678	19.322	1.345							
					0.442	99.9439	0.229				
								-	3.24	19.101	95.49
4	200	1.120	18.880	1.291							
					0.571	199.888	0.151				
								-	5.76	18.595	50.90
5	400	1.691	18.309	1.222							
					0.816	399.776	0.111				
								-	6.25	17.901	43.48
6	800	2.507	17.493	1.123							
7	200	2.292	17.708	1.149							
8	50	2.085	17.915	1.174							

Tested by : Daneal.G
Lab Expert

Processed by : Getu.M
Geotechnical Engineer

Checked by :- Biruk A.
Senior Geotechnical Engineer

Approved by :- Bethlehem B.
Geotechnical Lab S/P Manager

Please make sure that this document is the correct version before use

Figure B-36 Snapshot of consolidation test data for category-2

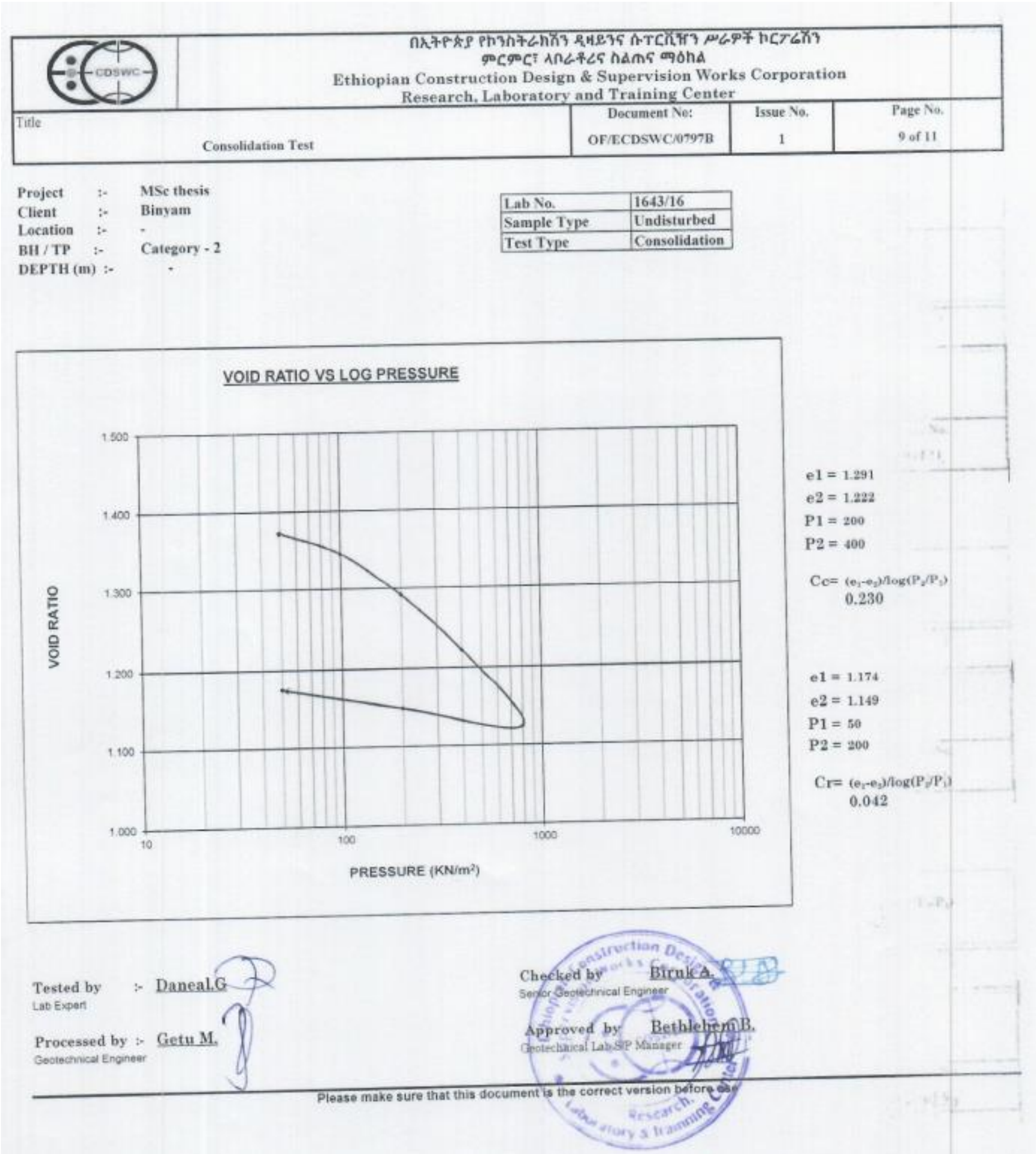
በኢትዮጵያ የኮንስትራክሽን ዲዛይንና ሱፐርቪዥን ሥራዎች ኮርፖሬሽን
ምርምር፣ ላቦራቶሪና ስልጠና ማዕከል
Ethiopian Construction Design & Supervision Works Corporation
Research, Laboratory and Training Center

Title	Document No:	Issue No.	Page No.
Consolidation Test	OF/ECDSWC/0797B	1	9 of 11

Project :- MSc thesis
Client :- Binyam
Location :- -
BH / TP :- Category - 2
DEPTH (m) :- -

Lab No.	1643/16
Sample Type	Undisturbed
Test Type	Consolidation

Tested by :- Daneal.G
Lab Expert

Processed by :- Getu M.
Geotechnical Engineer

Checked by :- Biruk A.
Senior Geotechnical Engineer

Approved by :- Bethlehem B.
Geotechnical Lab.S/P Manager

Please make sure that this document is the correct version before use

Figure B-37 Snapshot of void ratio-pressure plot for category-2

B.8.3 Category-3 Subgrade Soil

በኢትዮጵያ የኮንስትራክሽን ዲዛይንና ሱፐርቪዥን ሥራዎች ኮርፖሬሽን
ምርምር፣ ላቦራቶሪና ስልጠና ማዕከል
Ethiopian Construction Design & Supervision Works Corporation
Research, Laboratory and Training Center

Title	Document No:	Issue No.	Page No.
Consolidation Test	OF/ECDSWC/0797A	1	10 of 11

Project :- MSc thesis
Client :- Binyam Gezahegn
Location :- -
BH / TP :- Category - 3
DEPTH (m) :- -

Lab No.	1644/16
Sample Type	Undisturbed
Test Type	Consolidation

Specimen data

BEFORE TEST

Weight of sample & Ring (gm)	239.20
Weight of Ring (gm)	108.90
Weight of sample (gm)	206.00
Weight of Dry Sample (gm)	91.90
Weight of Initial Moisture (gm)	114.10
Initial Moisture content (M_o) (%)	124.16
Initial Void Ratio : $e_o = (G_s/r_d)-1$	1.442
Height of Solids : $H_s = H_o/(1+e_o)$ (mm)	8.189
Initial Saturation : $S_o = (M_o*G_s)/e_o$ (%)	218.63

Specific Gravity (G_s)	2.54
Sample Diameter (D) (mm)	75.00
Sample Thickness (H_o) (mm)	20.00
Area (A) (cm^2)	44.18
Volume (V) (cm^3)	88.37
Bulk Density (r_b) (gm/cm^3)	2.331
Dry Density (r_d) (gm/cm^3)	1.040

AFTER TEST

Weight of Sample + Ring (gm)	240.60
Weight of Dry Sample + Ring (gm)	200.80
Weight of Ring (gm)	108.90
Weight of Wet Sample (gm)	131.70
Weight of Dry Sample (gm)	91.90
Final Moisture Content (M_f) (%)	43.31

Over all settlement (mm)	2.396
Volume change (cm^3)	10.59
Final Volume (cm^3)	77.78
Final Bulk Density (gm/cm^3)	1.693
Final Dry Denssity (gm/cm^3)	1.182

ONE - DIMENSIONAL CONSOLIDATION TEST CALCULATION SHEET

Sample diameter (D)	75.00 mm	Height H_O	20.0 mm
Height of solids H_S =	8.189	Initial Voids ratio e_o =	1.44

Voids Ratio					COMPRESSIBILITY			COEFFICIENT OF CONSOLIDATION			
					Incremental						C_v
Increment N°	Pressure Kpa	Cumulative compression (ΔH) mm	Consolidated height H = H_O-DH mm	Voids Ratio e=H-HS/Hs	Height change δH mm	Pressure change δp Kpa	m_v = (δH/H_1)*(1000 / δp) m^2/MN	t_{50} min	t_{90} min	H = 1/2(H_1+ H_2)	(0.848*H^2)/t_{90} m^2/year
								-	-		
1	0	0.000	20.000	1.442							
					0.977	49.972	0.978	-	11.56	19.512	27.93
2	50	0.977	19.023	1.323							
					0.318	49.972	0.335	-	4.00	18.864	75.44
3	100	1.295	18.705	1.284							
					0.401	99.9439	0.215	-	4.84	18.505	59.99
4	200	1.696	18.304	1.235							
					0.492	199.888	0.134	-	12.25	18.058	22.57
5	400	2.188	17.812	1.175							
					0.615	399.776	0.086	-	4.00	17.505	64.96
6	800	2.803	17.197	1.100							
7	200	2.609	17.391	1.124							
8	50	2.396	17.604	1.150							

Tested by : Daneal.G
Lab Expert

Processed by : Getu.M
Geotechnical Engineer

Checked by :- Biruk A.
Senior Geotechnical Engineer

Approved by :- Bethlehem B.
Geotechnical Lab S/T Manager

Please make sure that this document is the correct version before use

Figure B-38 Snapshot of consolidation test data for category-3

በኢትዮጵያ የኮንስትራክሽን ዲዛይንና ሱፐርቪዥን ሥራዎች ኮርፖሬሽን
ምርምር፣ ላቦራቶሪና ስልጠና ማዕከል
Ethiopian Construction Design & Supervision Works Corporation
Research, Laboratory and Training Center

Title	Document No:	Issue No.	Page No.
Consolidation Test	OF/ECDSWC/0797B	1	11 of 11

Project :- MSc thesis
Client :- Binyam
Location :- -
BH / TP :- Category - 3
DEPTH (m) :- -

Lab No.	1644/16
Sample Type	Undisturbed
Test Type	Consolidation

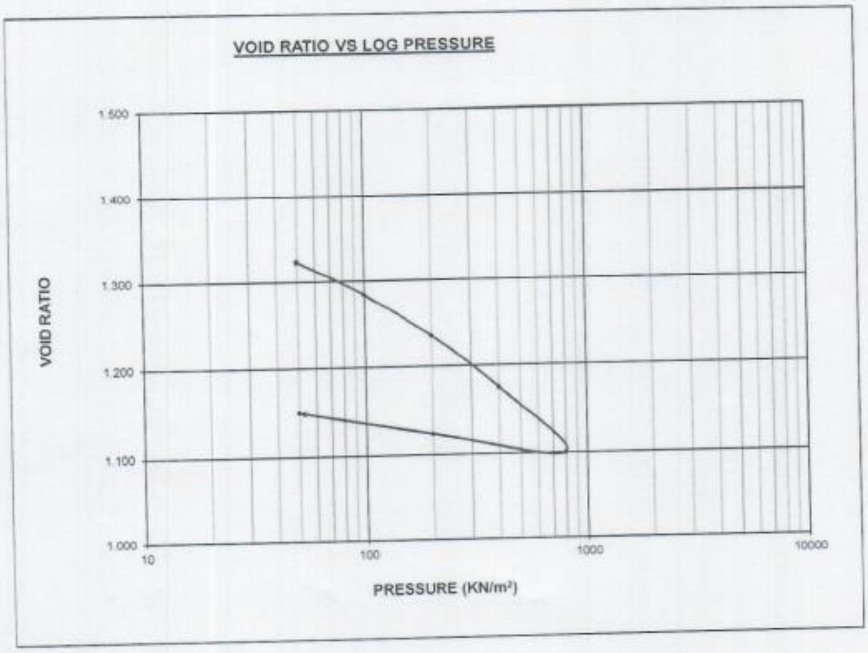

e1 = 1.235
e2 = 1.175
P1 = 200
P2 = 400

Cc= $(e_1-e_2)/\log(P_2/P_1)$
0.200

e1 = 1.150
e2 = 1.124
P1 = 50
P2 = 200

Cr= $(e_1-e_2)/\log(P_2/P_1)$
0.043

Tested by :- Daneal.G
Lab Expert

Processed by :- Getu M.
Geotechnical Engineer

Checked by Biruk A.
Senior Geotechnical Engineer

Approved by Bethlehem B.
Geotechnical Lab S/P Manager

Please make sure that this document is the correct version before use

Figure B-39 Snapshot of void ratio-pressure plot for category-3

B.9 Free Swell Index Determination

Table B-36 Free swell test

Subgrade category	Category-1		Category-2		Category-3	
Test No	1	2	1	2	1	2
Graduated cylinder No	A	B	C	D	E	F
Mass of oven dry specimen [gm]	10	10	10	10	10	10
Volume of soil specimen in distilled water [ml]	13.5	14.1	13.8	14.5	15.8	14.8
Volume of soil specimen in kerosene [ml]	12	12	11.8	12	12.8	12.5
Free swell index [%]	12.5	17.5	16.9	20.8	23.4	18.4
Average Free swell index [%]	15.0		18.9		20.9	

B.10 Mineral Identification Using XRD Analysis

B.10.1 Category-1 Subgrade Soil

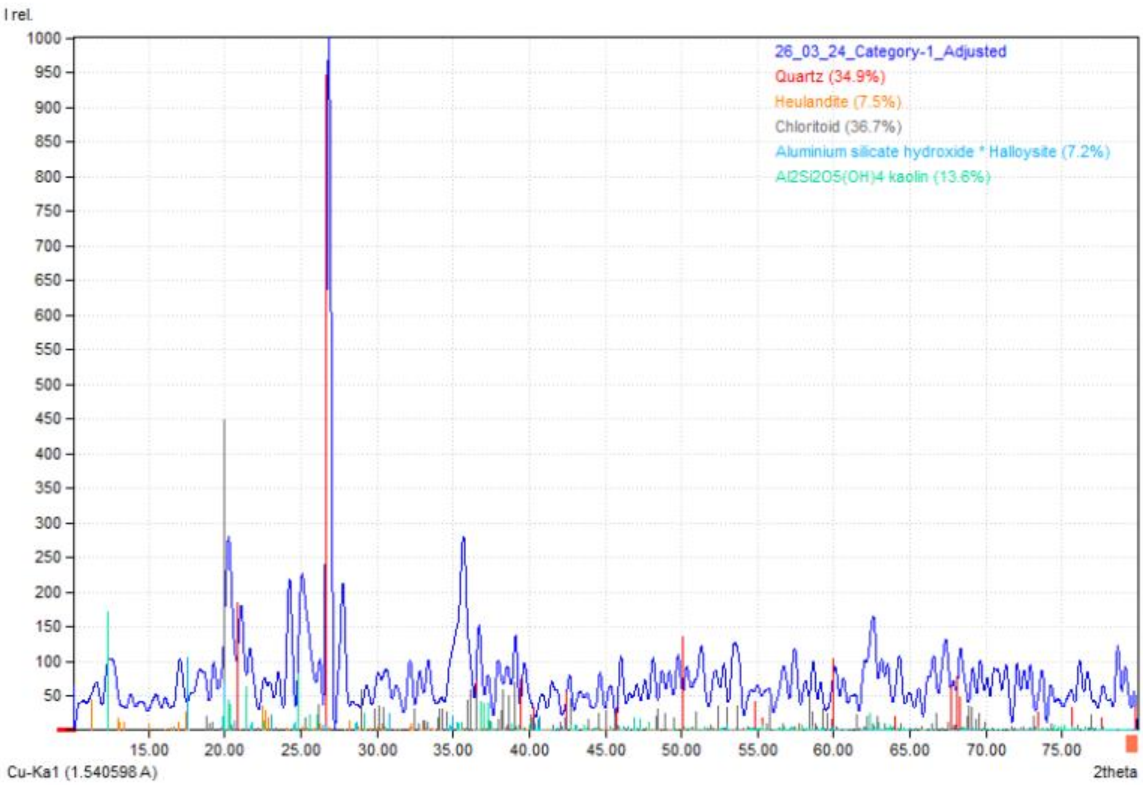

Figure B-40 Snapshot of diffraction pattern graphics from MATCH software for Category-1

B.10.2 Category-2 Subgrade Soil

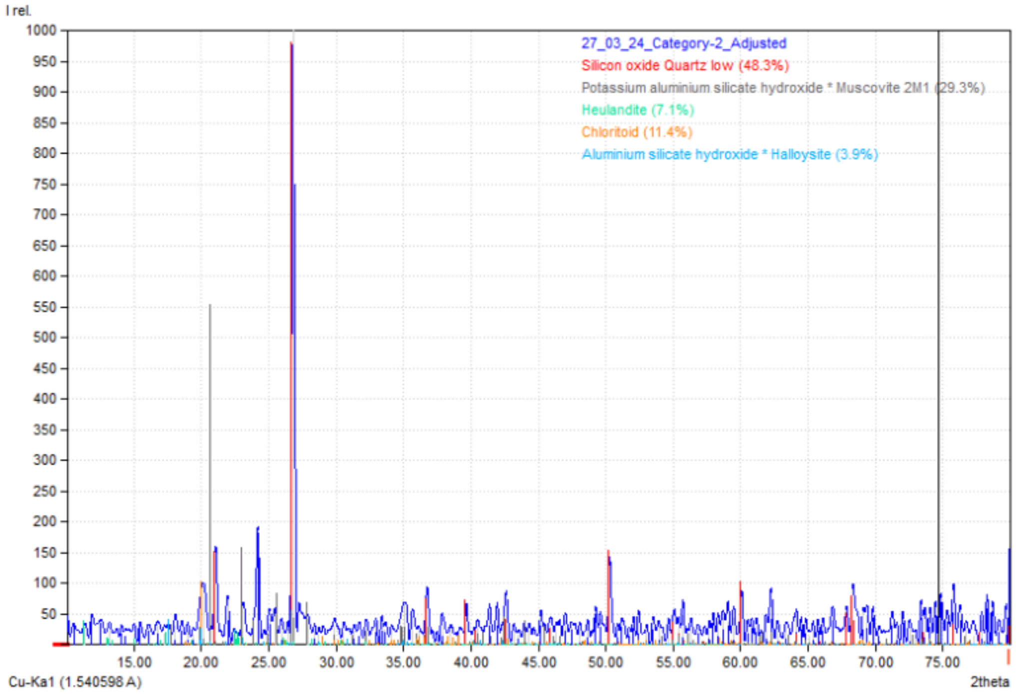

Figure B-41 Snapshot of diffraction pattern graphics from MATCH software for Category-2

B.10.3 Category-3 Subgrade Soil

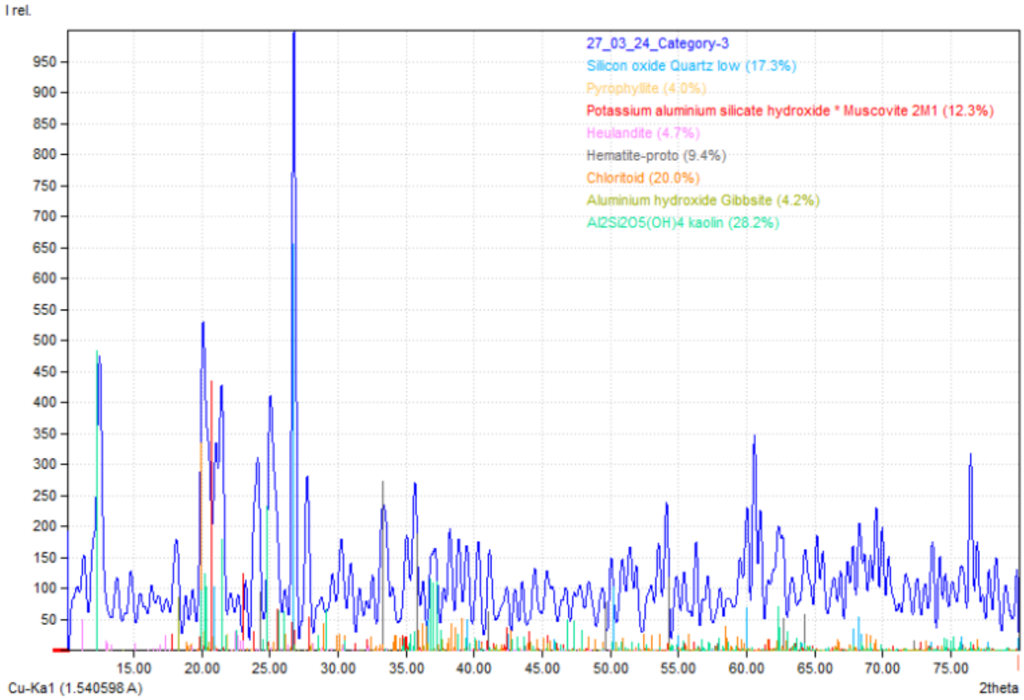

Figure B-42 Snapshot of diffraction pattern graphics from MATCH software for Category-3

B.10.4 Replacement Material

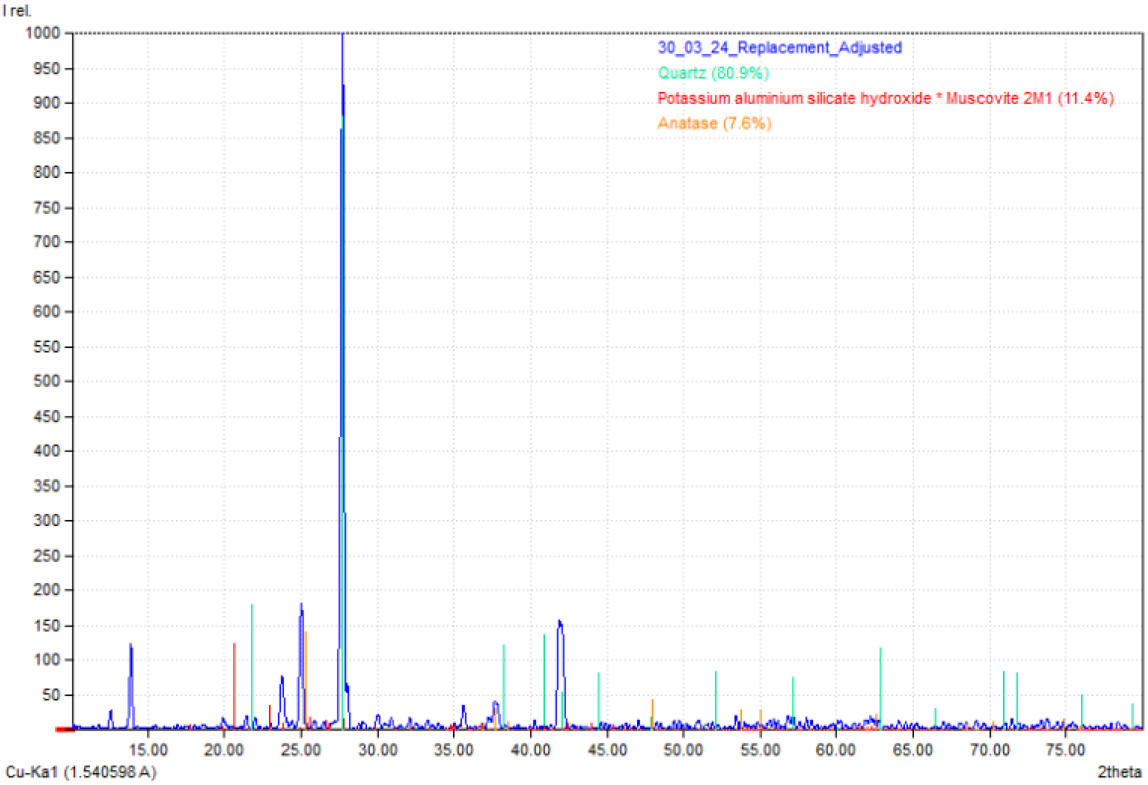

Figure B-43 Snapshot of diffraction pattern graphics from MATCH software for Replacement

B.11 Determination of Major and Minor Oxides Using Silicate Analysis

	GEOLOGICAL INSTITUTE OF ETHIOPIA	**Doc. Number: GLD/F5.10.2**	**Version No: 1**
	Geochemical Laboratory Desk		Page **1**of **1**
Document Title:-	**Complete Silicate Analysis Report**	**Effective date:**	**Nov. 2022**

Customer Name:-Biniyam Gezahegn

Sample type :- Soil

Sample Preparation:-200 Mesh

Date Submitted:-19/02/2024

Issue Date:-08/04/2024

Request No:- GLD/RQ/843/24

Report No:- GLD/RN/3063/24

Number of Sample:- Three(03)

Analytical Result: In percent (%) Element to be determined Major Oxides & Minor Oxides.

Analytical Method: $LiBO_2$ FUSION, HF attack, GRAVIMETERIC, COLORIMETRIC and AAS

Collector's code	SiO_2	Al_2O_3	Fe_2O_3	CaO	MgO	Na_2O	K_2O	MnO	P_2O_5	TiO_2	H_2O	LOI	Weight of Sample
Category -1	40.50	22.30	12.56	<0.01	<0.01	0.80	0.26	0.32	0.32	1.94	12.12	9.93	500gm
Category -2	41.76	20.42	11.16	<0.01	0.50	<0.01	0.50	0.38	0.30	2.12	14.30	9.84	500gm
Category -3	41.32	23.92	10.66	<0.01	<0.01	<0.01	0.24	0.20	0.24	1.60	10.71	11.33	500gm

Note:- This result represent only for the sample submitted to the laboratory.

- LOI = Loss on Ignition

Analysts	Checked By	Approved By	Quality Control
Haimanot Bayeh			
Kindie Kasahun	Nigist Fikadu	Lidet Endeshaw	Gosa Haile
Melkamu Debalka			
Shashe Haile			

Geochemical Laboratory Desk Page 1

Figure B-44 Snapshot of Silicate analysis report from Geological Institute of Ethiopia

B.12 Determination of DCP Value

B.12.1 Category-1 Subgrade Soil

Table B-37 DCP penetration data for category-1

B	E	F	B	E	F	B	E	F	B	E	F
0.0	0.0	0.0	10.0	235.0	27.0	20.0	505.0	31.0	30.0	720.0	22.0
1.0	13.0	13.0	11.0	264.0	29.0	21.0	530.0	25.0	31.0	744.0	24.0
2.0	39.0	26.0	12.0	290.0	26.0	22.0	552.0	22.0	32.0	766.0	22.0
3.0	63.0	24.0	13.0	316.0	26.0	23.0	572.0	20.0	33.0	788.0	22.0
4.0	86.0	23.0	14.0	337.0	21.0	24.0	590.0	18.0	34.0	809.0	21.0
5.0	109.0	23.0	15.0	365.0	28.0	25.0	610.0	20.0	35.0	830.0	21.0
6.0	132.0	23.0	16.0	390.0	25.0	26.0	631.0	21.0	36.0	851.0	21.0
7.0	158.0	26.0	17.0	415.0	25.0	27.0	653.0	22.0	37.0	871.0	20.0
8.0	186.0	28.0	18.0	445.0	30.0	28.0	676.0	23.0	38.0	892.0	21.0
9.0	208.0	22.0	19.0	474.0	29.0	29.0	698.0	22.0	39.0	910.0	18.0

B = Cumulative number of blows [blow], E = Cumulative penetration [mm], and F = Penetration rate [mm/blow]

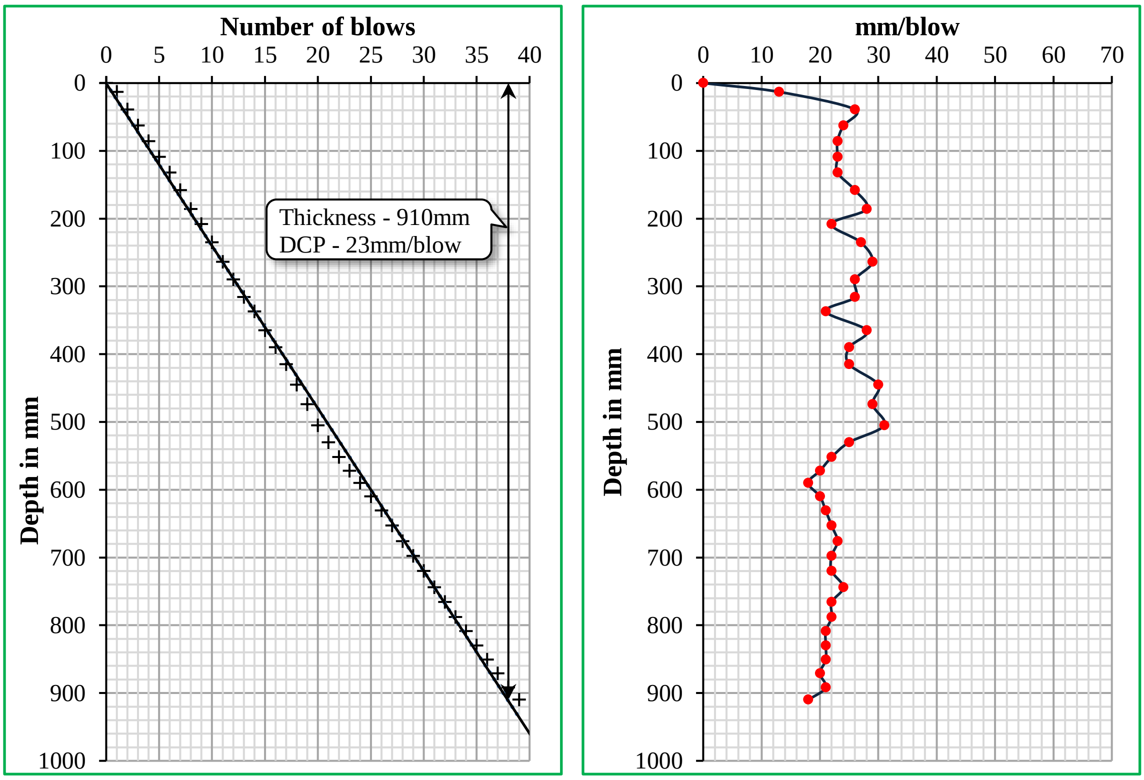

(a) (b)

Figure B-45 Penetration curves for category-1; (a) Number of blows-depth curve, and (b) Penetration rate-depth curve

B.12.2 Category-2 Subgrade Soil

Table B- 38 DCP penetration data for category-2

B	E	F	B	E	F	B	E	F	B	E	F
0.0	0.0	0.0	10.0	215.0	19.0	20.0	515.0	31.0	30.0	775.0	22.0
1.0	23.0	23.0	11.0	238.0	23.0	21.0	543.0	28.0	31.0	797.0	22.0
2.0	51.0	28.0	12.0	266.0	28.0	22.0	567.0	24.0	32.0	822.0	25.0
3.0	80.0	29.0	13.0	299.0	33.0	23.0	591.0	24.0	33.0	847.0	25.0
4.0	102.0	22.0	14.0	330.0	31.0	24.0	617.0	26.0	34.0	866.0	19.0
5.0	123.0	21.0	15.0	355.0	25.0	25.0	645.0	28.0	35.0	884.0	18.0
6.0	143.0	20.0	16.0	381.0	26.0	26.0	669.0	24.0	36.0	902.0	18.0
7.0	162.0	19.0	17.0	410.0	29.0	27.0	696.0	27.0	37.0	910.0	8.0
8.0	180.0	18.0	18.0	445.0	35.0	28.0	725.0	29.0			
9.0	196.0	16.0	19.0	484.0	39.0	29.0	753.0	28.0			

B = Cumulative number of blows [blow], E = Cumulative penetration [mm], and F = Penetration rate [mm/blow]

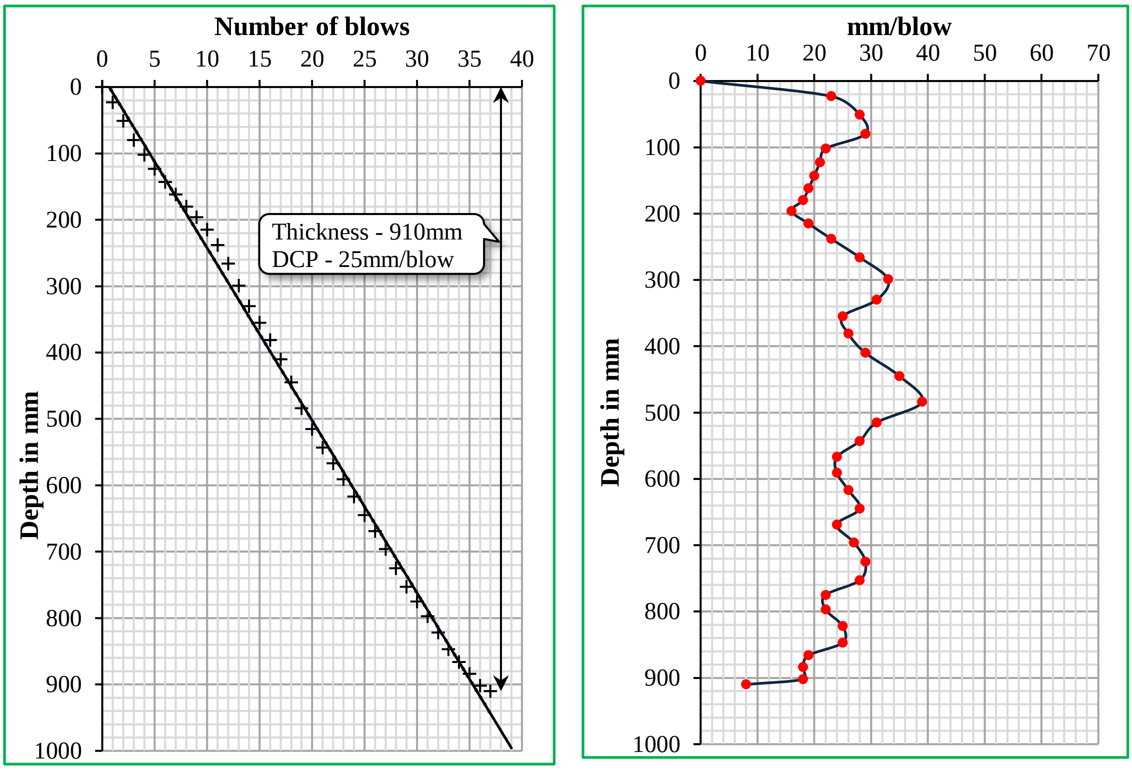

(a) (b)

Figure B-46 Penetration curves for category-2; (a) Number of blows-depth curve, and (b) Penetration rate-depth curve

B.12.3 Category-3 Subgrade Soil

Table B-39 DCP penetration data for category-3

B	E	F	B	E	F	B	E	F	B	E	F
0.0	0.0	0.0	6.0	321.0	57.0	12.0	642.0	53.0	18.0	890.0	40.0
1.0	46.0	46.0	7.0	379.0	58.0	13.0	690.0	48.0			
2.0	96.0	50.0	8.0	432.0	53.0	14.0	743.0	53.0			
3.0	164.0	68.0	9.0	492.0	60.0	15.0	785.0	42.0			
4.0	216.0	52.0	10.0	533.0	41.0	16.0	820.0	35.0			
5.0	264.0	48.0	11.0	589.0	56.0	17.0	850.0	30.0			

B = Cumulative number of blows [blow], E = Cumulative penetration [mm], and F = Penetration rate [mm/blow]

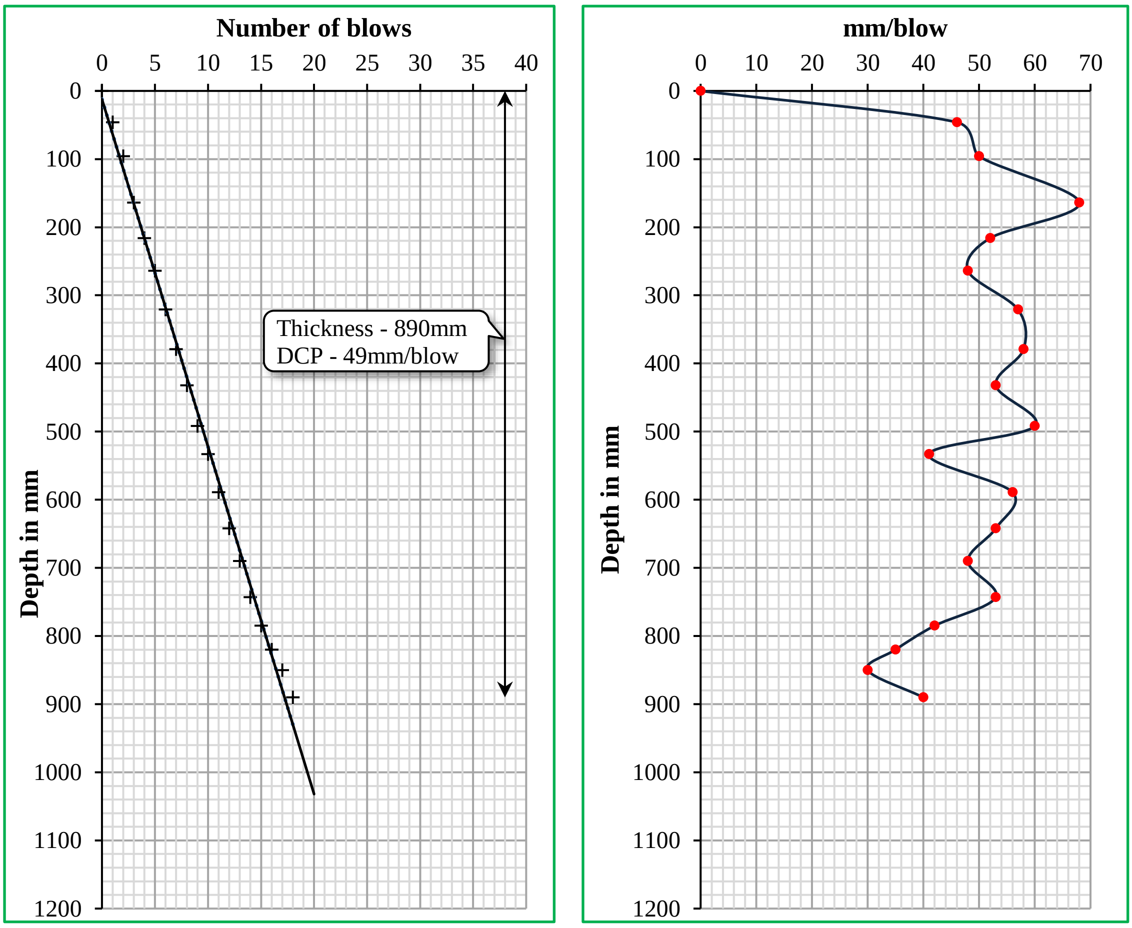

(a) (b)

Figure B-47 Penetration curves for category-3; (a) Number of blows-depth curve, and (b) Penetration rate-depth curve

B.13 Determination of Field Bulk Density and Unit Weight

Table B-40 Bulk density and unit weight test data

Subgrade category	Cagtegory-1		Cagtegory-2		Cagtegory-3	
Test No	1	2	1	2	1	2
Mass of wet soil + core cutter [gm]	2301.2	2325.1	2283	2362	2259	2247
Mass of core cutter [gm]	1100.8	1100.4	1136	1135	1137	1136
Mass of wet soil [gm]	1200.4	1224.7	1147	1227	1123	1111
Volume of core cutter [cm3]	719.1	719.1	719.1	719.1	719	719
Bulk density of soil [g/cm3]	1.669	1.703	1.596	1.706	1.56	1.55
Average Bulk density of soil [g/cm3]	1.686		1.651		1.553	
Unsaturated unit weight [KN/m3]	16.54		16.19		15.24	
Saturated unit weight [KN/m3]	17.26		16.23		16.32	

CDSWC

በኢትዮጵያ የኮንስትራክሽን ዲዛይንና ሱፐርቪዥን ሥራዎች ኮርፖሬሽን

ETHIOPIAN CONSTRUCTION DESIGN & SUPERVISION WORKS CORPORATION

Geotechnical Laboratory Testing Report	OF/ECDSWC/ 0996	1	1 of 11

Client Ref.:-	GL/093/2024
Date Received:-	19/02/2024
Reported on:-	22/03/2024

Lab No. :- 1642/16 - 1645/16
Submitted by :- BINYAM GEZAHEGN
Project :- Thesis
Station :- ....
Test Requested :- As Stated Below
Reported to :- BINYAM GEZAHEGN
Customer Contact Address:- Binyam G. /0911478642/
Date of Sampling :- --------

No.	Testing Date	Test Type	Standard Method	Soil Samples Test Results			
				Lab. No. :- 1642/16	Lab. No. :- 1643/16	Lab. No. :- 1644/16	Lab. No. :- 1645/16
				Sample Id.:- Category-1	Sample Id.:- Category-2	Sample Id.:- Category-3	Sample Id.:- Replacement Material
				Identification remark:-			
				3	3	3	1
1	26/02/2024-15/03/2024	Volumetric Shrinkage Limit (%)	ASTM D427	21.62	19.43	27.29	-
2		Swelling Pressure (Kpa)	ASTM D4546	Nil	3.00	11.00	-
3		Consolidasion	ASTM D2435				
		P_c		240	230	118	-
		eo		1.270	1.427	1.442	-
		Cc		0.154	0.230	0.200	-
		Cr		0.040	0.042	0.043	-
4		Triaxial Shear UU	ASTM D2850				
		C (Kpa)		247.53	74.08	116.29	92.20
		Ø(Degree)		3.98	10.71	3.45	21.20

REMARK:- The samples were collected & submitted to the laboratory by client.
:- Sample results relate only to items tested.
:- Lab No.:- 1645/16 remolded triaxial UU test, OMC & MDD was given by the client.

Processed by :- Getu M. — Geotechnical Engineer
Checked By :- Biruk A. — Senior Geotechnical Engineer
Approved By :- Bethelhem B. — Geotechnical Lab S/P Manager

Among the major services rendered by the Geotechnical and Material Laboratory Testing s/processes of Ethiopian Construction Design & Supervision Works Corporation are
•In Geotechnical Laboratory -Testing the engineering properties of Soil Mechanics and Rock Mechanics.
•In Material Testing Laboratory - Testing the engineering properties of various Construction materials, such as Aggregates, Asphalts/Bitumen/, Cements, Rocks, Water, Reinforcement steel bars, Hollow Blocks, Bricks, Ceramics, Tiles,Asphalt & Concrete Core Tests, Concrete Mix Designs, Asphalt Mix Designs, Sampling of the soil and construction materials, and so on.

Please make sure that this document is the correct version before use.

Figure B-48 Summary of test result from ECDSWC

APPENDIX C

MODEL PARAMETER DETERMINATION

C.1 Material Model Parameters

C.1.1 Reference Secant Stiffness Modulus (E_{50}^{ref})

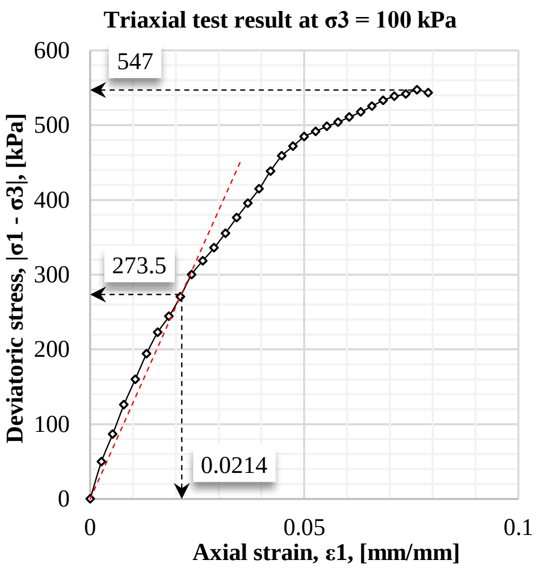

For category-1 (set 1)

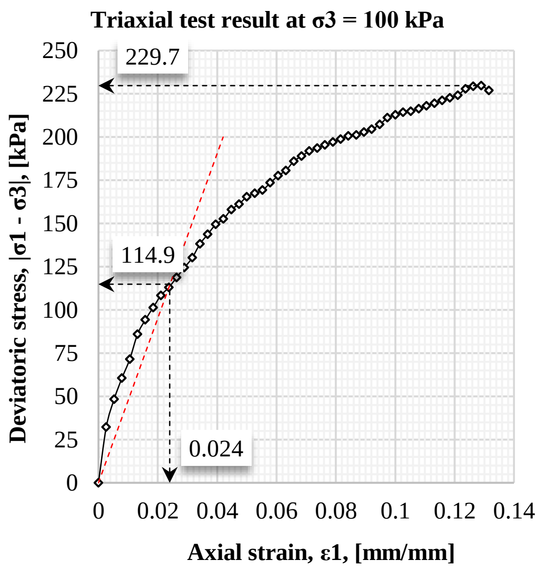

For category-2 (set 1)

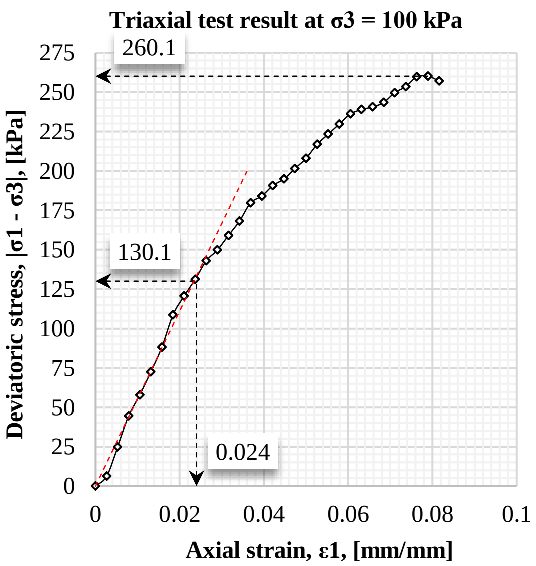

For category-3 (set 1)

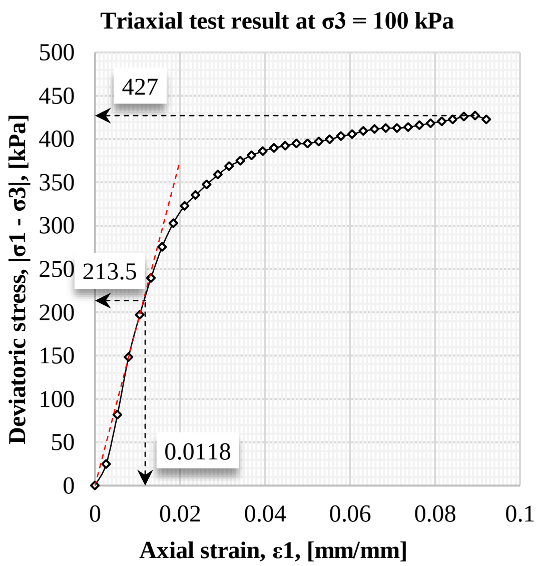

For replacement (set 1)

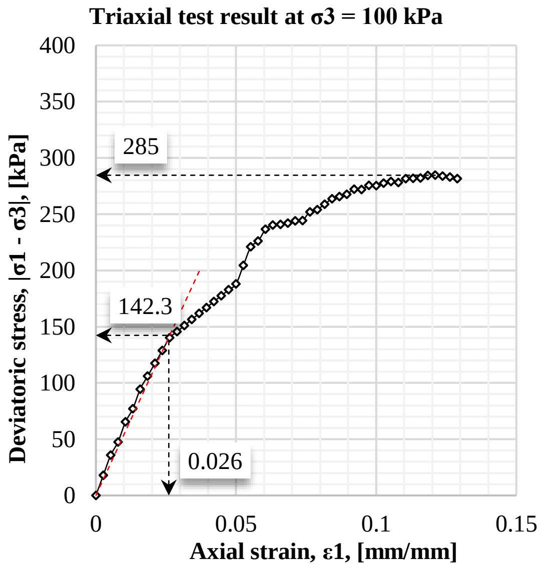

For category-1 (set 2)

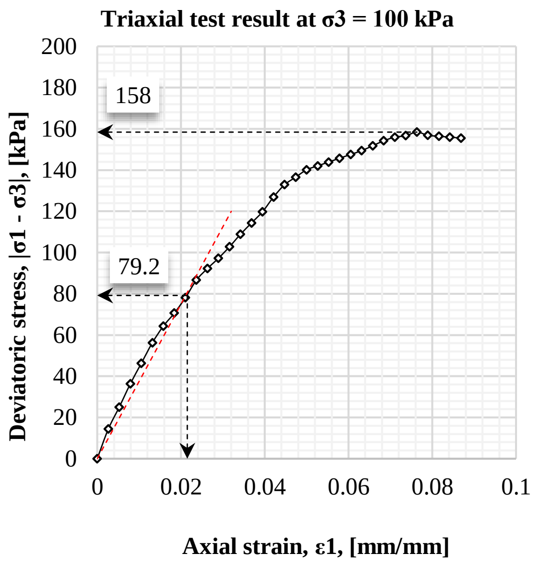

For category-2 (set 2)

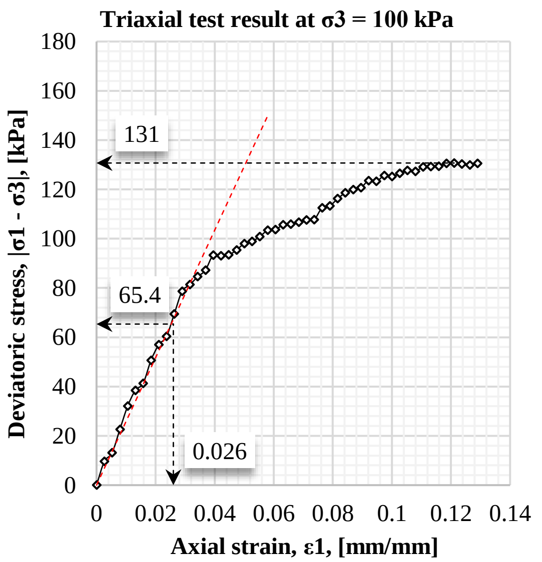

For category-3 (set 2)

Figure C-1 Secant stiffness modulus determination curves from triaxial test data

$E_{50} = \frac{|\sigma_1 - \sigma_3|_{50\%}}{\varepsilon_1}$, for σ_3 = 100kPa, $E_{50} = E_{50}^{ref}$. Thus, E_{50}^{ref} computed data is presented in the table below.

Table C-1 Secant stiffness modulus for subgrade soils and replacement material

	Category-1		Category-2		Category-3		Replacement
	Set 1	Set 2	Set 1	Set 2	Set 1	Set 2	Set 1
E_{50}^{ref}, kPa	12,780	5,473	4,786	3,684	5,419	2,514	18,096

C.1.2 Reference Tangent Stiffness Modulus (E_{oed}^{ref})

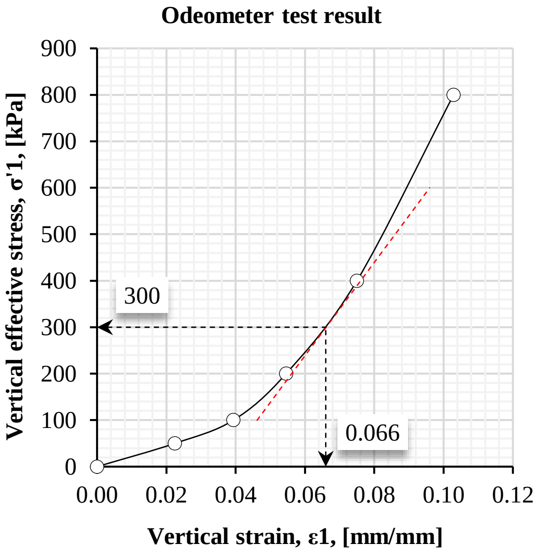

For category-1 (Primary compression)

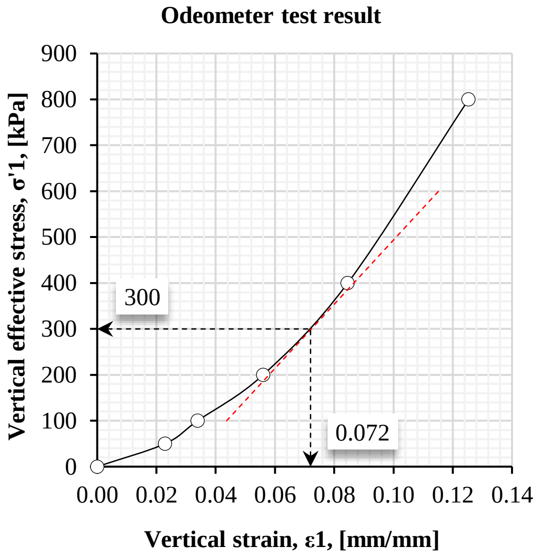

For category-2 (Primary compression)

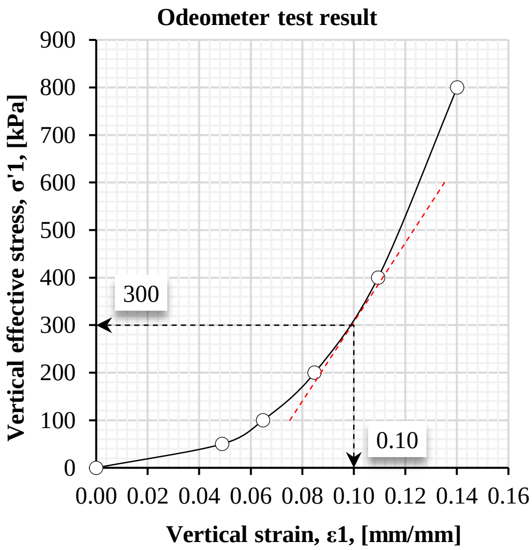

For category-3 (Primary compression)

$E_{oed} = \frac{\sigma_1'}{\varepsilon_1}$, after rearranging the equation (2-2), E_{oed}^{ref} was determined. Shear strength parameters from Table 4-10 were used and for MH soils, m = 0.8 was used based on correlation given by Obrzud and Andrzej [47].

Figure C-2 Tangent stiffness modulus determination curves from consolidation test data

Thus, E_{oed}^{ref} computed data is presented in the table below.

Table C-2 Tangent stiffness modulus for subgrade soils

	Category-1		Category-2		Category-3	
	Set 1	Set 2	Set 1	Set 2	Set 1	Set 2
E_{oed}^{ref}, kPa	4,356	3,178	3,171	2,738	2,783	1,938

Note: for set 1 test data, the difference between E_{50}^{ref} and E_{oed}^{ref} is very significant, hence, the default PLAXIS setting, $E_{50}^{ref} = E_{oed}^{ref}$, was used. The same setting was applied for replacement material.

C.1.3 Reference Unloading/Reloading Stiffness Modulus (E_{oed}^{ref})

Default value suggested by PLAXIS: $E_{ur}^{ref} \approx 3E_{50}^{ref}$ was used. As a result, E_{ur}^{ref} computed data is presented in the table below.

Table C-3 Reference unloading/reloading modulus for subgrade soils and replacement material

	Category-1		Category-2		Category-3		Replacement
	Set 1	Set 2	Set 1	Set 2	Set 1	Set 2	Set 1
E_{oed}^{ref}, kPa	38,341	16,420	14,359	11,052	16,257	7,541	54,288

C.1.4 Reference Shear Modulus at Very Small Strains (G_0^{ref})

Benz [49], presented the form of most of the correlations between the Standard Penetration Test (SPT) and very small strain stiffness as, $G_0 = A((N_{60})_{60})^B (G_0$ in MPa units). For cohesive soils, A = 15.56 and B = 0.68 are recommended. SPT values were obtained using correlation with DCP value by Parry et al. [72] as shown in Figure C-3.

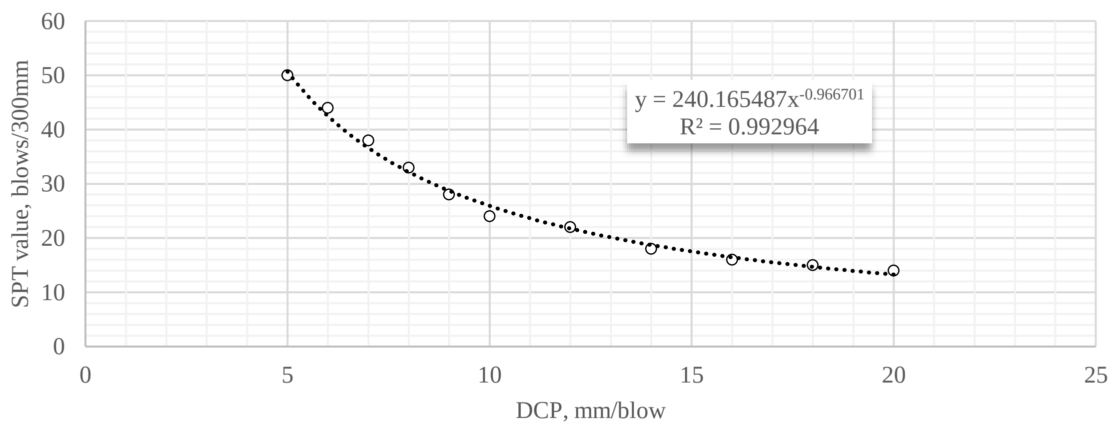

Figure C-3 SPT-DCP correlation [72]

Thus, G_0^{ref} computed data is presented in the table below.

Table C-4 SPT and Reference shear modulus at very small strains for subgrade soils

	Category-1	Category-2	Category-3
SPT [N]	11.4	10.9	5.5
G_0^{ref}, [MPa]	81.6	78.8	49.8

C.1.5 Shear Strain ($\gamma_{0.7}$)

Obrzud and Andrzej [47] presented approximated experimental data for $\gamma_{0.7}$. For PI ≥ 15, it is reported as, $\gamma_{0.7} = 10^{1.15\log(PI)-5.1}$ and used in this study. Thus, $\gamma_{0.7}$ computed data is presented in the table below.

Table C-5 Shear strain for subgrade soils

	Category-1	Category-2	Category-3
$\gamma_{0.7}$	0.00021	0.00023	0.00026

APPENDIX D

PLAXIS OUTPUT DATA

D.1 Deformation Analysis

D.1.1 Using Set 1 Test Result Input Data

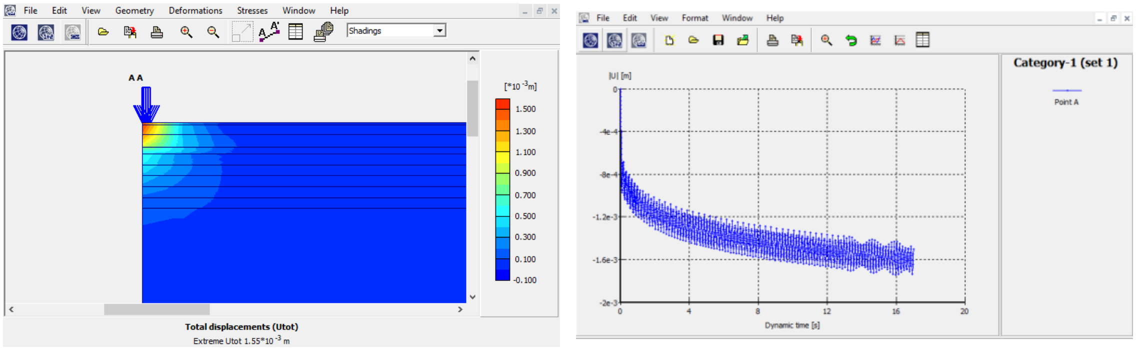

(a) (b)

Figure D-1 Category-1 analysis output data (with no undercut)

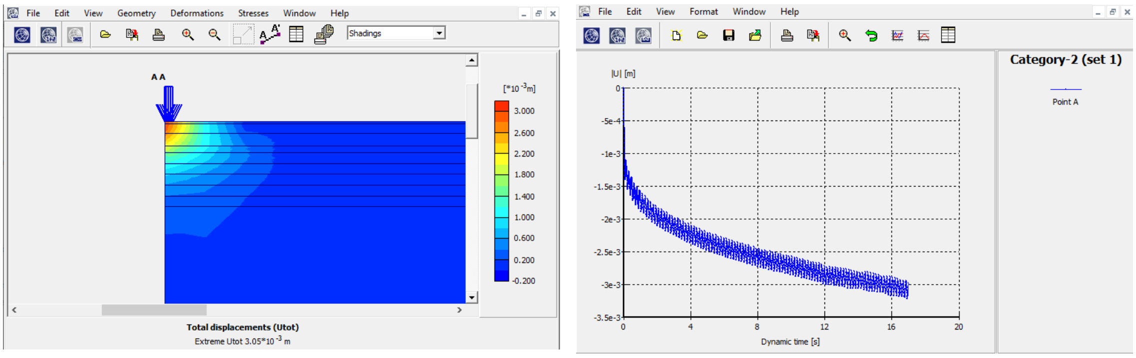

(a) (b)

Figure D-2 Category-2 analysis output data (with no undercut)

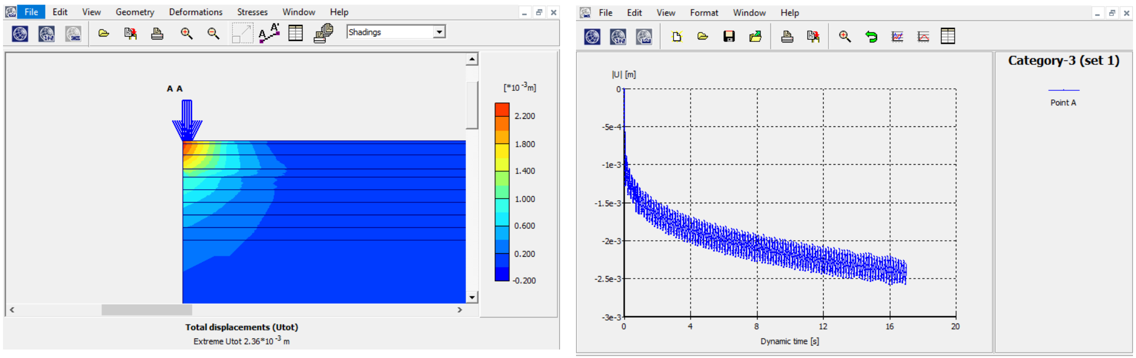

(a) (b)

Figure D-3 Category-3 analysis output data (with no undercut)

<u>**Note**</u>: (a) Deformation shadings (zoomed), and (b) Dynamic Time-Deformation curve snapshot

D.1.2 Using Set 2 Test Result Input Data

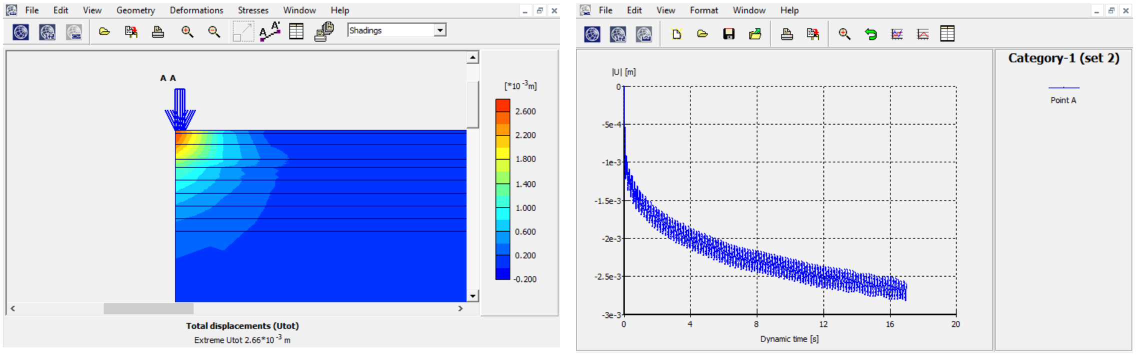

(a) (b)

Figure D-4 Category-1 analysis output data (with no undercut)

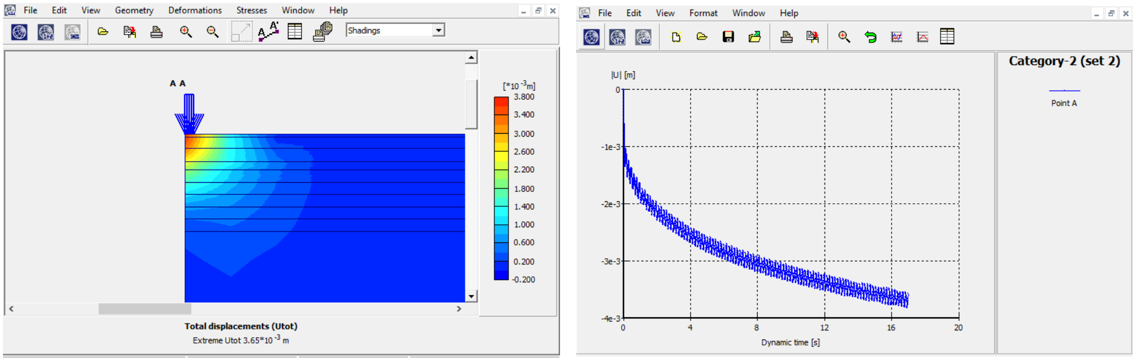

(a) (b)

Figure D-5 Category-2 analysis output data (with no undercut)

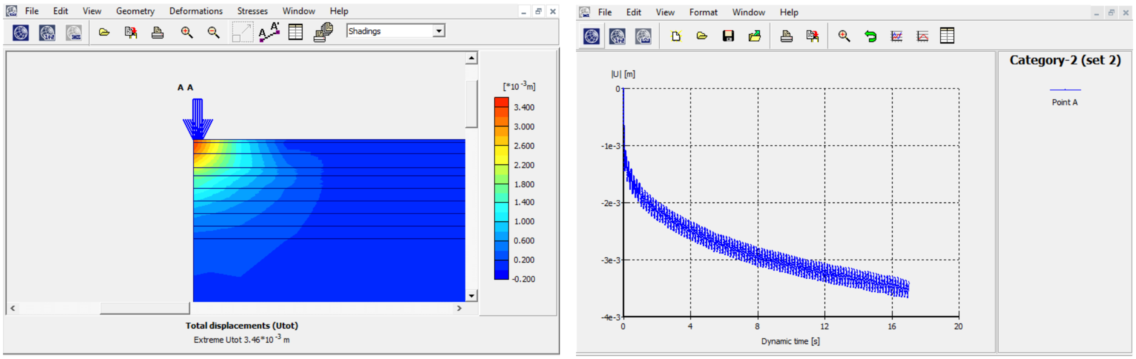

(a) (b)

Figure D-6 Category-2 analysis output data (with 20 cm undercut)

<u>Note</u>: (a) Deformation shadings (zoomed), and (b) Dynamic Time-Deformation curve snapshot

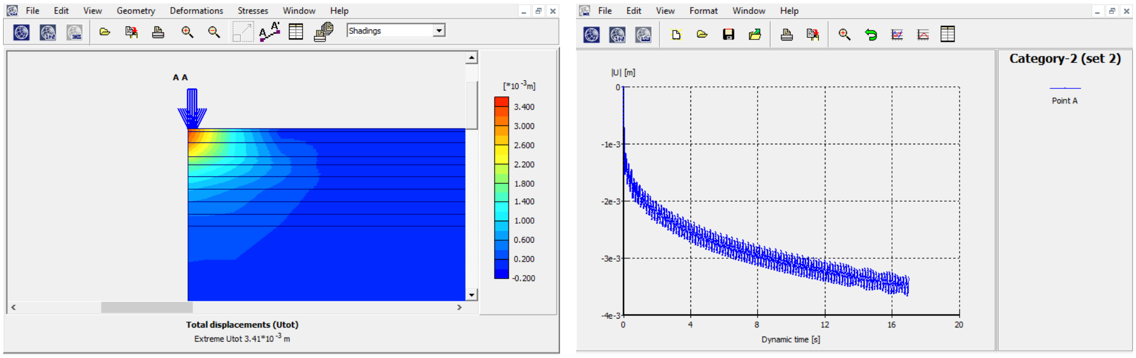

(a) (b)

Figure D-7 Category-2 analysis output data (with 40 cm undercut)

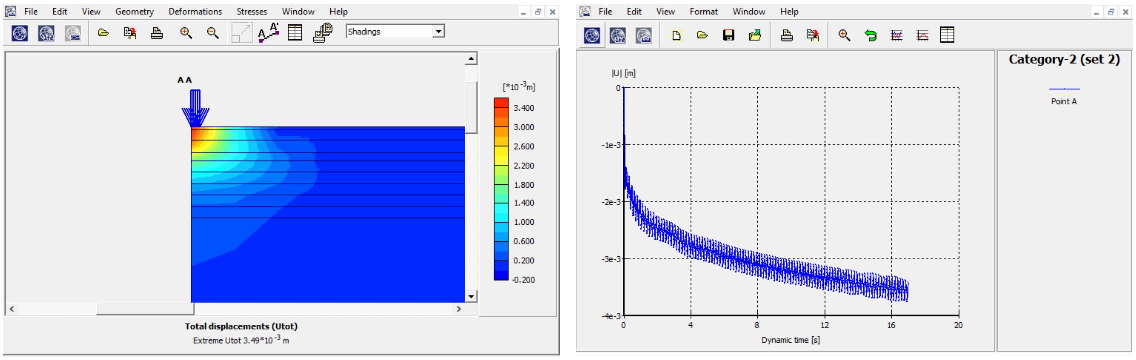

(a) (b)

Figure D-8 Category-2 analysis output data (with 60 cm undercut)

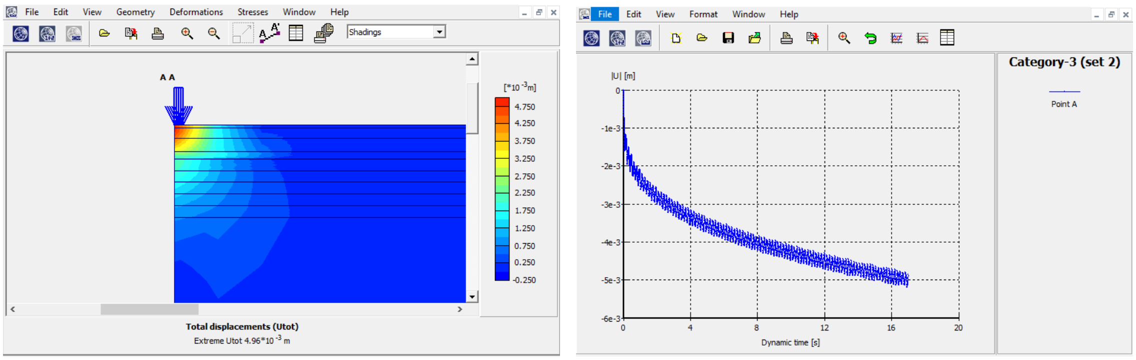

(a) (b)

Figure D-9 Category-3 analysis output data (with no undercut)

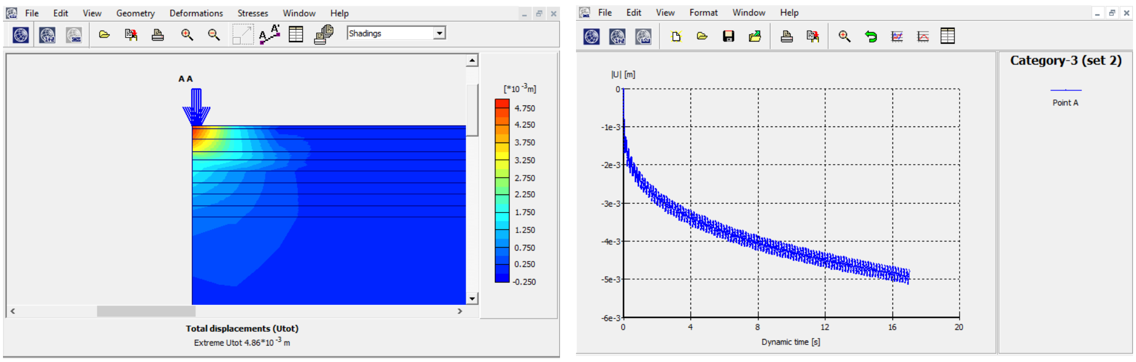

(a) (b)

Figure D-10 Category-3 analysis output data (with 20 cm undercut)

Note: (a) Deformation shadings (zoomed), and (b) Dynamic Time-Deformation curve snapshot

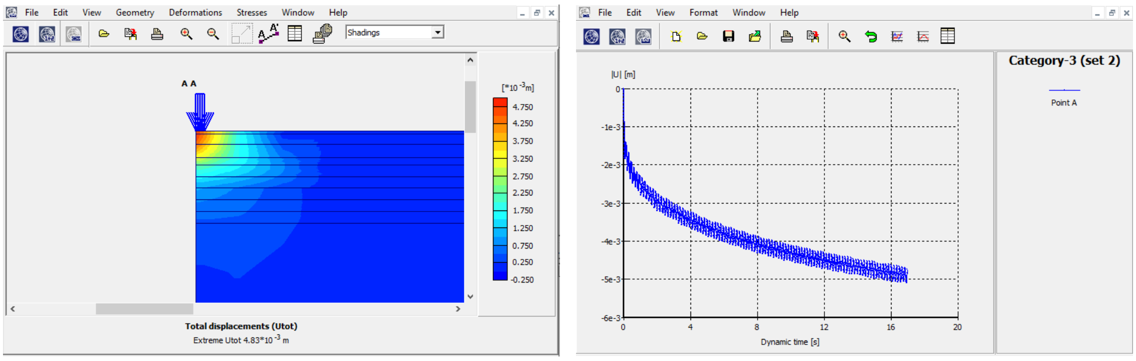

(a) (b)

Figure D-11 Category-3 analysis output data (with 40 cm undercut)

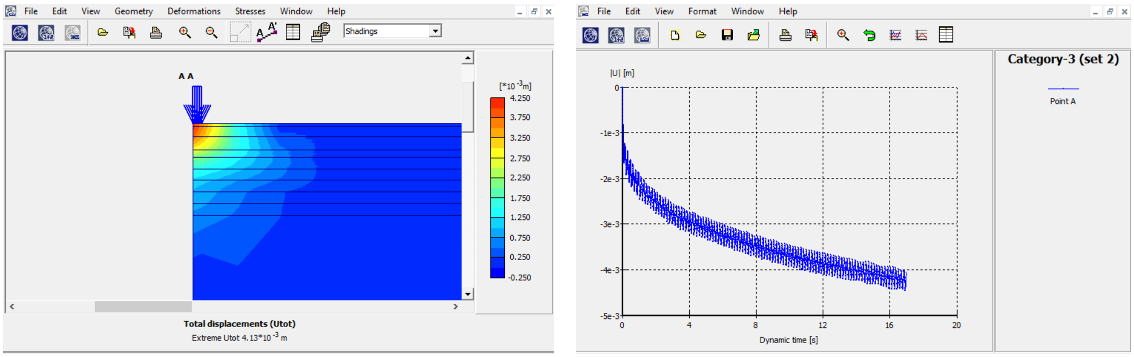

(a) (b)

Figure D-12 Category-3 analysis output data (with 60 cm undercut)

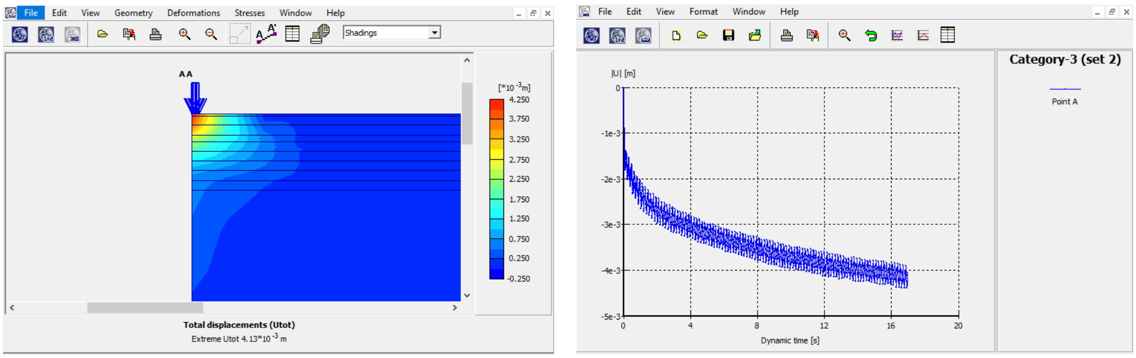

(a) (b)

Figure D-13 Category-3 analysis output data (with 80 cm undercut)

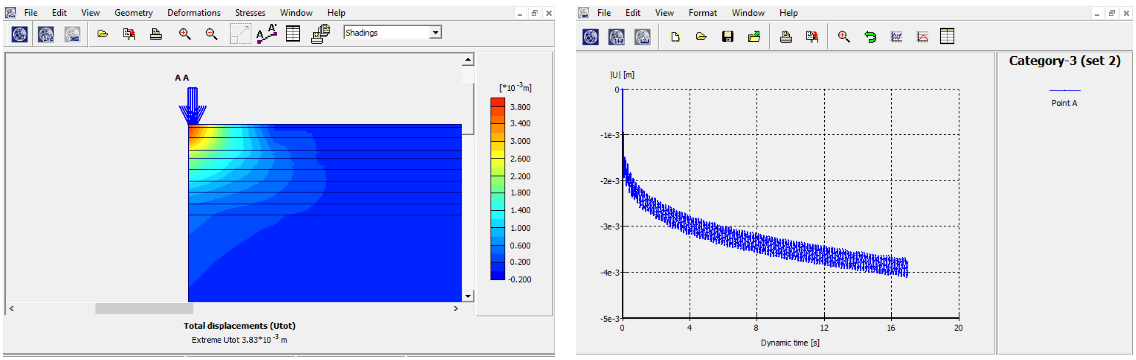

(a) (b)

Figure D-14 Category-3 analysis output data (with 100 cm undercut)

Note: (a) Deformation shadings (zoomed), and (b) Dynamic Time-Deformation curve snapshot

APPENDIX E

PHOTOS OF TEST PROGRAM

Hereunder pictures taken during the process of the test program are presented.

DCP in-situ test

Undistrubed and core cut samples

Test pit logging

Sample preparation

Moisture content determination

Liquid limit test

Sieve analysis

Linear shrinkage test

Specific gravity determination

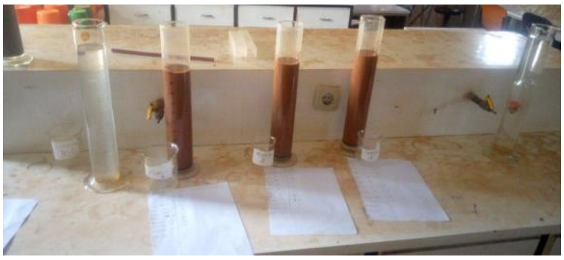

Hydrometer analysis

Compaction test

Soaked CBR specimens

Triaxial compression test

Specimen after test (triaxial)

Free swell index test